



AR-008-399

DSTO-RR-0013

O

T

A Review of Rolling Element
Bearing Vibration "Detection,
Diagnosis and Prognosis"

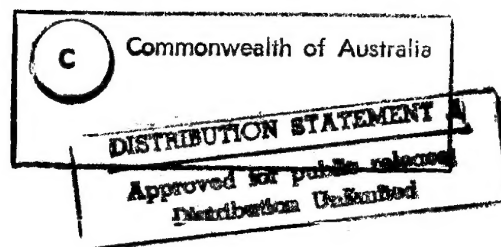
Ian Howard

19950214 074

S

APPROVED
FOR PUBLIC RELEASE

R



A Review of Rolling Element Bearing Vibration "Detection, Diagnosis and Prognosis"

Ian Howard

DSTO-RR-0013

Aeronautical and Maritime Research Laboratory
Airframes and Engines Division

ABSTRACT

Rolling element bearings are among the most common components to be found in industrial rotating machinery. They are found in industries from agriculture to aerospace, in equipment as diverse as paper mill rollers to the Space Shuttle Main Engine Turbomachinery. There has been much written on the subject of bearing vibration monitoring over the last twenty five years. This report attempts to summarise the underlying science of rolling element bearings across these diverse applications from the point of view of machine condition monitoring using vibration analysis. The key factors which are addressed in this report include the underlying science of bearing vibration, bearing kinematics and dynamics, bearing life, vibration measurement, signal processing techniques and prognosis of bearing failure.

APPROVED FOR PUBLIC RELEASE

DTIC QUALITY INSPECTED 4

DEPARTMENT OF DEFENCE

DEFENCE SCIENCE AND TECHNOLOGY ORGANISATION

Accession For	
NTIS GRA&I	<input checked="checked" type="checkbox"/>
DTIC TAB	<input type="checkbox"/>
Unannounced	<input type="checkbox"/>
Justification	
By	
Distribution/	
Availability Codes	
Dist	Avail and/or Special
A-1	

Published by

*DSTO Aeronautical and Maritime Research Laboratory
GPO Box 4331
Melbourne Victoria 3001 Australia*

*Telephone: (03) 626 7000
Fax: (03) 626 7999
© Commonwealth of Australia 1994
AR No. 008-399
OCTOBER 1994*

APPROVED FOR PUBLIC RELEASE

A Review of Rolling Element Bearing Vibration "Detection, Diagnosis and Prognosis"

EXECUTIVE SUMMARY

The art of machine condition monitoring is knowing what to look for, and successful diagnosis is having the ability to measure it and to correlate the results with known failure mechanisms.

Vibration analysis has been used as a condition monitoring tool for bearing fault detection and diagnosis, probably ever since the first use of bearings when the symptoms were "something sounds strange". This report reviews some of the important factors which influence the bearing vibration, including different machine types, bearing types and modes of failure. Much has been written about vibration analysis for bearing fault detection over the last twenty five years. A review completed over twenty years ago provided comprehensive discussion on bearings, their rotational frequencies, modes of failures, resonance frequencies and various vibration analysis techniques. The more common techniques which were used at that time included time and frequency domain techniques. These comprised techniques such as RMS, crest factor, probability density functions, correlation functions, band pass filtering prior to analysis, power and cross power spectral density functions, transfer and coherence functions as well as cepstrum analysis, narrow band envelope analysis and shock pulse methods. It is interesting to note that these are the techniques which have continued to be used and have been further developed over the past two decades for bearing fault detection and diagnosis.

A large number of vibration signal processing techniques for bearing condition monitoring have been published in the literature across the full range of rotating machinery. Condition monitoring can be divided up into three main areas, detection, diagnosis and prognosis. Detection can often be as simple as determining that a serious change has occurred in the mechanical condition of the machine. Diagnosis in effect determines the location and type of the fault, while prognosis involves estimation of the remaining life of the damaged bearing.

Over the past decade, the understanding of signal processing techniques and their application to bearing fault detection has increased tremendously. The amount of information which can be gained from the vibration measured on rotating machinery is immense. It would be anticipated that the general use of advanced signal processing techniques will become more widespread in the future.

The review commences with an examination of the underlying science of bearing vibration including the modes of failure, how the failure mode influences the bearing dynamics and resulting forces, the transmission of the stresses through the structure, the external noise and vibration environment, the measurement of the vibration and the effect of the class of machine on the diagnostic techniques which need to be used to detect impending failure. Then follows an outline of the kinematic relationships between bearing components and the status of modelling of bearing dynamics, a discussion of bearing life and the major influencing parameters, a summary of the latest advanced signal processing techniques and their application to bearings and a review of the state of the art of bearing prognosis.

Rather than comparing the effectiveness of the various signal processing techniques for bearing fault detection, an emphasis has been placed upon discussion of the underlying factors associated with bearings, their modes of failure and the vibration environment and class of machine. The next logical step would be to undertake a detailed comparison of techniques for the various modes of failure, class of machine, vibration environment, etc.

Author

Ian Howard

Airframes and Engines Division

Bachelor of Mechanical Engineering (Honours) 1983,
The University of Western Australia.

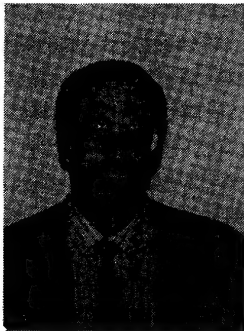
Ph.D in Mechanical Engineering 1987 - Structural
dynamic modelling using the receptance systems
approach, The University of Western Australia.

Postdoctoral Research on an Australian Research
Grant Scheme - Investigation of the mechanism of
noise and vibration generation in rolling element
bearings, March 1987 - April 1988, The University of
Western Australia.

Research Scientist, Aeronautical Research
Laboratory, Defence Science and Technology
Organisation, Melbourne, May 1988 - December 1993.
Development of advanced signal processing
techniques for vibration condition monitoring of
bearings and fixed axis and moving axis gears in
helicopter transmissions.

Visiting Senior Scientist, Technology Integration
Inc., Bedford, Massachusetts, November 1991 -
January 1993. Application of advanced signal
processing techniques for bearing fault detection of the
Space Shuttle Main Engine Oxygen Turbopump,
NASA Marshall Contract NAS8-38955.

Lecturer in Applied Mechanics, Department of
Mechanical Engineering, Curtin University of
Technology, Perth Western Australia, January 1994 -
present. Research interests include signal processing
and dynamic modelling of rotating machinery
vibration.



Contents

1.0	INTRODUCTION	1
2.0	UNDERLYING SCIENCE	2
2.1	Mode of failure	2
2.1.1	Fatigue	3
2.1.2	Wear	3
2.1.3	Plastic deformation	3
2.1.4	Corrosion	4
2.1.5	Brinelling	4
2.1.6	Lubrication	4
2.1.7	Faulty installation	4
2.1.8	Incorrect design	5
2.1.9	Expected vibration signature	5
2.2	Dynamic response to damage	6
2.3	Force propagation and transmission path effects	7
2.4	External noise and vibration	7
2.5	Vibration measurement	8
2.6	Effect of class of machine	9
3.0	BEARING KINEMATICS AND DYNAMICS	11
3.1	Bearing kinematics	11
3.2	Vibration models of localised defects	14
3.3	Bearing dynamic modelling	17
4.0	BEARING LIFE	19
4.1	Rolling bearing fatigue life	19
4.2	Rolling element bearing lubrication	23
4.3	Summary of bearing life	24
5.0	SIGNAL PROCESSING TECHNIQUES	24
5.1	Time domain techniques	25
5.2	Frequency domain techniques	31
5.3	Envelope analysis	34
5.4	Cepstrum analysis	45
5.5	Time-frequency analysis	46
5.5.1	The short time Fourier transform	46
5.5.2	The Wigner-Ville distribution	49
5.5.3	The continuous wavelet transform	51
5.6	Higher order spectral analysis	54
5.6.1	Definition of bispectrum	54
5.6.2	Determining the existence and strength of quadratic coupling	56
5.6.3	Application to bearing fault detection and diagnosis	61
5.7	Adaptive noise cancellation	66
5.8	The Haar transform	67
5.9	Summary of techniques	68
6.0	BEARING PROGNOSIS	71
7.0	DISCUSSION	72
7.1	Future research program	74
8.0	CONCLUSION	75
	ACKNOWLEDGMENTS	75
	REFERENCES/BIBLIOGRAPHY	76

1.0 Introduction

Vibration analysis has been used as a condition monitoring tool for bearing fault detection and diagnosis, probably ever since the first use of bearings when the symptoms were "something sounds strange". This report reviews some of the important factors which influence the bearing vibration, including different machine types, bearing types and modes of failure. Much has been written about vibration analysis for bearing fault detection over the last twenty five years. An early review can be found in [Houser, et al, 1973], which provides comprehensive discussion on bearings, their rotational frequencies, modes of failures, resonance frequencies and various vibration analysis techniques. The more common techniques which were used at that time included time and frequency domain techniques. These comprised techniques such as RMS, crest factor, probability density functions, correlation functions, band pass filtering prior to analysis, power and cross power spectral density functions, transfer and coherence functions as well as cepstrum analysis, narrow band envelope analysis and shock pulse methods. It is interesting to note that these are the techniques which have continued to be used and have been further developed over the past two decades for bearing fault detection and diagnosis.

Much of the early work on bearing dynamics and vibration analysis was carried out by Mechanical Technology Inc., Latham, New York. They were the first to develop narrow band envelope analysis which was originally called the High Frequency Resonance Technique [Darlow, et al 1974]. Envelope analysis has been the one technique which has stood out above all others for bearing fault detection since that time. It is widely recognised as being the best approach for most rotating machinery bearing diagnosis [Chivers, et al, 1986], even in high noise environments, such as helicopter transmissions.

Comprehensive and complex bearing dynamic models have been developed, for example by P.K. Gupta [Gupta, 1975 - 1990] using the generalised equations of motion for the rolling elements, cage, and raceways. The dynamic models include effects such as roller-race interaction, roller-cage interaction, cage-raceway interaction, lubricant drag and churning, roller skew, cage instabilities, material properties of the bearing components, operating conditions such as speed, load, misalignment and preloads. The more advanced models [Gupta, 1984] are also capable of handling geometrical imperfections such as variations in rolling element size, race curvature, bearing element imbalance and cage geometry, allowing various bearing defects to be simulated.

Bearing fatigue life is determined by a variety of factors including material properties, lubricant properties, speed, load, size and number of rolling elements, etc. Fatigue life prediction theories were originally developed in the 1940's. Since that time, significant improvements have been made in bearing materials and processing in particular, resulting in a dramatic increase in rolling element bearing life and reliability. Much of the research and development work which led to advances in bearing technology was spurred on by the requirements for advanced aircraft gas turbine engines, where there has been an increasing need for bearings with longer life, higher reliability, and higher speed capability.

A large number of vibration signal processing techniques for bearing condition monitoring have been published in the literature across the full range of rotating machinery. Condition monitoring can be divided up into three main areas, detection, diagnosis and prognosis. Detection can often be as simple as determining that a serious change has occurred in the mechanical condition of the machine. Diagnosis in effect determines the location and type of the fault while prognosis involves estimation of the remaining life of the damaged bearing.

The following review commences with an examination of the underlying science of bearing vibration including the modes of failure, how the failure mode influences the bearing dynamics and resulting forces, the transmission of the stresses through the structure, the external noise and vibration environment, the measurement of the vibration and the effect of the class of machine on the diagnostic techniques which need to be used to detect impending failure. Then follows an outline of the kinematic relationships between bearing components and the status of modelling of bearing dynamics, a discussion of bearing life and the major influencing parameters, a summary of the latest advanced signal processing techniques and their application to bearings and a review of the state of the art of bearing prognosis.

2.0 Underlying Science

The underlying science of rolling element bearing vibration which will be examined here from the aspects of detection, diagnosis and prognosis of bearing damage, involves consideration of a number of factors including the mode of failure, kinematics and dynamics, stresses and forces generated at the roller/race interface, transmission path effects, external noise, transducer measurement and the class of machine. Each of these influences will be outlined in some detail.

2.1 Mode of failure

The actual mode of bearing failure which occurs for any particular rotating machine can have a major influence on the resulting vibration which is measured externally. The normal service life of a rolling element bearing rotating under load is determined by material fatigue and wear at the running surfaces. Premature bearing failures can be caused by a large number of factors, the most common of which are fatigue, wear, plastic deformation, corrosion, brinelling, poor lubrication, faulty installation and incorrect design [Stewart, 1983, Eschmann, et al, 1985, Harker, et al, 1989, Sachs, 1992 and Herraty, 1993]. Often there can be overlap between factors for a particular bearing failure or a bearing may start to fail in one particular mode which then leads on to other failure modes.

2.1.1 *Fatigue*

A bearing subject to normal loading will fail due to material fatigue after a certain running time. Fatigue damage begins with the formation of minute cracks below the bearing surface [Tsushima, 1993 and Yoshioka, 1993]. As loading continues, the cracks progress to the surface where they cause material to break loose in the contact areas. The actual failure can manifest itself as pitting, spalling or flaking of the bearing races or rolling elements. If the bearing continues in service, the damage spreads since the localised stresses in the vicinity of the defect are increased. The surface damage severely disturbs the rolling motion of the rolling elements which leads to the generation of short time impacts [Boto, 1971] repeated at the appropriate rolling element defect frequency. As the damage spreads the periodic repetitive nature of the impacts will diminish as the motion of the rolling element becomes so irregular and disturbed that it becomes impossible to distinguish between individual impacts. If the bearing were to continue in service, the damage would spread to the other raceways or rolling elements and eventually lead to increasing friction between the components and cage failure followed thereafter by complete seizure. A large number of references deal specifically with the vibration resulting from localised fatigue failure [Stewart, 1983, McFadden, et al, 1985, Swansson, et al, 1984 and Gore, et al, 1984].

2.1.2 *Wear*

Wear is another common cause of bearing failure. It is caused mainly by dirt and foreign particles entering the bearing through inadequate sealing or due to contaminated lubricant. The abrasive foreign particles roughen the contacting surfaces giving a dull appearance. Severe wear changes the raceway profile and alters the rolling element profile and diameter, increasing the bearing clearance. The rolling friction increases considerably and can lead to high levels of slip and skidding, the end result of which is complete breakdown. A discussion on the effects of general wear on the resulting measured vibration can be found in [Sunnarsjo, 1985]. Increasing wear will gradually introduce geometric errors in the bearing. Non-uniform diameters of worn rolling elements will cause cage frequency vibration and harmonics to be produced [Hine, 1989] as the sequence of balls rotating through the load zone is periodic with the cage rotation frequency. Geometric form errors of the race ways will result in multiple harmonics of shaft speed being produced. This will be compounded if the bearing clearance increases to the extent that looseness of the bearing arrangement occurs.

2.1.3 *Plastic deformation*

Plastic deformation of bearing contacting surfaces can be the result of a bearing subject to excessive loading while stationary or undergoing small movements. The result is indentation of the raceway as the excessive loading causes localised plastic deformation. In operation, the deformed bearing would rotate very unevenly producing excessive vibration and would not be fit for further service. If left to operate, localised fatigue damage would quickly appear.

2.1.4 *Corrosion*

Corrosion damage occurs when water, acids or other contaminants in the oil enter the bearing arrangement. This can be caused by damaged seals, acidic lubricants or condensation which occurs when bearings are suddenly cooled from a higher operating temperature in very humid air. The result is rust on the running surfaces which produces uneven and noisy operation as the rust particles interfere with the lubrication and smooth rolling action of the rolling elements. The rust particles also have an abrasive effect and generate wear. The rust pits also form the initiation sites for subsequent flaking and spalling.

2.1.5 *Brinelling*

Brinelling manifests itself as regularly spaced indentations distributed over the entire raceway circumference, corresponding approximately in shape to the Hertzian contact area. Three possible causes of brinelling are (1) static overloading which leads to plastic deformation of the raceways, (2) when a stationary rolling bearing is subject to vibration and shock loads and (3) when a bearing forms the loop for the passage of electric current. In all cases, the result will be repetitive indentations of the raceways. In some instances, a large number of indentations may occur as the bearing may occasionally be turned slightly. The bearing operation will be noisy and uneven in the presence of brinelling with each indentation acting like a small fatigue site producing sharp impacts with the passage of the rolling elements. Continued operation will lead to the development of spalling at the indentation sites and increasing distributed damage.

2.1.6 *Lubrication*

Inadequate lubrication is one of the common causes of premature bearing failure as it leads to skidding, slip, increased friction, heat generation and sticking. At the highly stressed region of Hertzian contact, when there is insufficient lubricant, the contacting surfaces will weld together, only to be torn apart as the rolling element moves on. The three critical points of bearing lubrication occur at the cage-roller interface, the roller-race interface and the cage-race interface [Keba, 1990]. Lubricant starvation or improper lubricant selection can have severe consequences as the increased temperature can anneal the bearing elements reducing hardness and fatigue life as well as degrading the lubricant. Excessive wear of the bearing elements results, followed by catastrophic failure.

2.1.7 *Faulty installation*

Faulty installation can include such effects as excessive preloading in either radial or axial directions, misalignment, loose fits or damage due to excessive force used in mounting the bearing components. Radial preloading results in noisier running and usually also in increased temperature differences between the inner and outer races. The increased temperature differences are likely to increase the undesirable preloads, causing higher contact pressures leading to premature fatigue, heavy rolling element wear, overheating and eventual seizure. Oval preloading can result from out-of-round shafts or housings, causing deformation of the inner or outer raceways leading to additional radial

preloading. A preload can also be generated by misalignment of the inner and outer races relative to one another causing the rolling elements to run under preload in the apex zones. Such misalignment generates a uniformly wide wear track at the rotating raceway extending over the entire circumference. At the stationary raceway, the track will be of uneven width extending diagonally over the raceway. Excessive axial preload originates from too tight an adjustment in the axial direction during installation. Premature fatigue, heavy rolling element wear and overheating will be the end result. If improper mounting methods are used in the assembly of the bearing in the rotating machine, indentation or scoring damage of the raceways or rolling elements can be caused. Even if the damage is small, it can develop into premature spalling.

2.1.8 Incorrect design

Incorrect design can involve poor choice of bearing type or size for the required operation, or inadequate support by the mating parts. Incorrect bearing selection can result in any number of problems depending on whether it includes low load carrying capability or low speed rating. The end result will be reduced fatigue life and premature failure. Inadequate support can give rise to excessive clearance of the mating parts of the bearing resulting in relative motion such as slippage of the inner race on the shaft. Fretting can occur if the slippage is slight and continuous, generating abrasive metal particles. The looseness will be self perpetuating and will lead to increased friction and temperature resulting in catastrophic failure.

2.1.9 Expected vibration signature

The vibration symptoms of the various modes of failure mentioned above are complex and can be difficult to predict. Apart from the classical localised fatigue of rolling elements or raceways, which has a deterministic repetitive vibration pattern [McFadden, et al, 1985, Swansson, et al, 1984 and Stewart, 1983], the vibration symptoms of the other forms of bearing failure are by no means easy to detect or diagnose in the early stages. Those failure modes which result in asperity-asperity interaction of the contacting bearing components such as lubrication failure, wear or corrosion, will produce impulsive noise and vibration due to the elastic deformation and recovery of the asperities. The frequency of the vibration which is produced is determined by the size of the surface features and the sliding and rolling velocities. The resulting vibration from the asperity interactions will consist of random sequences of small impulses which excite all natural modes of the bearing and supporting structure. The natural frequencies which correlate with mean impulse rise time or mean interval between the impulses will be more strongly excited than the others. General vibration trending is likely to be the only means of detecting the slight change in the vibration in the early stages of these failure modes. As the damage progresses and subsequent localised damage results, the typical fatigue vibration pattern should be produced. However for those instances where no localised damage results, and no significant shaft related vibration is produced, little or no vibration warning may be given before complete seizure occurs. Examples include cage failure and lubrication starvation. In these cases it would be hoped that other forms of condition monitoring such as temperature or oil

debris monitoring would detect the increasing deterioration in bearing condition.

One of the major difficulties in detecting and diagnosing the vibration resulting from various modes of failure is the rapidly changing nature of the vibration signal as the mechanical condition changes. Each new spall which is generated produces a whole family of impacts. As the edges of the spall wear down, so the sharpness of the impacts will decrease, altering the vibration pattern. Each change in the rolling element or raceway geometrical profile can dramatically alter the vibration signal, as can changes in the lubrication condition. These effects would be more pronounced under higher speed and load conditions. For some classes of rotating machinery, these effects can mean that almost continuous monitoring is required to correctly detect and diagnose bearing condition [Coffin, 1986 and Jong, et al, 1991], whilst for other machinery, a short vibration snapshot once a month can accurately diagnose bearing condition [Brown, Appl. Note No. 209-11].

2.2 *Dynamic response to damage*

The dynamic response of the rotating bearing elements as they encounter the various modes of failure determine the resulting vibration [Boto, 1971, Gore, et al, 1984, McFadden, et al, 1985 and Swansson, et al, 1984]. The rolling elements of undamaged loaded rotating bearings undergo complex forces and moments including static forces such as shaft loads and designed preloads, as well as dynamic forces including those due to centrifugal loads, fluid pressure, traction, friction and hysteresis. For a given bearing operating at a constant shaft speed and load, all of the various forces will be in quasi-equilibrium and their sum will be small. When a rolling element encounters a fault, a rapid localised change in the elastic deformation of the elements takes place, and a transient force imbalance occurs.

When a loaded ball encounters a spall, there will be a sudden relaxation of the loading, or, if a ball encounters a high spot or a piece of debris, a sudden increase in loading will occur. The transient forces which are produced will result in rapid accelerations of the bearing components and complex motions can occur including oscillatory contact and impacts between the balls and races, balls and cage, and cage and races as well as skidding or slipping of the balls and cage.

A simple model of the contact action when a ball encounters a spall was first developed by [Boto, 1971] and later clarified by [Swansson, et al, 1984] where it was shown that the energy transferred to the impact point was proportional to the square of the velocity. The resulting acceleration of the impacted bearing race is also proportional to the energy of impact. The dominant factors in the impact action were found to include the defect size, bearing geometry and speed.

Dynamic modelling of the complicated bearing motion when defects are encountered is possible and can include localised changes to the profiles of the raceways and rolling elements [Gupta, 1975-1984]. However, experimental

verification of the results has not been undertaken except for limited examples [Gupta, et al, 1985]. The measurement of the fundamental components of motion such as cage mass centre velocity, cage angular velocity, roller mass centre and angular velocity, etc., is an extremely difficult task and prone to errors because of the general vibration environment in which the measurements have to be made.

2.3 *Force propagation and transmission path effects*

If the forces, stresses and acceleration of bearing components could be measured directly, the task of monitoring the health of the bearing would be quite simple. Unfortunately, for the majority of rotating machinery, external measurement of the machine velocity or acceleration is the only means of vibration measurement which is possible. The internal forces and stresses have to propagate through the structure, being attenuated at each joint and interface, damped by the internal damping of the structure and modified by the frequency response of the system. The short impact duration and sharp rise times of the stress wave front mean that a wide range of natural frequencies and modes can be excited in the structure. The higher frequency stress waves (having smaller amplitudes) are attenuated the most as their transmission depends to a greater extent upon the fitting and accuracy of contacting surfaces and the presence of fluid between joints, than it does for the lower frequency components. These transmission path effects ensure that the vibration which is finally measured by the transducer is a poor replica of the original internal forcing function, particularly for complex paths from source to transducer.

The excitation of a range of natural frequencies and modes by the stress wave provides a convenient method of detecting the transient force imbalance, each time a defect is encountered. If significant damage occurs, the resonances which are excited will increase in amplitude. By demodulating the natural frequencies, the excitation action is recovered, and if the repetition rate can be related to the bearing frequencies then diagnosis of the bearing damage can follow [Bell, 1985]. In this way, the transmission path effect directly helps in the detection and diagnosis phase of bearing condition monitoring, even though by its very nature it hinders the recovery and analysis of the internal forces and stresses.

2.4 *External noise and vibration*

In laboratory situations, bearing test rigs can be run and vibration measured which is almost free from external machinery vibration [Howard, 1989]. However, most industrial rotating machinery will contain components such as gears, pumps, turbines, injectors, etc., which will produce additional noise and vibration. The overall machinery vibration is often of much higher magnitude than the bearing vibration and can dominate the measurements. A good example of this is the High Pressure Oxygen Turbopump on the Space Shuttle Main Engine. As well as the vibration from other machinery components, the transducers mounted externally to the Turbopump are also measuring the vibration from the combustion noise of the engines, acoustic resonances in the fluid and general flow noise [Coffin, et al, 1986].

For bearing fault detection and diagnosis, the influence of external noise and vibration will change the type and nature of the signal processing techniques which are required for effective condition monitoring. For those rotating machines which are relatively free from external influences, simple rudimentary techniques should be just as effective as the more advanced approaches. The key is to recognise, for each machine type, what the nature and influence of external noise and vibration effects will be.

2.5 *Vibration measurement*

A number of transducer types exist for measuring machinery noise and vibration, including proximity probes, velocity transducers, accelerometers, acoustic emission transducers, microphones, and lasers. The measurement of machine casing acceleration is the most common method used for bearing fault detection. This is normally achieved by mounting a piezoelectric accelerometer externally on the machine casing, preferably near or on the bearing housing, or on a portion of the casing where a relatively rigid connection exists between the bearing support and the transducer. This will allow the bearing vibration to transmit readily through the structure to the transducer. Accelerometers have the advantage of providing a wide dynamic range and a wide frequency range for vibration measurement. They have been found to be the most reliable, versatile and accurate vibration transducer available.

Velocity transducers are used for measuring the velocity of the machine casing to which they are attached. They are capable of measuring down to almost DC. Most machines will have a flat velocity frequency response from near DC to 2 kHz. For slow speed rotating machinery, velocity is often used when a vibration velocity magnitude measurement is required. They have not found wide acceptance for bearing fault detection as the wider frequency range available with accelerometers has been found to be better, even for slow speed rotating machinery [Smith, 1982, Teo, 1989 and Mechefske, et al, 1992].

Proximity probes are used for bearing fault detection by mounting directly on the outer race to measure outer race deflection at each ball pass [Kim, 1984, Kim, 1987 and Philips, 1978, Philips, 1982 and Philips, 1989]. A number of probes are used including eddy current, strain gauge and fibre optic transducers. Whilst giving a very clear image of the ball pass deflection of the outer race from which diagnostics such as ball speed ratio can be made, it necessitates modification and installation of the transducer into the bearing housing to provide a clear view of the bearing outer race. Whilst this could be readily achieved in most instances at the manufacturing stage, for a large number of bearings it is not possible after production. This is seen as a severe limitation on its use as opposed to the external mounting of accelerometers.

For non-contacting vibration measurement, lasers and microphones can be used [Smith, 1992]. A number of laser velocity measurement systems are now available where the surface velocity of the machine is measured by the laser using the Doppler shifting principle. Surface acceleration can be derived electronically by differentiation of the velocity signal. Frequency ranges up to

100 kHz have been reported. Comparison of the accelerometer and laser measurements on the same machine at the same time confirmed that they contain essentially the same information for the purposes of bearing fault detection. Microphones measuring the acoustical response of the machine have also been found to be effective in certain instances. The parabolic microphone in particular has been shown to be effective as a remote acoustic monitor of rolling element bearings and has been used effectively on railcar bearing detection and diagnosis [Smith, 1988]. By locating the microphone statically at a distance of approximately 20 feet from the train, the parabolic microphone is capable of eliminating off axis sound and concentrating on the direct sound. As the train rolls past at a fixed speed, the acoustic signatures of defective bearings can be detected. A speed limit was detected below which the technique was found to not work as the audible sound dropped off.

Acoustic emission (AE) transducers [Bannister, 1984, McFadden, 1984, et al, Bannister, 1985, Bagnoli, et al, 1988, Hawman, 1988, Berryman, et al, Czaja, 1990, Li, et al, 1990, Tandon, et al, 1990, Tavakoli, 1991 and Holroyd, 1993] are receiving greater attention for use in bearing condition monitoring. They are designed to detect the very high frequency stress waves which are generated when cracks grow under load and when short time impacts are generated as defects are encountered. The common frequency range for AE transducers is from approximately 50kHz up to 2 MHz. The stress wave activity is inherently transient in nature and each transient burst will propagate from the source out through the machine structure until it is damped through the many reflections and is no longer detectable. Having obtained the AE signal, simple processing procedures are used to detect bearing damage. Because of the high frequency nature of the signal, most of the noise and vibration from other machinery components will not be present. The AE signal can then be enveloped and processed using simple techniques such as threshold counts and level trending.

In practice, the main difficulties in working with AE signals are in calibration and in making repeatable and transferable measurements [Holroyd, 1993]. However, these problems can be overcome with care to provide repeatable periodic as well as continuous measurements. The cost of AE hardware has also started to reduce significantly, and the signs are that AE will play a major role in machine condition monitoring in the future.

2.6 *Effect of class of machine*

A large number of bearing fault detection case studies exist in the published literature. Some questions worth asking are, why is there such a variety of vibration monitoring techniques in use and why do some techniques work in some instances and not in others? One reason for the variability in technique success can be attributed to the effect of machine class. Table 1 illustrates the concept of machine class using some common types of rotating machinery.

Table 1. Degree of difficulty of bearing fault detection as a function of machine class.

Class of Machine	Degree of Difficulty for Bearing Fault Detection	Machine Type
Easiest	1	Fans, Electric Motors, Generators
Slightly Complicated	2	Compressors, Pumps
Complicated	4	Industrial Gearboxes
Difficult	5	Turbines including Gas Turbine Engines
More Difficult	7	Helicopter Transmissions
Most Difficult	10	Specialised Rotating Machinery with Extreme Noise Environments

The easiest machines from the point of view of bearing fault detection are those where the transducers can be mounted directly on the bearing housing and where there is little vibration from other machine components. Examples include fans, electric motors and generators. The next easiest machine class will be those with the same characteristics as the previous except there will be some interference from the vibration of the machine. Examples include pumps and compressors. Although the transducer can be mounted directly on the bearing housing, the measured vibration will be contaminated with components from the machine.

The next class includes industrial gearboxes, where the transducer can no longer be mounted directly on the bearing housing. However, the transmission path from the internal bearings to the casing is relatively straight forward. The general machine vibration environment will be dominated by the gear mesh vibration requiring more complex techniques for bearing fault diagnosis. Bearing fault detection of gas turbine engines is an example of the next more difficult machine class where the transmission path from the internal bearings to the external transducer is complex and will need to occur over a relatively long distance. The vibration environment will be more severe due to the presence of combustion noise.

The next machine class includes machines such as helicopter main rotor gearboxes. The transmission path from the internal bearings to the externally mounted transducer is indirect, and especially so in the case of the moving planetary gears which involve a variable path for the planet bearing vibration as a function of planet carrier rotation. The vibration environment includes a multiplicity of high amplitude gear mesh components which cover the frequency region up to 20 kHz. In this class of machine, none of the simple detection techniques are likely to work, especially for the planetary bearings.

The most difficult machines to monitor will be those where the vibration environment is extreme. Examples include rocket engines, where combustion vibration and related pumping and acoustic resonances completely dominate the vibration. In such instances novel or unusual diagnostic techniques have to be developed to detect bearing failure, often at the later stages of development. By recognising the machine class for each particular application, techniques should be used which are most appropriate for that class. If a simple technique will be effective in providing enough warning of impending failure then it should be used in preference to the more complicated techniques.

3.0 Bearing Kinematics and Dynamics

An understanding of bearing geometry and kinematics is essential for bearing fault detection as it determines the rotational speeds of the bearing elements with respect to each other and the theoretical bearing fault frequencies.

3.1 Bearing kinematics

A number of articles deal with bearing geometry and kinematics including [Palmgren, 1947 and Eschmann, et al, 1985]. Figure 1 shows a schematic of a typical angular contact rolling element bearing in the general case with rotating inner and outer races.

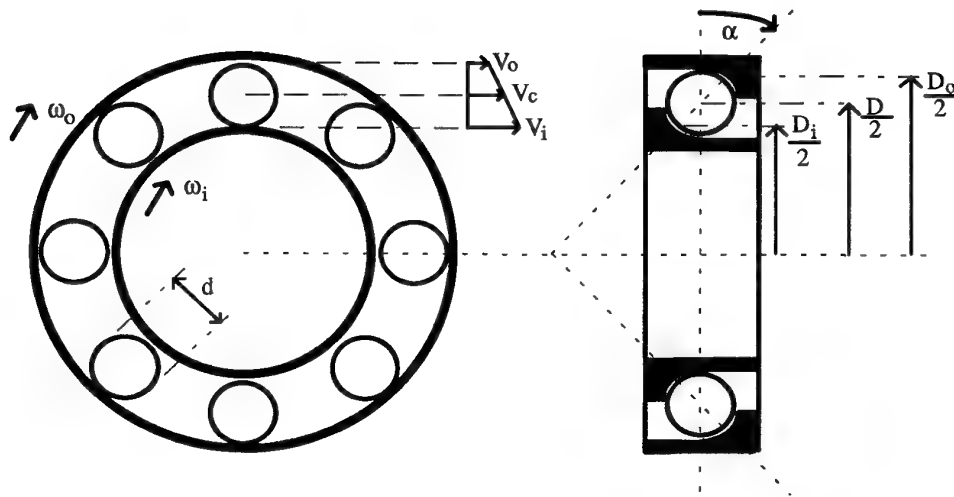


Figure 1. Schematic of a rolling element angular contact bearing.

From the geometry, assuming a constant operating contact angle α , the pitch circle diameter of the bearing D can be approximated by,

$$D = \frac{D_i + D_o}{2}, \quad (1)$$

where D_i is the diameter of the inner ring raceway and D_o is the diameter of the outer ring raceway. The race diameters can be expressed in terms of the pitch circle diameter, contact angle and ball diameter d to give,

$$D_i = D - d \cos(\alpha), \quad (2)$$

and,

$$D_o = D + d \cos(\alpha), \quad (3)$$

The circumferential velocity of the bearing components can be derived in terms of the angular velocity (rad/sec) and radius (m), assuming pure rolling conditions. The inner race circumferential velocity is given by,

$$V_i = \omega \frac{D_i}{2}, \quad (4)$$

the outer race velocity is given by,

$$V_o = \omega \frac{D_o}{2}. \quad (5)$$

The circumferential velocity of the cage, V_c , is the average of the velocity of the inner and outer races assuming no slip occurs,

$$V_c = \frac{V_i + V_o}{2}, \quad (6)$$

which after substitution of equations (2), (3), (4) and (5), becomes,

$$V_c = \frac{\omega(D - d \cos(\alpha))}{4} + \frac{\omega(D + d \cos(\alpha))}{4}. \quad (7)$$

Conversion of the circumferential velocity from m/sec to angular frequency revolutions/sec (Hz) by dividing through by πD and rearranging to give the cage frequency in Hz rather than velocity gives,

$$f_c = \frac{f_i(1 - \frac{d}{D} \cos(\alpha))}{2} + \frac{f_o(1 + \frac{d}{D} \cos(\alpha))}{2}. \quad (8)$$

Equation (8) is the theoretical cage or fundamental train frequency (FTF) for rolling element bearings. Often, one of the raceways will be stationary, the most common being the outer race. In this case, equation 8 can be further simplified to the familiar form,

$$f_c = \frac{f_i(1 - \frac{d}{D} \cos(\alpha))}{2}. \quad (9)$$

The frequency of rotation of the rolling elements with respect to the inner races can likewise be derived by,

$$f_{ri} = f_c - f_i, \quad (10)$$

which by substitution of equation (8) becomes,

$$f_{ri} = \frac{f_o(1 + \frac{d}{D} \cos(\alpha))}{2} - \frac{f_i(1 + \frac{d}{D} \cos(\alpha))}{2}. \quad (11)$$

With Z rolling elements, the expression for the ball pass frequency on the inner race can be found using equation (11) to give,

$$f_{bpf_i} = \frac{Z(f_o - f_i)(1 + \frac{d}{D} \cos(\alpha))}{2} \quad (12)$$

and when the outer race is stationary, this leads to the familiar expression for the ball pass frequency on the inner race,

$$f_{bpf_i} = \frac{-Zf_i(1 + \frac{d}{D} \cos(\alpha))}{2} \quad (13)$$

The frequency of rotation of the rolling elements with respect to the outer race can likewise be derived by,

$$f_{ro} = f_o - f_c, \quad (14)$$

which by substitution of equation (8) gives,

$$f_{ro} = \frac{f_o(1 - \frac{d}{D} \cos(\alpha))}{2} - \frac{f_i(1 - \frac{d}{D} \cos(\alpha))}{2} \quad (15)$$

With Z rolling elements, the expression for the ball pass frequency on the outer race becomes,

$$f_{bpfo} = \frac{Z(f_o - f_i)(1 - \frac{d}{D} \cos(\alpha))}{2} \quad (16)$$

and when the outer race is stationary, this leads to the familiar expression for the ball pass frequency on the outer race,

$$f_{bpfo} = \frac{-Zf_i(1 - \frac{d}{D} \cos(\alpha))}{2} \quad (17)$$

The frequency of rotation of the rolling elements about their own axes of rotation can also be derived. The frequency of rotation assuming no slip, is given by the frequency of rotation of the cage with respect to the inner race multiplied by the diameter ratio of the inner race to the ball diameter,

$$f_{bsf} = f_{ri} * \frac{D_i}{d} \quad (18)$$

This can be rewritten using equations (2) and (11) to give,

$$f_{bsf} = \frac{f_o - f_i}{2} \frac{D}{d} (1 - (\frac{d}{D} \cos(\alpha))^2), \quad (19)$$

which is the general form of the ball spin frequency.

Equations (8), (12), (16) and (19) are the general forms of the bearing defect frequency equations presented in the literature assuming no slip and with both races rotating. In practise, slip will almost always be present, and the theoretical expected frequencies will have to be adjusted in a suitable manner. The derivation as illustrated in Figure 1 has assumed positive rotations to be clockwise and negative rotations to be anticlockwise. Thus, as given in equations (8), (12), (16) and (19), a final negative value will denote anticlockwise rotation of the rolling elements. These bearing equations are summarised in Table 2.

Table 2. Summary of the general bearing defect frequency equations.

Bearing Element	Frequency Equations
Inner Race Defect Frequency	$fbpfi = \frac{Z(f_o - f_i)(1 + \frac{d}{D} \cos(\alpha))}{2}$
Outer Race Defect Frequency	$fbpfo = \frac{Z(f_o - f_i)(1 - \frac{d}{D} \cos(\alpha))}{2}$
Cage Rotational Frequency	$f_c = \frac{f_i(1 - \frac{d}{D} \cos(\alpha))}{2} + \frac{f_o(1 + \frac{d}{D} \cos(\alpha))}{2}$
Ball or Roller Spin Frequency	$fbsf = \frac{f_o - f_i}{2} \frac{D}{d} (1 - (\frac{d}{D} \cos(\alpha))^2)$

3.2 Vibration models of localised defects

The bearing frequency equations provide a theoretical estimate of the frequencies to be expected when various defects occur on the bearing elements, based upon the assumption that an ideal impulse will be generated whenever a bearing element encounters the defect. For localised bearing faults such as spalling and pitting, sharp force impacts will be generated as discussed in section 2.1. These impacts will excite structural resonances and the resulting vibration will be measured by the transducer mounted externally on the machine casing. The measured vibration for each impact will consist of an exponentially damped sinusoidal oscillation each time a localised defect is encountered.

Comprehensive theoretical models of the vibration generation mechanism and the influence of various parameters such as loading and the transmission path have been developed and extended to include single and multiple localised defects [McFadden, et al, 1984, 1985, Su, et al, 1992 and 1993]. The initial model developed by McFadden, [McFadden, 1984], considers the vibration produced as the rolling elements encounter the point defect to consist of a series of impulses representing the transient force imbalance to the machine structure. As the bearing rotates, the impulses occur periodically with a frequency which is dependent on the location of the defect, as given in Table 2. Defects on the inner race of a bearing with a stationary outer race are considered and the model

considers the variations in the load around the bearing using the Stribeck equation assuming the bearing is operating under radial load. The resulting modulation of the impulses with shaft rotation as the defect location rotates in and out of the load zone was considered as well as the modulation due to the variation in transmission path from the impulse location to the transducer as the shaft rotates. By considering the response of a typical structural resonance, the vibration measured from each impulse was assumed to take the form of an exponentially decaying sinusoid. The resulting vibration as measured by the transducer was shown to be a combination of the periodic impulses, modulation due to rotation through the load zone, the variations in amplitude of the transfer function as the defect rotates with the shaft and the exponential decay of the impulses due to internal structural damping. The complete model was experimentally verified for an inner race defect using vibration measured from a bearing test rig which confirmed that for inner race localised defects the predominant features as measured in the vibration consist of shaft frequency harmonics, the inner race defect frequencies, modulated by shaft frequencies, and multiple harmonics thereof.

The model was later extended to include the influence of multiple defects on the inner race [McFadden, 1985] by treating them as the sum of a number of localised defects at different phase angles around the inner race. The influence of multiple defects was explained by the reinforcement and cancellation of spectral lines due to the differing phase angles in the spectra from the individual impulses. The model was validated by experiments on a bearing test rig with two defects on the inner race.

Su, et al [Su, et al, 1992] extended the original work by McFadden to characterise the vibrations measured from bearings subject to various loading conditions and with defects located on any of the bearing components. The main development of the work was the determination of the periodic characteristics of various loading and transmission path effects and their influence on the vibration. These effects are generally associated with the misalignment or dynamic unbalance of the shaft, the axial or radial loading, the preload and manufacturing imperfections. When the shaft rotates, some of these influences maintain their spatial locations around the bearing while others revolve. Where there is relative angular velocity between the defect and the effect then a modulation or periodicity arises.

Table 3 presents the main causes of periodicities and the resulting effect of defects on the various bearing components as listed in [Su, et al, 1992] where f_s represents shaft frequency, f_c represents cage frequency and f_{bsf} represents rolling element spin frequency on its axis.

The table shows that for an outer race defect, with fixed outer race, the periodicity will be a function of the unbalance of the shaft and the diameter errors of the rollers. The eccentric loading due to unbalance rotates at the shaft frequency f_s so that the periodic variation occurs with frequency f_s . A bearing with rolling element diameter variations under preload conditions will be subject to a non-uniform loading distribution which will revolve with the cage assemble. Consequently the periodic variation will occur with frequency f_c .

Table 3. Periodic characteristics of bearings with defects under various loadings and transmission path effects [Su, et al, 1992].

Causes of Periodicities	Outer Race Defects	Inner Race Defects	Rolling Element Defects
Stationary Loading	No Effect	f_s	f_c
Shaft Unbalance	f_s	No Effect	$f_s - f_c$
Rolling Element Diameter Variations	f_c	$f_s - f_c$	No Effect
Transmission Path variations	No Effect	f_s	f_c f_{bsf}

For an inner race defect, the defect will rotate with shaft frequency. For stationary loading, and with the influence of transmission path effects, the resulting variation will be periodic with shaft frequency f_s . For variations in rolling element diameters, since the relative angular frequency between the loading and the defect will be $f_s - f_c$, the resulting variation will be periodic with $f_s - f_c$.

For a roller defect, the defective roller revolves with the cage frequency and the defect contacts the inner and outer race alternately. The relative angular frequencies between the defective roller and the loadings will be f_c for stationary loading and $f_s - f_c$ for shaft unbalance loading. The contact point for the defect will move alternately from the inner race to the outer race at a frequency of $2 \times f_{bsf}$. The influence of the transmission path variations will then occur at f_{bsf} giving rise to the corresponding periodic frequency variations.

For each of the above defects, the prominent defect frequencies will be those as given in Table 2. The periodic frequencies given in Table 3 will cause sidebands to appear about the defect frequencies and multiple harmonics thereof. The possible frequencies which will occur in a rolling element bearing under various loading conditions are summarised in Table 4.

Table 4. Possible spacings of main bearing defect frequencies and sidebands.

Frequency Lines	Outer Race Defect	Inner Race Defect	Rolling Element Defect
Major harmonics of spectral lines	f_{bpfo}	f_{bpfi}	$2 \times f_{bsf}$
Spacing of sidebands	f_s f_c	f_s $f_s - f_c$	f_c $f_s - f_c$ f_{bsf}

For situations with multiple bearing defects, the measured response will be the sum of the induced vibrations from each defect. The phase differences between impulses will either cause cancellation or reinforcement of the bearing defect frequencies.

Having obtained a model to predict the possible bearing frequencies, harmonics and sidebands for the various types of localised fatigue damage, the pattern of expected frequencies can be searched for as part of routine bearing condition monitoring. Further work has shown that the analysis of the magnitude of the defect frequencies relative to each other improves reliability [Su, et al, 1993].

The modelling of bearing failures other than localised spalling has received little attention, although the effect of variations in roller diameters is well understood [Wardle, 1988 and Hine, 1989]. In particular, the effects of lubrication starvation, wear, corrosion, skidding and slippage of the rolling elements and cage failure, upon the measured vibration is relatively unknown. For these areas, dynamic modelling using the generalised equations of motion can provide answers as seen in the next section.

3.3 *Bearing dynamic modelling*

Dynamic modelling of rolling element bearings first commenced over 30 years ago using quasi-static analysis [Hamrock, 1983] before there was a general awareness of elastohydrodynamic lubrication, and coulomb friction was assumed to occur at the race contact. This led to the commonly known "race control" theory which assumed that pure rolling occurred at one of the ball-race contacts with all of the spinning required for dynamic equilibrium of the balls taking place at the other, or "non-controlling" race contact. This analysis proved to be quite effective for predicting fatigue life but less useful for predicting cage slip, which normally occurs at high speeds and light loads. This work was later extended by allowing a frictional resistance to gyroscopic moments at the non controlling as well as the controlling race which was adequate for predicting bearing performance under conditions of dry-film lubrication or whenever an absence of elastohydrodynamic lubrication occurs. Elastohydrodynamic lubrication was introduced into the modelling in the mid 1960's including more precise viscosity-pressure and temperature relationships and traction data for the lubricant, and several computational programs evolved as a result. This work is categorised as quasi-static because it applies only when steady state conditions prevail. However, under transient conditions only a truly dynamic analysis will suffice.

The first attempts at complete dynamic models of rolling element bearings occurred in the mid 1970's [Gupta, 1975], when Gupta solved the generalised differential equations of motion of the ball in an angular contact ball bearing operating under elastohydrodynamic lubrication conditions. The formulation of the equations of motion provided for the inclusion of initial conditions and a complete transient and steady state motion was thus obtained, giving predictions about ball motion, the amount of skid and wear rates, for various ball-race traction characteristics. This work was extended to include cylindrical roller bearing analysis and a more general ball bearing model [Gupta, 1979],

where emphasis was placed upon ball-cage and race-cage interactions and the treatment of drag and churning losses to include a more realistic assessment of the lubrication. A substantial fraction of the bearing torque is due to the cage, and the inclusion of detailed cage analysis was found to be important even for low-speed applications.

The development of comprehensive dynamic simulation models of the performance of bearings greatly increases our understanding of the interactions which influence bearing motion. Bearing misalignment was found to significantly influence the ball-cage and race-cage interactions and hence the stability of cage motion. The increased radial to axial load ratios promote skidding which couples with the lubricant behaviour to impose accelerations on the ball which ultimately influence the ball-cage interaction. The lubricant behaviour and the large load variations on the balls were found to play dominant roles not only in determining the extent of skidding but also in establishing the overall stability of cage motion.

Over time, the models have increased in complexity and elegance as the representations of all forces and moments approach reality [Gupta, 1984]. Although improvements in computational efficiency have been achieved, the degree of computational complexity is a major problem. It usually limits the scope of the bearing simulation to a few shaft revolutions so the problems have to be carefully formulated for analysis. Some dynamic models are readily available for general use, an example of which is ADORE (Advanced Dynamics Of Rolling Elements) [Gupta, 1984], which is a general purpose computer program with extensive documentation on the formulation and operation of the simulation. The capabilities of the program range from a simple equilibrium analysis to highly sophisticated dynamic simulations, where the influence of geometric imperfections of the bearing elements and the transient operating conditions on the overall dynamic performance of the bearing may be investigated. It allows bearing designers, manufacturers, and users to model actual bearing configurations with varying levels of sophistication.

One difficulty with the use of complex dynamic models lies in experimentally verifying the predicted results. Measurements of the important effects such as lubricant drag and churning moments are difficult to make, and achieving the required accuracy is a formidable task. An example of an experimental validation is given in [Gupta, et al, 1985], where the various components of general motion of the cage are measured in an angular contact ball bearing and compared to analytical predictions. Specifically, the general motion of the cage predicted by simulation up to operating limits of 2 million DN is compared with experimental data. Both the computer predictions and experimental data indicate a certain critical shaft speed at which the cage mass centre begins to whirl. The predicted and measured whirl velocities are in good agreement and the axial and radial velocities of the cage mass centre agree within the tolerance band of the expected experimental error. The cage angular velocity was not reliably measured at high speeds due to experimental difficulties. At low speeds, however, there was a fair agreement between the experimental data and the analytical predictions. Another more recent example of analytical and experimental comparison can be found in [Boesiger, et al, 1992] where tests with precision angular-contact ball bearings verified important features such as

friction threshold for stability, cage motion and instability frequency. Cage stability was found to be highly sensitive to cage-ball friction and exhibited a constant characteristic frequency, which was independent of speed, external vibration, radial load, and preload.

Bearing analytical modelling can have significant benefits for machine condition monitoring. In the more advanced models [Gupta, 1984] any arbitrary variation in bearing internal geometry, geometric imperfections and operating conditions can be treated. This can include effects such as misaligned races, race shrink fits with the housing and shafts, and thermal and mechanical distortion of the races, cage and rolling elements. Geometric imperfections such as variations in rolling element size, race curvature variation, bearing element imbalance and cage geometry variation can likewise be included. The dynamic simulation of these imperfections can greatly increase our understanding of the fundamental science of bearing vibration such as the transient forces which arise when imperfections are encountered and the resulting transient dynamics of the bearing elements. The effects of general wear can also be simulated and with inclusion of life prediction correction factors for materials and operating conditions into the dynamic models [Gupta, et al, 1990], an increased level of sophistication in the implementation of fatigue life models can be made. Thus, a much closer link can be made between the three areas of vibration condition monitoring, analytical dynamic modelling and fatigue life for rolling element bearings, which enhances our understanding of rolling element bearings and the vibration generated at the onset of incipient failure.

4.0 Bearing Life

The useful life of rolling element bearings has historically been considered to be limited by the onset of fatigue or spalling of the raceways and rolling elements, assuming that the bearing was properly selected and mounted, effectively lubricated and protected against contaminants. A large number of recent articles have been written on the subject of bearing fatigue life, including [Hamrock, et al, 1983, Zaretsky, 1986 and Anderson, 1990].

4.1 Rolling bearing fatigue life

Fatigue in rolling element bearings is caused by the application of repeated stresses on a finite volume of material. It occurs at the weakest point of the material where on the microscale there is a large dispersion in material strength or resistance to fatigue because of the inhomogeneities in the material. Because bearing materials are complex alloys, they are not homogeneous or equally resistant to failure at all points. As a result, a group of supposedly identical specimens will exhibit wide variations in failure times when operated in the same way. To be able to predict how long a particular bearing will run under a specific load, we must have an accurate, quantitative estimate of the life dispersion or scatter and an estimate of the life at a given survival rate or reliability level.

Fatigue life prediction theories have been around since the 1940's [Anderson, 1990]. The Lundberg-Palmgren theory provided a dramatic step forward in life prediction of rolling element bearings by determining bearing dynamic capacity and fatigue lives. Specific dynamic capacity formulae were developed as a result of analytical and experimental work, based upon statistics. The factors which are important in determining dynamic capacity and fatigue life include, 1) Size of rolling elements, 2) Number of rolling elements per row, 3) Number of rows of rolling elements, 4) Conformity between rolling elements and races, 5) Contact angle under load, 6) Material properties, 7) Lubricant properties, 8) Operating temperature and 9) Operating speed. The first five factors were incorporated in bearing dynamic capacity formulas developed from the Lundberg-Palmgren theory and the remaining factors are taken into account using life adjustment factors. Examples of the specific dynamic capacity formulas can be found in [Hamrock, et al, 1983] for various bearing types.

The Weibull distribution, originally developed in the 1940's, is based upon the theory that fatigue lives of a homogeneous group of rolling element bearings can be related according to the equation [Hamrock, et al, 1983],

$$\ln \ln\left(\frac{1}{S}\right) = e \ln\left(\frac{L}{A}\right), \quad (20)$$

where S is the probability of survival, L is the fatigue life and e and A are constants. The equation results from a statistical theory of strength based on probability theory using the "weakest link" theory. Using equation (20), bearing fatigue lives can be plotted as a straight line on the Weibull plot, (log log vs. log), so that the life at any reliability level can be determined. Of most interest are the L_{10} life ($S = 0.9$) and the L_{50} life ($S = 0.5$) and bearing load ratings are based on the L_{10} life. The L_{10} life is calculated in practice from the load on the bearing and the bearing dynamic capacity or load rating given in manufacturers' catalogues and engineering journals, by using the equation,

$$L = \left[\frac{C}{Fe} \right]^m, \quad (21)$$

where C is the basic dynamic capacity or load rating, Fe is the equivalent bearing load, and m is the load-life exponent which is dependent upon the contact arrangement (3 for elliptical contacts such as ball bearings and 10/3 for rectangular contacts such as rolling element bearings).

Since the development of the Lundberg-Palmgren theory, significant advances have been made in rolling element bearing material quality and in the understanding of the role of lubrication in bearing life through the development of elastohydrodynamic theory. In particular, improvements in bearing materials and processing in the last 30 years have contributed greatly to the large increase in rolling element bearing life and reliability. Some of the more significant milestones, with the approximate year of their introduction, are given in Table 5 [Anderson, 1990].

Table 5. Significant Milestones in bearing Material and Manufacturing technology

Significant Milestones	Year of Introduction	Improvements
Vacuum degassing and vacuum melting	1958	Releases entrapped gasses & reduces quantity of harmful inclusions
Non-destructive testing (eddy current & ultrasonic methods)	1962	Better detection & elimination of material faults
Argon atmosphere protection during teeming	1963	Improved material homogeneity & cleanliness
Recognition of importance of grain flow direction	1963	Improved resistance to fatigue of parallel grain flow
Recognition of importance of hardness differential	1965	Improved fatigue life with optimum hardness differential between rolling elements & races
Vacuum induction melting followed by vacuum arc remelting (VIMVAR)	1971	Further improvements in material homogeneity & cleanliness
M50 Nil material (carburizable M-50)	1984	Improved life & fracture toughness over through hardened M-50

Much of the research and development work which led to advances in bearing technology has been spurred on by the requirements for aircraft turbine engine bearings where there has been an increasing need for bearings with longer life, higher reliability, and higher speed capability.

The improvements in bearing materials, lubrication and manufacturing technology which have occurred since the development of the original Lundberg-Palmgren theory, have led to increases in bearing life by a factor of 100 and large discrepancies between predicted and actual bearing dynamic capacity and fatigue lives. One of the initial means of addressing the problem was to include empirical correction factors to account for various environmental or design factors which were assumed to be multiplicative in their effect on bearing life giving rise to the following life equation,

$$L_A = (\tilde{D})(\tilde{E})(\tilde{F})(\tilde{G})(\tilde{H})L_{10}, \quad (22)$$

where \tilde{D} refers to the materials factor, \tilde{E} refers to the metallurgical processing factor, \tilde{F} refers to the lubrication factor, \tilde{G} refers to the speed effect factors and \tilde{H} refers to the misalignment factor. The new adjusted life equation L_A , is based upon the original L_{10} life, equation (21). Various procedures can be found for calculating the adjustment factors and detailed discussions can be found in the manufacturers' catalogues and engineering journal papers [Hamrock, et al, 1983].

The recognition of some of the shortcomings of the original Lundberg-Palmgren theory and improvements in the understanding of the theory behind bearing life and the influence of advanced fracture mechanics and lubrication, have led to the development of alternative bearing fatigue life theories. Some of the deficiencies in the original theory include the recognition only of sub-surface originated failures, the absence of surface tangential force effects and the inability of the theory to explain variances in bearing life behaviour from the

Weibull distribution in both very low and high probability of failure regimes [Anderson, 1990]. In particular, the theory doesn't recognise a non-zero life at zero probability of failure. Significant improvements in bearing material cleanliness and manufacturing methods have resulted in situations where bearings can have a minimum life, where there may be a minimum or threshold stress level below which fatigue may not occur.

These limitations in the Lundberg-Palmgren theory have provided the impetus for the development of more comprehensive bearing life prediction methodologies such as those mentioned in [Anderson, 1990]. Tallian and co-workers have included into mathematical models many of the features which are missing in the original theory including the effects of material strength, material defect characteristics, surface roughness parameters, lubrication conditions and the effects of sliding and tractive forces in the contact. They initially introduced the concept of competing failure modes by subdividing fatigue failures into spalling fatigue and surface distress, [Tsushima]. The effect on fatigue life of surfaces which deteriorate with bearing running time is treated, where wear and the presence of surface damaging debris in a contaminated lubricant are the major life influencing parameters. Traction and asperity slope effects are included where the effective traction coefficient as a function of film thickness/roughness ratio is estimated from experimentally observed changes.

In the early 1980's, a unified model was developed by Tallian to include a crack growth relationship and defect populations in the contact material and at the contact surfaces. Gupta, [Gupta, et al, 1990], utilised the model to calculate fatigue lives of a range of bearing types at a number of temperatures, loads, and traction coefficients for comparison with the standard ANSI/AFBMA fatigue life calculation. Ioannides and Harris also extended the original Lundberg-Palmgren theory based upon an elemental calculation of the risk of fatigue and the use of a material fatigue limit below which fatigue will not occur. In the work by Tallian and Ioannides and Harris, much better agreement was obtained between field experience and theory of fatigue lives for a range of bearings including those under high speed conditions such as in aircraft turbine engines, as compared to the original Lundberg-Palmgren theory.

The utility and effectiveness of these theories in producing better life estimates depends in part on the quality of inputs to the calculation scheme. The theories present the mechanics for inputting variables but not for calculating their values. These must be determined in detailed investigations. A key element in the use of these theories is whether or not the input variables such as fatigue limit are invariant or whether they change with time or are application-dependent. If they are application-dependent, every use of the theory would require auxiliary investigations to determine their value, and the ease of use of the theory would be seriously impaired.

Doubt has been cast on the suitability of using through hardened alloys such as VIMVAR M-50 for extremely high speed applications such as advanced transmission and engine applications, [Anderson, 1990]. At speeds approaching 3 million DN, cracks originating at inner race spalls have been found to propagate through the inner ring resulting in catastrophic failure. Changing to a

high quality carburizable alloy, such as case carburized CBS 1000M, was found to eliminate the problem.

Recent work enhancing the speed capability of tapered rolling element bearings in particular has included 1) Optimisation of roller and cone angles and roller size for minimum heat generation and cone rib stresses, 2) Crowning of rollers to eliminate end stresses under less than perfect alignment, 3) Shaping of roller ends and cone rib guide flanges, together with super finishes to improve elastohydrodynamic conditions and eliminate surface peeling, 4) Analysis of cage designs to minimise cage stresses, 5) Use of advanced case-carburized materials such as CBS 1000M for improved life and reliability at ultra high speeds and 6) Use of under-race lubrication and cooling, together with cup cooling for effective internal lubrication, and bearing clearance and temperature management.

4.2 Rolling element bearing lubrication

In rolling element bearing application, the lubricant can have a marked effect on bearing life and load capacity [Hamrock, et al, 1983, Zaretsky, 1986, and Anderson, 1990]. The required points of lubricant in a bearing are the cage-rolling element interface, the cage-race interface and the race-rolling element interface. Improper lubricant selection or lubricant starvation at these interfaces will quicken the process of bearing failure, particularly for higher temperature applications. A lubricant fulfils four main functions for bearing operation, 1) Provide a separating film between rolling and sliding contacting surfaces thus preventing wear, 2) Act as a coolant to maintain proper bearing temperature, 3) Prevent the bearing from being contaminated by dirt and other contaminants and 4) Prevent corrosion of bearing surfaces.

A number of lubrication regimes can be identified depending on the type and thickness of the intervening film. The well known Stribeck-Hersey curve can be used to distinguish four lubrication zones depending on the coefficient of friction and a parameter ZN/P , where Z is the viscosity of the fluid, N is the velocity and P is the load as discussed at length in [Zaretsky, 1986]. As the parameter ZN/P increases, so the film thickness between surfaces increases and four lubrication zones can be identified, boundary, mixed, elastohydrodynamic and hydrodynamic. At high values of ZN/P , which occur at high speeds, low loads, and at high viscosity, the surfaces are completely separated by a thick ($>0.25 \mu\text{m}$) lubricant film corresponding to hydrodynamic lubrication where friction is determined by the rheology of the lubricant. For higher load situations where elastic deformation of the surfaces occurs, elastohydrodynamic lubrication can be identified. The film thickness can range from 0.025 to $2.5 \mu\text{m}$. As the film thickness becomes thinner, surface interactions start to occur. This regime of increasing friction, which combines asperity interactions and fluid film effects, is referred to as the mixed lubrication regime.

Finally, at low values of the ZN/P parameter, boundary lubrication occurs which is characterised by the following, 1) Complex interactions including metallurgy, surface topography, physical and chemical absorption, corrosion, catalysis and reaction kinetics, 2) Formation of protective surface films to

minimise wear and surface damage, 3) Surface film formation dependent upon chemistry of the film-forming agent, as well as the surface of the solid and other environmental factors, and 4) The effectiveness of the films in minimising wear, as determined by their physical properties, which include shear strength, thickness, surface adhesion, film cohesion, melting point or decomposition temperature, and solubility [Zaretsky, 1986].

Rolling element bearings are designed to operate in the elastohydrodynamic region. For operation at higher speeds, lubrication, cooling and optimisation of lubrication design to minimise centrifugal effects becomes increasingly important. Centrifugal effects in particular make conventional jet lubrication techniques less and less effective as DN values increase and it becomes more and more difficult to provide lubricant to the critical interior contacts which require both lubrication and cooling. This has led to the design of under-race lubrication systems [Anderson, 1990] where oil is pumped radially outwards through slots in the inner ring. The centrifugal effects then fling the oil outwards to cover the cage, rolling element and outer race contact points. For sustained bearing operation at conditions approaching 3 million DN, under-race lubrication systems are particularly effective at maintaining the required lubrication.

Lubrication plays a critical role in rolling element bearings as far as their operation and fatigue lives are concerned. One of the major modes of bearing failure is due to lubrication problems including lubricant starvation or degraded lubrication. A proper understanding of lubrication is required for dynamic modelling of rolling element bearings including the effects of churning, drag and traction forces as seen in section 3.3. The influence of lubrication problems on the vibration generated in bearings is still unclear.

4.3 *Summary of bearing life*

Bearing life is central to bearing vibration condition monitoring. For most classes of rotating machinery, the ability to detect and diagnose the presence of a damaged bearing is not sufficient. Of more importance is the extent of the damage and the effect upon bearing life. Will the machine operate until the next scheduled maintenance without failure or is failure imminent? This will depend not only on the mode of failure, but on the class of machine, lubrication conditions and type of bearing material used in the bearing. Prognosis of bearing damage, that is how much bearing life is left, can thus be seen to be a complex variation of a number of parameters and will be discussed in more detail in section 7.

5.0 *Signal Processing Techniques*

Signal processing techniques for bearing fault detection and diagnosis by vibration analysis have been used for many years and a review of published

literature indicates the enormous number of techniques which are available. This section details those techniques which can be used on vibration signals from standard accelerometer-type transducers where an analogue voltage-time signal is available for measurement and processing (section 2.5). This excludes techniques such as shock pulse or spike energy, where dedicated hardware is used to provide an automatic diagnosis of bearing condition. Further information on these techniques can be found in the literature [Andersson, Swansson, 1984 and Shea, 1992].

5.1 Time domain techniques

One of the simpler detection and diagnosis approaches is to analyse the measured vibration signal in the time domain. Whilst this can be as simple as visually looking at the vibration signal, other more sophisticated approaches can be used [Dyer, et al, 1978, Swansson, et al, 1984, Alfredson, et al, 1985, Bannister, 1985, Lai, 1990, Khan, 1991, Martin, et al, 1992 and Li, et al, 1992], such as trending time domain statistical parameters. A number of statistical parameters can be defined such as RMS, peak, crest factor, kurtosis [Dyer, et al, 1978, Lai, 1990 and Khan, 1991], clearance factor, impulse factor, shape factor [Li, et al, 1992] and beta moments based upon the beta distribution [Martin, et al, 1992].

The simplest technique of visually looking at portions of the time waveform should not be discounted too lightly, as an enormous amount of information can be obtained in this manner such as the presence of amplitude modulation, shaft frequency components, shaft unbalance, transients and higher frequency components. This is illustrated in Figure 2 which shows 0.1 seconds of acceleration data measured from a gear test rig containing an implanted inner race bearing defect where the sampling frequency was 100 kHz.

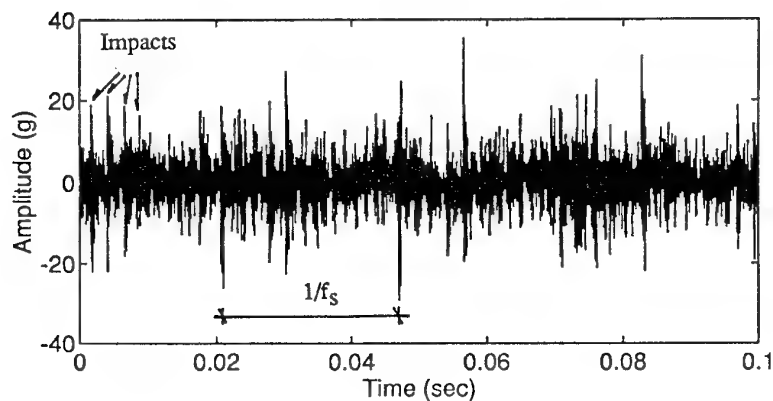


Figure 2. Vibration data from a gear test rig with an implanted inner race bearing defect.

From the visual image of the vibration, repetitive impacts can be observed corresponding to the rotation of the rolling elements past the race damage and the general impression of modulation occurring at the time period corresponding to every shaft revolution of the inner race $1/f_s$ is apparent. The high frequency transient nature of some components of the vibration signal can be seen by zooming in on the first 10 msec of the data as shown in Figure 3.

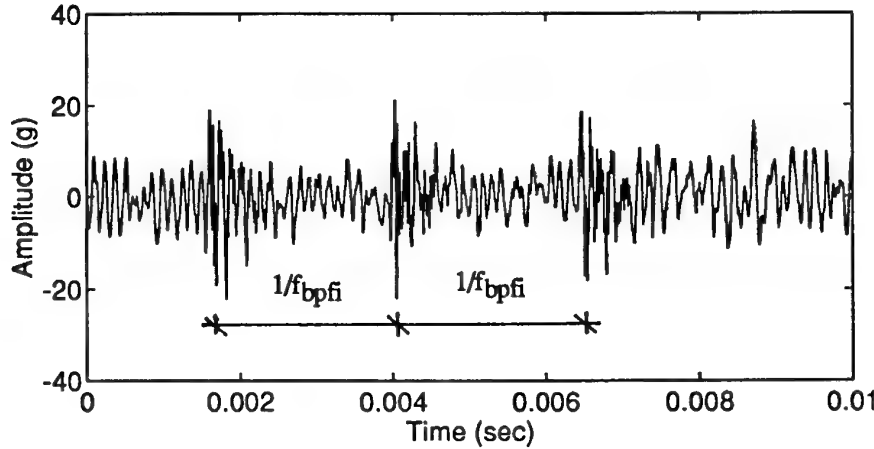


Figure 3. Short segment of vibration data showing inner race impacts.

The short segment of the vibration data contains three impacts which are spaced at intervals of the ball pass frequency on the inner race, $1/f_{bpfi}$. Each impact excites the resonances of the structure which gradually decay due to damping which is present in the system. Often a quick glance at the time waveform can indicate the presence of repetitive impacts and by linking the recurrent timing of the impacts to the frequency of a rotating component, the diagnosis of a bearing fault is achieved.

Time domain statistical parameters have been used as one-off and trend parameters in an attempt to detect the presence of incipient bearing damage. The most common statistical parameters are the peak, RMS, crest factor and kurtosis which can be defined for a discrete signal as,

$$peak = \frac{1}{2}(\max(x(t)) - \min(x(t))), \quad (23)$$

$$RMS = \sqrt{\frac{1}{N} \sum_{i=1}^N (x(i) - \bar{x})^2}, \quad (24)$$

$$CrestFactor = \frac{peak}{RMS}, \quad (25)$$

and

$$Kurtosis = \frac{\frac{1}{N} \sum_{i=1}^N (x(i) - \bar{x})^4}{RMS^4}, \quad (26)$$

where \bar{x} denotes the mean value of the discrete time signal $x(t)$ having N data points. Two approaches may be used for time domain statistics. The first is to compute the statistical parameters for the whole frequency range of the signal as digitised, and the second is to break the signal up into discrete frequency bands and obtain the parameters for each band [Dyer, et al, 1978]. A large number of studies have been undertaken to investigate the use of these parameters for detection of bearing damage and for trending to determine their behaviour as bearing damage increases [Dyer, et al, 1978, Swansson, et al, 1984, Lai, 1990 and Khan, 1991] as discussed in more detail in section 7. For vibration data measured from undamaged bearings, the levels of kurtosis and crest factor are approximately 3.0 and 3.5 respectively where the vibration data is relatively random. For the vibration data with the inner race bearing defect shown in Figure 3, the kurtosis was 4.57 and the crest factor was 6.53.

An illustration of the variation of time domain statistics with frequency band is shown in Figure 4, where the original vibration signal shown in Figure 2 (sampling frequency 100 kHz) is band pass filtered in the region of 20-40 kHz.

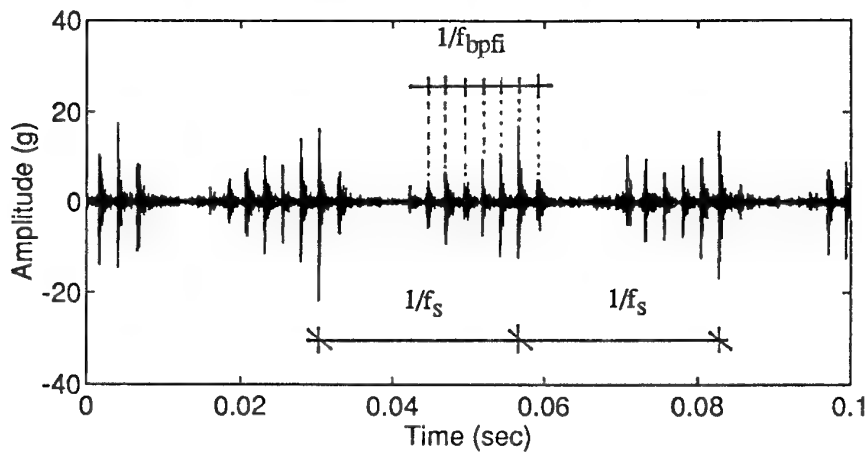


Figure 4. Gear test rig vibration data bandpass filtered from 20-40 kHz.

The visual impression from figure 4 reveals the presence of repeated transient impacts from the inner race damage, modulated at the shaft frequency. The highly transient nature is also revealed by the time domain statistics where the kurtosis rises to 25.3 and the crest factor increases to 10.3.

A recent study was undertaken by [Khan, 1991] where a number of rolling element bearing endurance tests were completed and the various parameters monitored throughout the bearing life. RMS and peak values of vibration cannot be used for single snap shot detection of bearing damage as the expected values for machinery vibration generally exhibit wide variability, whereas crest factor

and kurtosis are independent of the actual magnitude of the vibration level and respond more to the spikiness of the vibration signal. As such they provide early indication that significant changes have occurred in the vibration signal such as that which occurs during the early stages of bearing damage where impulsiveness becomes prominent in the vibration signal. One of the difficulties with crest factor and kurtosis is in their response to increasing damage. As the damage increases, the vibration pattern becomes more random, and as a consequence, the values of crest factor and kurtosis reduce to the undamaged levels, even in the various frequency bands.

A number of frequency bands can be chosen for computation and trending of the statistical parameters. Various investigators have used different numbers of bands with differing frequency ranges which seem to have been chosen arbitrarily. Khan [Khan, 1991] recommended the use of at least two frequency bands, one in the base band where it will be dominated by the defect frequencies, low order harmonics and sidebands (say below 5 kHz), and one in the pass band where it will be dominated by structural resonances (say 5-12.5kHz). The actual frequencies chosen will depend upon shaft rotational frequency and the structural resonances of the system. Table 6 shows typical values of time domain statistics from gear test rig data in four frequency bands, 0-40 kHz, 0-10 kHz, 10-20 kHz and 20-40 kHz. The frequency bands were chosen after analysis of the frequency content of the vibration measured from the gear casing. The frequency range 0-10 khz was dominated by the gear mesh harmonics, the range 10-20 kHz contained some gear mesh harmonics and a definite resonance structure and the range 20-40 kHz was dominated by structural resonances. The data was analysed with the bearings in the new condition and with an implanted inner race defect, and the statistical parameters are shown.

Table 6. Time domain statistical parameters in various frequency bands.

Frequency Band	Peak (g)	RMS (g)	Crest Factor	Kurtosis
New Bearing				
(0 - 40 kHz)	24.0	5.49	4.38	3.75
(0 - 10 kHz)	23.5	5.39	4.36	3.76
(10 - 20 khz)	3.63	0.92	3.92	3.27
(20 - 40 kHz)	2.08	0.48	4.33	3.48
Damaged Bearing				
(0 - 40 kHz)	35.3	5.4	6.53	4.57
(0 - 10 kHz)	23.03	4.87	4.73	3.64
(10 - 20 kHz)	10.61	1.52	6.94	7.42
(20 - 40 kHz)	17.42	1.69	10.33	25.36

The results shown in Table 6 indicate the effect different frequency bands have upon the various parameters in the presence of background noise such as gear mesh vibration. Although the results are from implanted defects which should not be taken as typical of naturally occurring race spalling, they illustrate the point that often frequency bands can be found which give rise to significant increases in various statistical parameters in the presence of bearing damage. Some work has been done to relate the influence of the parameters in various frequency bands as bearing damage increases. This will be treated in more detail in section 7.

The amplitude characteristics of a vibration signal $x(t)$ as detailed above, can also be expressed using the probability density distribution [Dyer, et al, 1978 and Randall, 1987]. The probability density of a signal can be estimated by determining the time duration for which a signal remains in a set of amplitude windows. For a typical window at amplitude x and of width Δx , the instantaneous probability $P(x)$ is defined as,

$$P(x \leq x(t) \leq x + \Delta x) = \sum_{i=1}^N \frac{\Delta t_i}{T}. \quad (27)$$

As the time domain statistics change with the nature of the vibration signal, so too does the probability density function. To illustrate the typical changes which can occur, Figure 5 shows the normalised probability density function for the band pass filtered time acceleration signal measured from the gear test rig with the implanted inner race fault shown in Figure 4, along the with corresponding band pass filtered signal for the undamaged bearing. The statistics for the two signals are given in Table 6.

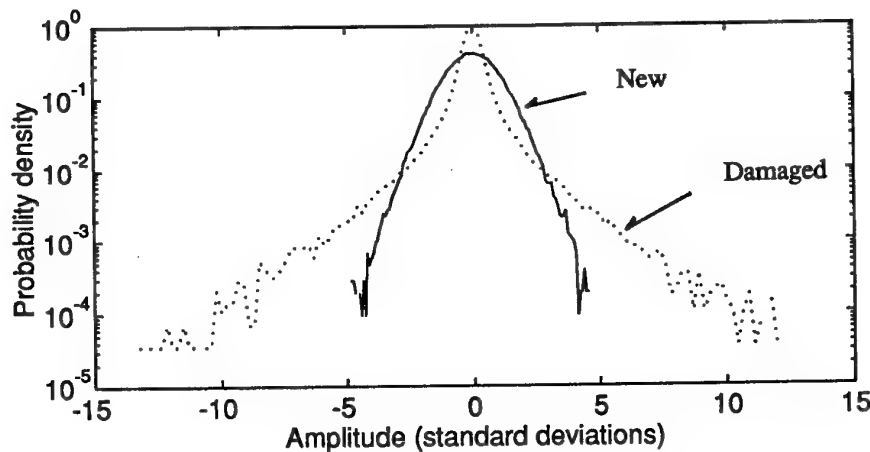


Figure 5. Normalised probability density function for a new and damaged bearing.

A large change can be observed in the probability density function from the undamaged bearing to the damaged bearing case, as denoted by the changes in the time domain statistics. For impulsive signals such as shown in Figure 4, the signal will spend a greater portion of time having a higher amplitude as shown by the increase in the tails of the probability function, over and above those obtained for non-impulsive signals. The changes in the characteristics of the probability density function can be enhanced by taking the integral of the density curve to obtain the probability of exceedence [Dyer, et al, 1978]. As the impulsiveness in the signal increases, due to incipient bearing damage, so too does the probability of exceedence above a certain threshold (say $3 \times$ standard deviation), which can be used as a trend parameter.

The success from computation and trending of time domain statistical parameters will depend to a large extent upon the mode of failure which is occurring, and the class of machine or vibration environment. This will be particularly so for measurement of the peak vibration level. If a certain mode of failure influences a narrow frequency band, then the overall peak amplitude will not be affected until the amplitude in the frequency band becomes the largest overall component, [Randall, 1985]. This can be alleviated by using a number of frequency bands to capture the initial increase in amplitude for each frequency band as shown in Table 6.

Other time domain parameters may be defined such as the clearance factor, impulse factor and shape factor, as developed by [Li, et al, 1992] and written in discrete form as,

$$ClearanceFactor = \frac{peak}{\frac{1}{N} \left(\sum_{i=1}^N \sqrt{|x(i)|} \right)^2}, \quad (28)$$

$$ImpulseFactor = \frac{peak}{\frac{1}{N} \sum_{i=1}^N |x(i)|}, \quad (29)$$

and

$$ShapeFactor = \frac{RMS}{\frac{1}{N} \sum_{i=1}^N |x(i)|}. \quad (30)$$

These three non-dimensional vibration amplitude parameters were found to be useful under simulation conditions using a Gaussian probability density function model of fatigue spalling. The Clearance and Impulse factors were the most useful with the Clearance factor being the most sensitive and generally robust for detection of incipient fatigue spalling.

Statistical moments can also be defined using the beta distribution [Martin, et al, 1992], where the probability density function is defined as,

$$p(x) = \frac{1}{B(b-a)^{\alpha+\beta-1}} (x-a)^{\alpha-1} (b-x)^{\beta-1}, \quad (31)$$

where $a < x < b$. For signal analysis purposes, a and b represent the minimum and maximum amplitudes in the time domain. The shape of the beta distribution is determined by the first two moments, which are also used to define the parameters α and β in equation (31). The higher moments are computed from the values α and β recursively. The moments based upon the beta distribution are claimed to have reduced sensitivity to noise than those based upon the Gaussian distribution and the preliminary results shown in [Martin, et al, 1992] look promising.

5.2 Frequency domain techniques

A number of publications deal with frequency domain techniques for rolling element bearing detection and diagnosis [Eshleman, 1980, Taylor, 1980, McFadden, et al, 1984, Alfredson, 1985, Randall, 1985, Hine, 1989, Mathew, 1989, Khan, 1991, Mechefske, et al, 1991, Serridge, 1991, Su, et al, 1992 and Su, et al, 1993]. A detailed presentation of the fundamentals of frequency analysis can be found in the book "*Frequency Analysis*", by Bruel and Kjaer [Randall, 1987], as well as in a number of digital signal processing texts, eg [Oppenheim, et al, 1975].

It is usual to refer to the power spectrum when investigating vibration data in the frequency domain. If a discrete time signal $x(t)$ represents a sampled periodic function with period T , the Fourier series expansion of $x(t)$ can be obtained from the Fourier integral,

$$X(f) = \frac{1}{T} \int_{-T/2}^{T/2} x(t) e^{-j2\pi ft} dt, \quad (32)$$

where f represents discrete equally spaced frequencies being multiples of the reciprocal of the period T . The power spectrum $P(f)$ can be defined as the magnitude or power obtained from the Fourier integral and can be estimated by,

$$P(f) = E[X(f)X^*(f)], \quad (33)$$

where $*$ represents complex conjugation and $E[\]$ represents the expected value. The FFT (Fast Fourier Transform) provides a fast and convenient means of computing the discrete Fourier transform of vibration data and a window function can be used to force the vibration data to appear periodic, which reduces leakage from one frequency component to another. A smooth estimate of the power spectrum computed from stationary random data can be obtained by averaging the spectrum obtained with equation (33) over a number of windowed data records and is often referred to as the Welch method of power spectrum estimation.

The FFT does not provide the only means of estimating the power spectrum of a discrete time signal. A large number of alternative spectral estimation procedures have been developed recently to overcome some of the inherent limitations of the FFT approach [Kay, et al, 1981] some of which are called, the maximum likelihood method, the auto regressive (AR) estimation technique and the moving average (MA) technique. Although these alternative approaches have largely been ignored by machine condition monitoring investigators, it is likely that they will become increasing popular, as has occurred with other areas of signal processing [Mechefske, et al, 1991].

An example of a power spectrum computed using the Welch method from vibration data measured from a gear test rig can be found in Figure 6.

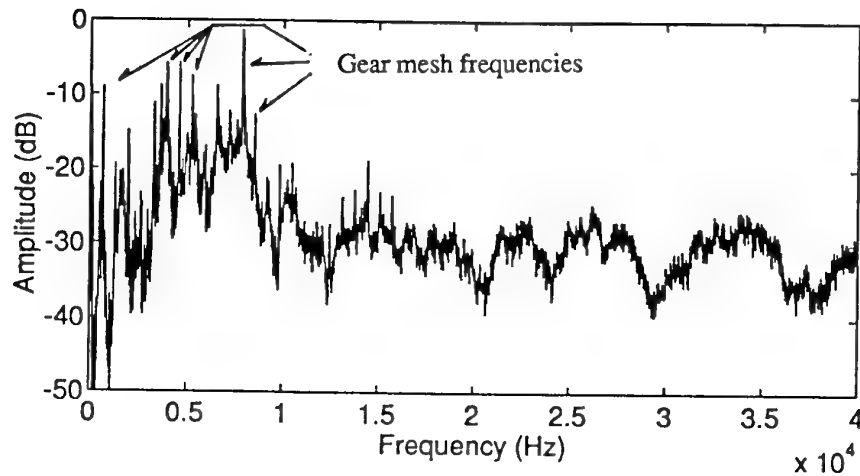


Figure 6. Power spectrum estimate from gear rig vibration data.

One of the main purposes in computing power spectra of vibration data is to identify the major frequency components which can be found in the spectrum and then use these components and their amplitudes for trending purposes. For bearing fault detection and diagnosis, a detailed knowledge of the bearing defect frequencies which can occur is required. As discussed in sections 2 and 3, a large number of bearing defect frequencies can possibly arise depending upon the actual mode of failure, the class of machine and the vibration environment [Eshleman, 1980, Taylor, 1980, McFadden, et al, 1984, Alfredson, 1985, Randall, 1985, Hine, 1989, Mathew, 1989, Khan, 1991, Mechefske, et al, 1991, Serridge, 1991, Su, et al, 1992 and Su, et al, 1993]. For classical localised race damage, (fatigue spalling) the major frequencies of interest which can arise are listed in Table 4. For other modes of failure such as lubrication starvation, contamination, misalignment, general wear, etc., the relevant frequencies which can occur are not readily apparent or understood or necessarily static in time. This makes detection and diagnosis of bearing damage using frequency analysis difficult for all but the straight forward cases of fatigue spalling.

Where the primary mode of bearing failure is localised fatigue spalling, both manual and automatic identification of bearing defect frequencies can be used. Manual identification involves human interaction using a digital signal analyser or equivalent, to manually search the spectrum for defect frequencies, harmonics or sidebands as listed in Table 4. For complex rotating machinery with a number of gears, shafts and bearings, the number of frequencies which must be included quickly becomes unwieldy and time consuming, and often automatic means of frequency identification are used. Automatic identification involves the searching of the spectrum for specific frequencies related to all relevant components and can include harmonics and sidebands of any of the defect frequencies. Its success will depend on the accuracy to which factors like speed variations, bearing slip and bearing geometry can be approximated, and other relevant influences such as the complexity of the spectrum, frequency resolution and preprocessing operations carried out on the spectrum to eliminate noise.

Rather than use frequency analysis primarily for diagnosis, one of its better uses is for detecting that something has occurred which may or may not point to a change in the mechanical condition of the machine. This is illustrated by references [Randall, 1985 and Serridge, 1991] dealing with spectrum comparison and trending techniques where a baseline spectrum is taken when the bearings are in good condition and the difference between the baseline and subsequent spectrum is used to highlight changes in mechanical condition. For bearing faults, often the changes will become apparent in the higher frequency ranges coinciding with increases in the amplitudes of structural resonances although this will be dependent upon the mode of failure and the vibration environment.

Spectrum comparison can readily be achieved semi-automatically and it has been suggested that increases of 6-8 dB are to be seen as significant, while changes of 20 dB are to be considered serious [Randall, 1985]. Trending of vibration data using spectrum comparison should be performed on a logarithmic amplitude scale (or dB) as equal changes on a logarithmic axis are equally serious. One of the difficulties with spectrum comparison is caused by small fluctuations in rotating speeds. Very small changes in shaft speeds can shift the position of peaks at different line numbers and/or within one bandwidth resulting in large amplitude differences and therefore false warnings. These problems can be overcome with the use of a logarithmic frequency axis (with constant percentage bandwidth) [Bruehl & Kjaer, 1990 and Serridge, 1991].

Constant percentage bandwidth spectra provide a means of compensating for speed fluctuations using a logarithmic frequency axis where a lateral shift in the frequency axis eliminates the effect of vibration components falling on different line numbers. A constant percentage bandwidth of 4 - 6 % can be used to give amplitude stability across a broad frequency range followed by spectrum comparison to give indications of changes in mechanical condition [Randall, 1993].

Trending of vibration spectra has been investigated by a number of people [Alfredson, et al, 1985, Randall, 1985, Mathew, 1989, Khan, 1991, Mechefske, et al, 1991 and Succi, 1991] and a number of spectral parameters can be defined for trending, or simple spectral amplitudes of significant components can be trended. Some of the more common spectral parameters are found in reference [Mechefske, et al, 1991], two of which are the matched filter root mean square (*Mfrms*) and the RMS of the spectral difference (*Rdo*), defined as,

$$Mfrms = 10 \log \left\{ \frac{1}{N} \sum_{i=1}^N \left(\frac{A_i}{A_i(ref)} \right)^2 \right\}, \quad (34)$$

and

$$Rdo = \left\{ \frac{1}{N} \sum_{i=1}^N (L_{ci} - L_{oi})^2 \right\}^{1/2}. \quad (35)$$

Mfrms is a direct comparison of spectral responses where *A_i(ref)* is the amplitude of the *i*th spectral line in the reference spectrum and *A_i* is the amplitude of the *i*th spectral line in the current spectrum. The RMS of the spectral difference, *Rdo*, involves finding the RMS of the difference between two spectra when the

amplitude of the spectral responses are given logarithmically where L_{ci} is the level (dB) of the current i th spectral line and L_{ri} is the level (dB) of the i th spectral line of the reference spectrum.

The success of spectral trending will be discussed in more detail in section 7.0. Suffice it to say that spectra can be very complex, especially when there are many defect-related harmonics and sidebands present, and rather than use parameters as given above, a problem exists in deciding which components or frequency bands to trend on [Khan, 1991] particularly for complex rotating machinery.

A further avenue for frequency domain analysis for bearing fault detection and diagnosis is to use so called waterfall or isoplot of spectra. This has been found to be particularly effective especially in severe noise environments [Coffin, et al, 1986 and Howard, 1993]. Various forms of display exist for visually representing the waterfall or isoplot. The traditional waterfall plot shows a three dimensional time-frequency plot with a number of frequency spectra at different times throughout the life of the mechanical component being shown, a typical example of which can be found in [Alfredson, et al, 1985]. A further means of displaying the time-frequency representation is as a two dimensional figure where the third dimension (amplitude) is shown as a colour variation and has proven to be a powerful means of indicating changes in mechanical condition particularly for situations with changing shaft speeds. The actual manner of visually displaying the time-frequency representation is normally very important and can greatly influence the amount of knowledge which can be gained about the vibration signal.

5.3 *Envelope analysis*

Envelope analysis has become one of the prominent vibration signal processing techniques for detection and diagnosis of rolling element bearing incipient failure. It was developed in the early 1970's by Mechanical Technology Inc. [Darlow, et al, 1974] and was originally called the high frequency resonance technique [McFadden, et al, 1984, Prashad, et al, 1984]. It has been known by a number of other names including amplitude demodulation [White, 1991 and Randall, 1987], demodulated resonance analysis, narrow band envelope analysis or just envelope analysis [Stewart, 1983, Bell, 1984, Courrech, 1985, Chivers, et al, 1986, Ratcliffe, 1990, Kim, et al, 1988, McMahon, 1991 and Mundin, et al, 1992], which now seems to be the more popular designation.

Fundamental to envelope analysis [McFadden, et al, 1984] is the concept that each time a localised defect in a rolling element bearing makes contact under load with another surface in the bearing, an impulse of vibration is generated as discussed in sections 2.1 and 2.2. The impulse will have an extremely short duration compared to the interval between impulses, and so its energy will be distributed across a very wide frequency range. The result is that various resonances of the bearing and the surrounding structure will be excited by the impacts. The excitation will normally be repetitive because the contacts between the defect and the mating surfaces in the bearing are essentially periodic. The frequency of occurrence of the impulses are referred to as the characteristic

bearing defect frequencies as shown in Tables 2, 3 and 4. It is usual to consider the resonance as being amplitude modulated at the characteristic defect frequency which makes it possible not only to detect the presence of a defect by the excitation of the resonance but also to diagnose the component of the bearing the defect is in. Envelope analysis provides a mechanism for extracting out the periodic excitation or amplitude modulation of the resonance.

The classical method of computing the narrow band envelope is to use analogue circuitry to bandpass filter the analogue vibration signal around a structural resonance and then to use full or half wave rectification followed by a smoothing circuit to recover the approximate envelope signal. A substantial review of analogue enveloping techniques can be found in [McFadden, et al, 1984] and a number of analogue enveloping "black boxes" are readily available on the market. Figure 7 shows the substantial steps involved in the analogue envelope process, [Bell, 1985].

One of the on-going difficulties with envelope analysis is how to determine the best frequency band to envelope. The majority of analogue enveloping devices on the market have a number of fixed frequency ranges which can be used. The fixed frequency bands may or may not encompass structural resonances which are excited by the bearing damage. As mentioned in section 5.2, spectrum comparison techniques, such as trending constant percentage bandwidth spectra, can be used to determine those frequency bands which have significantly increased (6 dB say) in amplitude, and are potential candidates for envelope analysis. For complex rotational machinery such as helicopter gearboxes, these frequency bands can be interspersed between some of the higher gear mesh harmonics. For envelope analysis to work effectively in these situations precise specification of the frequency band for filtering will be required, as well as sharp filters. Unfortunately, analogue enveloping does not readily meet either of these requirements.

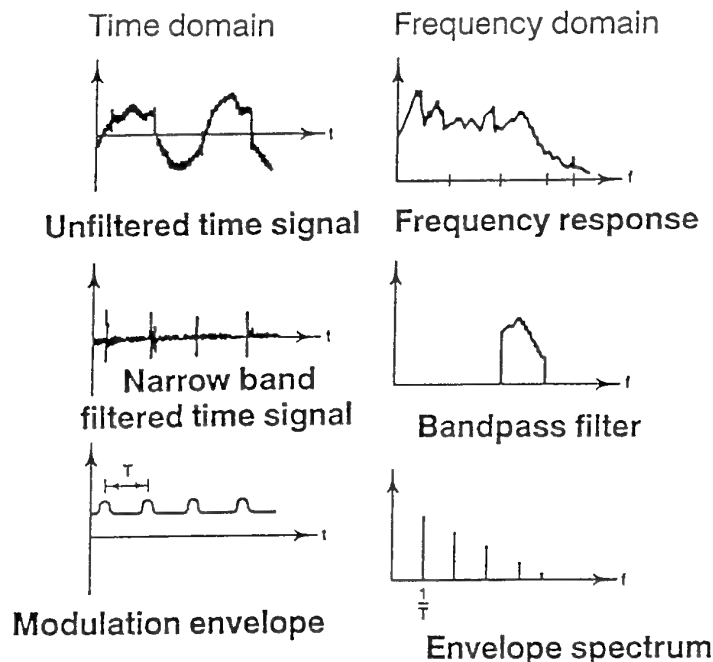


Figure 7. The principle of analogue enveloping.

An approximation which has been found useful in further investigating the effects of enveloping (by bandpass filtering followed by rectification and smoothing) is to replace the rectification by a squaring operation and the smoothing circuit by a lowpass filter; the operation can then be readily defined mathematically. Suppose that after bandpass filtering the vibration signal consists of N frequency components. This can be written in the time domain as [Berryman, et al],

$$x(t) = \sum_{i=1}^N a_i \cos(\omega_i t + \phi_i), \quad (35)$$

where ω_i is the i th frequency component in the passband with amplitude a_i and phase ϕ_i . After squaring, the signal can be written as,

$$x(t)^2 = \sum_{i=1}^N \sum_{j=1}^M a_i a_j \cos(\omega_i t + \phi_i) \cos(\omega_j t + \phi_j), \quad (36)$$

and by expansion this becomes,

$$x(t)^2 = \sum_{i=1}^N \sum_{j=1}^M \frac{1}{2} a_i a_j [\cos((\omega_i + \omega_j)t + \phi_i + \phi_j) + \cos((\omega_i - \omega_j)t + \phi_i - \phi_j)] \quad (37)$$

It can be seen that the squaring operation creates sum and difference frequencies from the original frequency components with the sum frequencies represented by the $(\omega_i + \omega_j)$ terms and the difference frequencies represented by the $(\omega_i - \omega_j)$ terms. After squaring, the signal is low pass filtered to remove the sum terms and leave the difference terms, analogous to the smoothing operation. The final envelope signal is then given by,

$$y(t) = \sum_{i=1}^N \sum_{j=1}^M \frac{1}{2} a_i a_j \cos((\omega_i - \omega_j)t + \phi_i - \phi_j). \quad (38)$$

It should be noted that all pairs of lines with the same frequency spacing in the original spectrum will add together to give a single frequency in the envelope signal. Whereas the original vibration signal may have been at a relatively high frequency, the resulting envelope signal only contains low frequency information.

An example can be used to clarify the preceding discussion. Consider a vibration signal having three frequency components at the frequency multiples 0.13, 0.18 and 0.19 of the sampling frequency in the presence of random noise which is bandpass filtered in the range from 0.1 to 0.2 of the sampling frequency. The spectrum will be as shown in Figure 8.

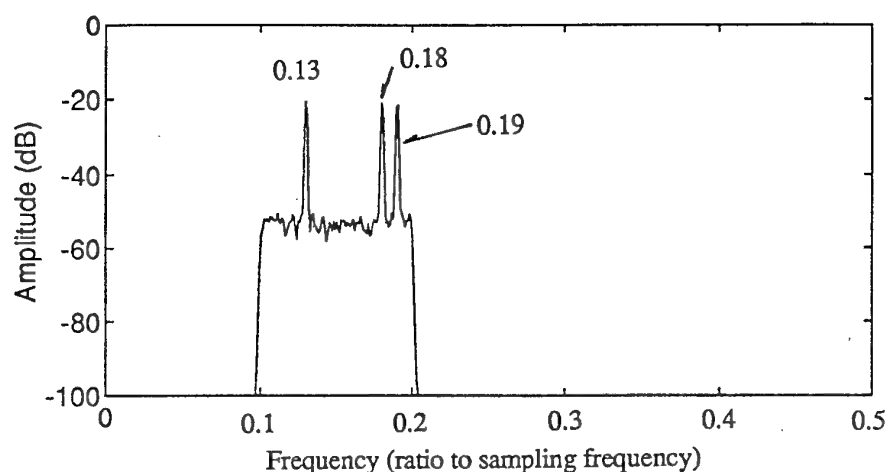


Figure 8. Power spectrum from simulated signal.

As indicated the signal contains frequency components in the range from 0.1 to 0.2 of the sampling frequency with three prominent frequencies appearing above the random noise floor. If the time signal is squared, then as discussed above the resulting signal will contain both sum and difference components. The sum components will occur at frequencies 0.26, 0.31, 0.32, 0.36, 0.37 and 0.38 of the sampling frequency while the difference frequencies will occur at DC, 0.01, 0.05 and 0.06, as illustrated in Figure 9. As indicated above, the squared bandpass filtered signal can be low pass filtered to remove the sum components and retain only the difference components, which effectively is the envelope signal.

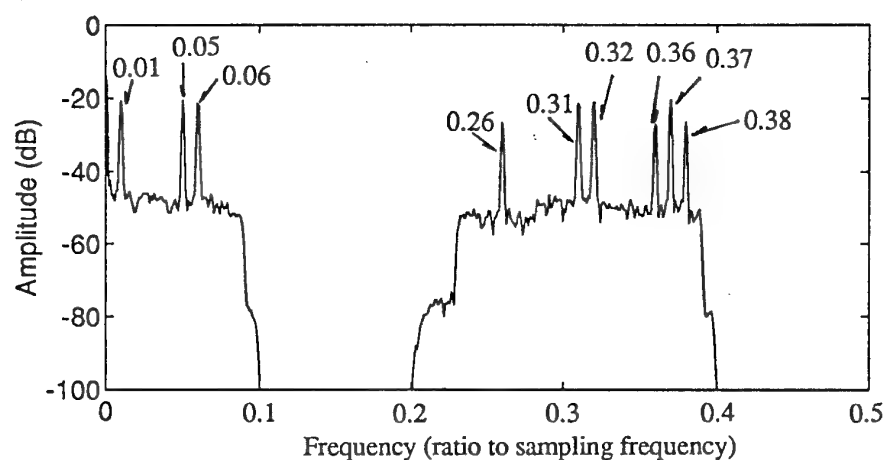


Figure 9. Power spectrum from the squared simulated signal.

An alternative to the analogue enveloping technique as outlined above is available using digital signal processing, as detailed in a number of references [Bell, 1985, Courrech, 1985, Randall, 1987 and Howard, 1991], and is most readily described in terms of the Hilbert transform and the analytic signal. An analytic signal is a complex time signal whose imaginary component is the Hilbert transform of the real part. Thus, if $a(t)$ represents the time signal,

$$\tilde{a}(t) = H\{a(t)\}, \quad (39)$$

and H is the Hilbert transform, then the analytic signal is defined as,

$$\hat{a}(t) = a(t) + j\tilde{a}(t), \quad (40)$$

where j is the complex operator. The Hilbert transform does not change the independent variable, so the result is in the same domain as the original function and it can be shown that the Hilbert transform corresponds to a 90 degree phase shift in the time domain. As a result, the Hilbert transform can be computed using a Fourier transform, by multiplying positive frequency components by $-j$ (a phase shift of -90 degrees) and negative frequency components by $+j$ (+ 90 degrees). This provides a convenient method for calculating the analytic signal as the negative frequencies of the resulting signal are zero, the positive frequencies are of double amplitude and the DC term remains the same. The analytic signal can thus be computed by Fourier transforming the time signal to the frequency domain, setting the negative frequency components to zero, doubling the positive frequency components and inverse transforming back to the time domain.

The analytic signal can also be represented in complex exponential form having both amplitude and phase,

$$\hat{a}(t) = |\hat{a}(t)|e^{j\theta(t)}, \quad (41)$$

where the amplitude is given by,

$$|\hat{a}(t)| = \sqrt{a(t)^2 + \tilde{a}(t)^2}, \quad (42)$$

and the phase is given by,

$$\theta(t) = \arctan\left[\frac{\tilde{a}(t)}{a(t)}\right]. \quad (43)$$

A general modulated signal can be represented as the real part of the analytic signal given by equation (40) and the amplitude of the analytic signal represents the amplitude modulation function (including the DC offset) as shown in equation (42) and as such corresponds to the envelope of the signal. The phase of the analytic signal represents the phase modulation (plus the carrier frequency component). The analytic signal thus provides a convenient means of obtaining both the amplitude and phase modulation of a signal.

A simple example can be used to help clarify the use of the analytic signal to compute the amplitude modulation or envelope function and the phase modulation [Randall, 1987]. If a real time signal is represented by a cosine function of frequency f_0 , then the Hilbert transform will be represented by a sine function, as shown by equations (44) and (45) respectively,

$$a(t) = \cos(2\pi f_0 t), \quad (44)$$

$$\tilde{a}(t) = \sin(2\pi f_0 t). \quad (45)$$

The amplitude modulation or envelope, as given by equation (42), will have unity amplitude, and the corresponding phase angle will be linearly increasing with time, given by $2\pi f_0 t$ with the slope of the phase curve representing the (constant) instantaneous frequency. Figure 10 shows the corresponding analytic signal as a right circular helix centred around the time axis, with the real and imaginary components corresponding to equations (44) and (45) respectively. The magnitude or envelope of the complex time signal is unity amplitude and the phase is a linear function increasing 2π per period.

A further simulated example can illustrate the use of envelope analysis to recover the amplitude modulation of a time domain signal. A cosine signal with a frequency of 5 kHz and amplitude of 1 can be used to represent the carrier signal to be amplitude modulated and a portion (0.01 seconds) of the signal is shown in Figure 11a. Figure 11b represents the modulating signal to be 50 % modulated with the carrier signal with a frequency of 500 Hz and the resulting amplitude modulated waveform is shown in Figure 11c. As discussed above, two mechanisms exist for recovery of amplitude modulation from a signal, firstly using the analytic signal and secondly by squaring the signal to generate sum and difference components and then low pass filtering to remove the high frequency sum components. Figure 11d shows the recovered amplitude modulation from the modulated waveform shown in Figure 11c using the analytic signal approach and Figure 11e shows the recovered modulation using the squaring and low pass filtering approach after some scale adjustment. As can be seen, both techniques accurately replicate the original modulating waveform shown in Figure 11b except in the region of the initial transient.

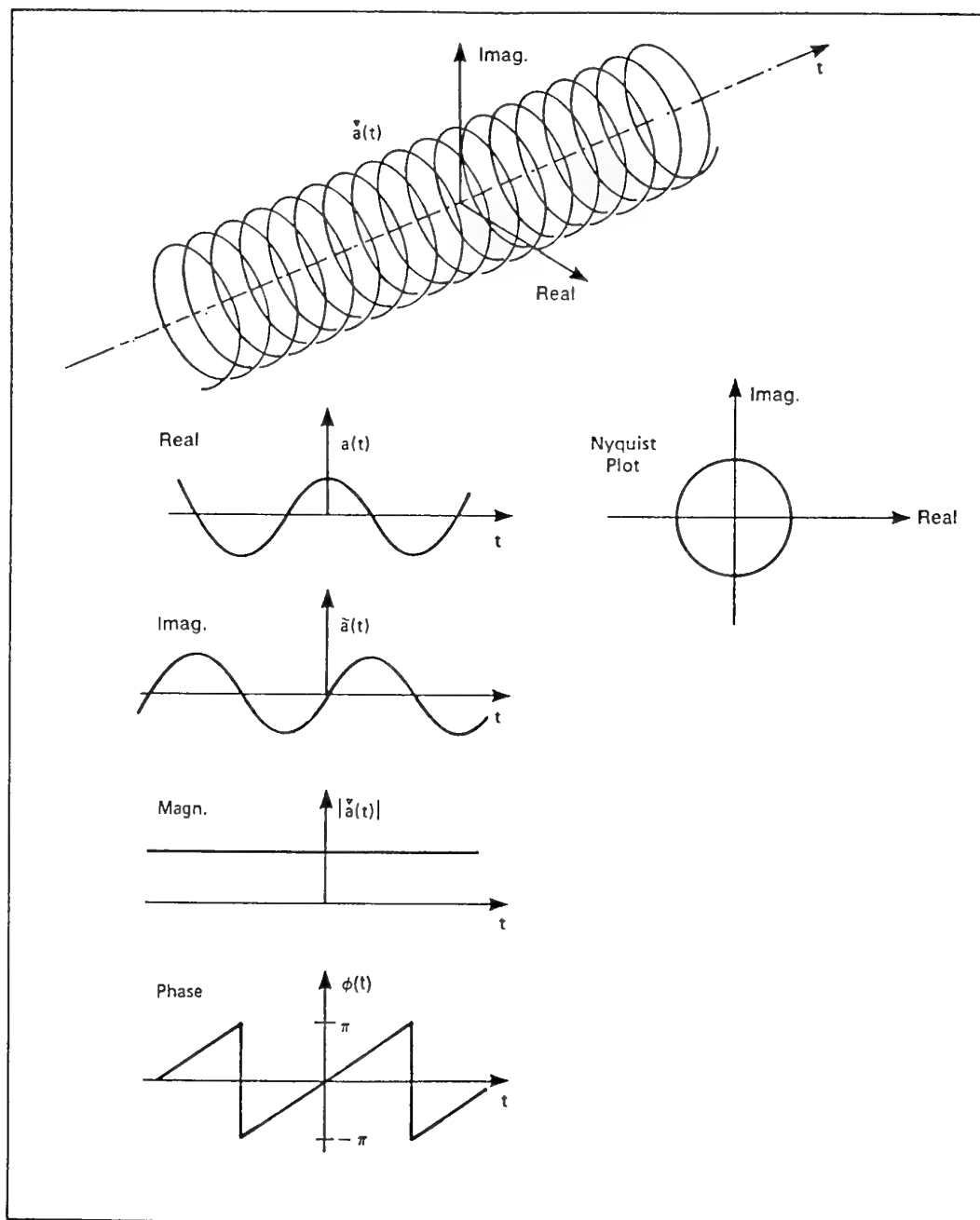


Figure 10. The analytic signal of a cosine time signal, [Randall, 1987].

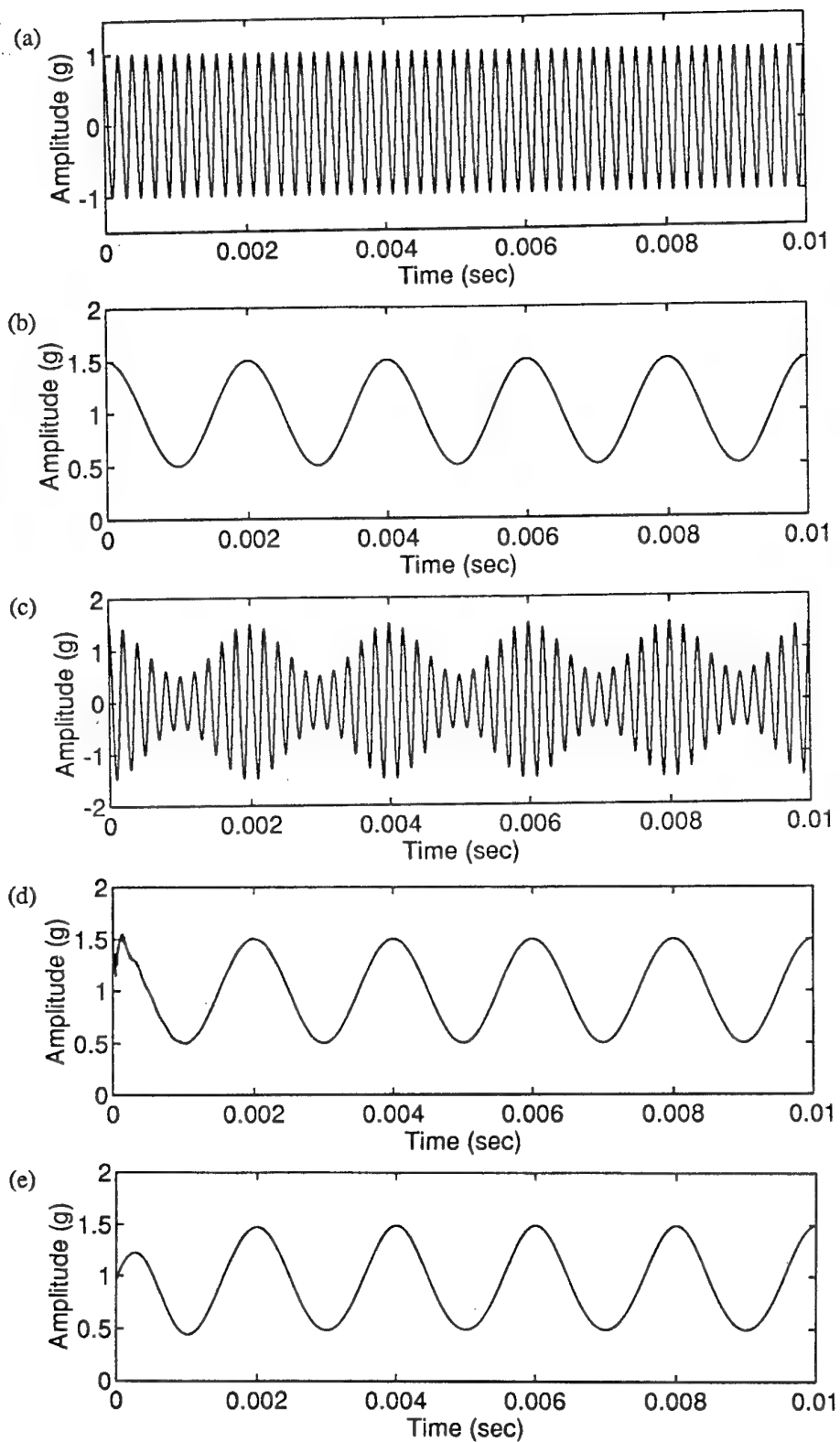


Figure 11. Simulated example of the recovery of amplitude modulation.

An example of envelope analysis using vibration data obtained from a gear test rig with an implanted inner race bearing defect will further illustrate the nature of envelope analysis. Figure 12a shows the narrow band envelope obtained from the vibration data measured from the gear test rig with the implanted inner race defect as discussed in section 5.2. The 0.1 seconds of envelope data was computed from the 20 - 40 kHz frequency band and coincides with the 0.1 seconds of bandpass filtered data shown in Figure 4. As expected, the envelope time signal effectively results from rectifying the original bandpass filtered data. Figure 12b shows the envelope power spectrum obtained from the envelope signal shown in Figure 12a and a number of harmonics of shaft frequency and inner race defect frequencies modulated by shaft frequencies can be observed, as indicated in Table 4.

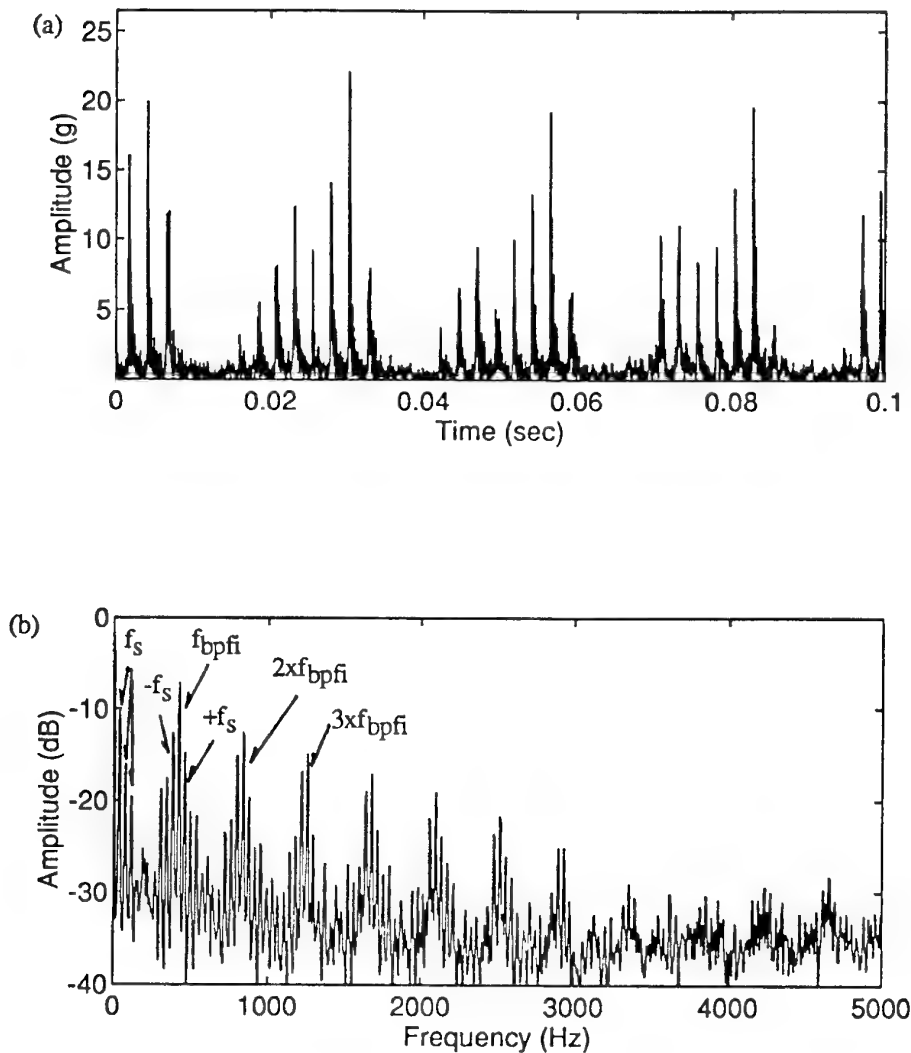


Figure 12. (a) Envelope time signal from the 20-40 kHz band. (b) Envelope power spectrum from the 20-40 kHz band.

The results presented above were obtained by using a line defect in the inner race of a bearing within a gear test rig. It has often been pointed out that results from test rigs with implanted defects should be treated with utmost caution as in many ways they will not be representative of the type and/or nature of naturally occurring defects, particularly because the modes of failure which occur in practice will not have such sharp profiles as is often the case with implanted defects. The sharp profile of the implanted line defect in the current data set provides the crisp clear impulses which can be seen in the bandpass filtered data and the resulting envelope data as shown above in Figures 4 and 12a respectively. It would be unusual to see such clear impulses in practice. However, the nature of the envelope spectrum shows a number of characteristics which correspond to the expected vibration spectral pattern for inner race damage as outlined in section 3.2 and Table 4.

A number of trend parameters and post-processing procedures can be found in the literature for envelope analysis. These encompass both bearing fault detection and diagnosis and rely upon the theoretical predictions of the typical spectral patterns which can arise for particular modes of failure as discussed in section 3.2. The most detailed of the post-processing procedures follow that originally developed by [Stewart, 1983] and reported in a number of other publications [Chivers, et al, 1986, Howard, 1991 and Munding, et al, 1992] and concerns the use of median filtering of the envelope spectrum followed by clipping, comb filtering and finally autocorrelation. Figure 13 shows the post-processing procedure originally proposed by [Stewart, 1983].

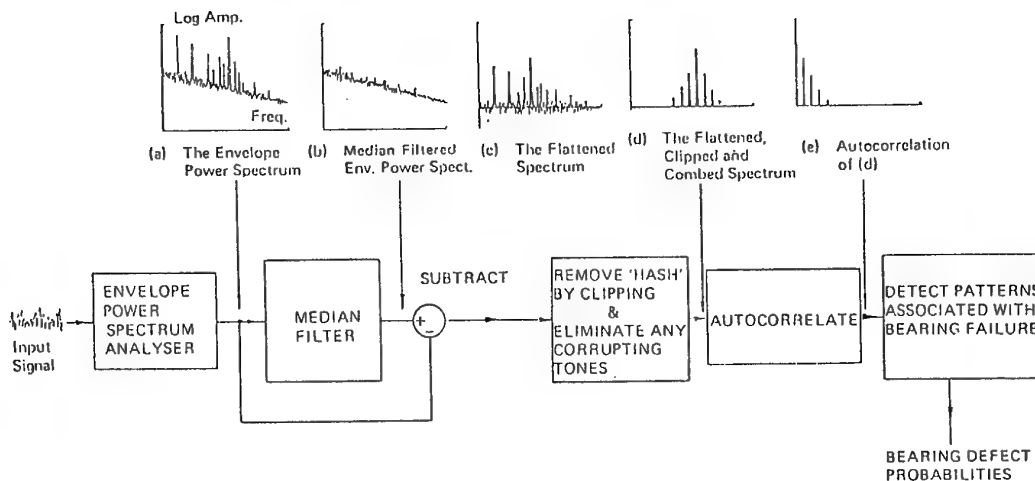


Figure 13. Envelope post-processing procedure using median filtering, clipping, comb filtering and autocorrelation, [Stewart, 1983].

The post-processing enables a number of defect parameters to be developed as indicated in Table 7, [Munding, et al, 1992].

Table 7. Bearing diagnostic parameters, [Mundin, et al, 1992].

	Diagnostic Indicator	Character	Purpose
Levels	BE	Band Energy (g)	Detects heavy damage
	BKv	Band Kurtosis	Detects localised damage
	EB	Base Energy	Detects distributed damage
Pattern Matching	OR DI	Outer Race Detection Index	Detects localised damage
	OR EI	Outer Race Energy Level	Detects localised damage confirm and trend
	IR DI	Inner Race Detection Index	Detects localised damage
	IR EI	Inner Race Energy Level	Detects localised damage confirm and trend
	RE DI	Rolling Elements Detection Index	Detects localised damage
	RE EI	Rolling Elements Energy Level	Detects localised damage confirm and trend

As detailed in Table 7, envelope post-processing can provide a number of bearing diagnostic parameters to help detect and diagnose bearing damage. The simplest of these parameters concerns the use of levels and comprise the energy in the selected frequency band which is used as a general utility parameter and the envelope kurtosis which is used as an indication of localised damage. The third level parameter is the amount of energy in the base band of the envelope spectrum and can be used to monitor the level of distributed damage. The pattern detection process is achieved by firstly calculating the anticipated bearing failure patterns (section 3.2, Table 4) and then correlating these patterns with the actual envelope power spectrum for each class of damage, whether it be outer race, inner race or rolling element damage. The degree of match of the expected bearing failure patterns and the actual tone spectrum is expressed as a percentage value called the detection index, (DI), while the associated energy in the failure pattern is called the energy level or energy index (EI).

The envelope post-processing procedure given by Stewart and outlined above, is certainly the most sophisticated procedure which has been found in the literature for interrogating the envelope signal and extracting trend parameters which can be used for detection and diagnosis of bearing failures. These procedures were developed specifically for detecting and diagnosing bearing faults in helicopter gearboxes which is one of the most difficult vibration environments to deal with, as discussed in section 2.6, and one in which envelope analysis and post-processing has consistently proved to be efficient [Chivers, et al, 1986]. For other classes of machines, less complicated procedures are likely to be successful although envelope analysis should still prove effective [McMahon, 1991].

5.4 Cepstrum analysis

Cepstrum analysis was developed in the 1960's [Bogert, et al, 1963] as a technique for processing seismological data for separating out the influence of echoes from data. Since the initial development, the areas of application have spread throughout the major signal processing fields [Childers, et al, 1977] and more recently in the area of vibration condition monitoring [Randall, 1980, Randall, 1983, Lyon, 1985, Courrech, 1985, Kershaw, 1986 and Mathew, 1987]. The cepstrum was originally defined as the "power spectrum of the logarithmic power spectrum", but a number of variations have also been developed. The most general definition is given as,

$$C(\tau) = F^{-1}\{\log F(x(t))\}, \quad (46)$$

where the original frequency spectrum $F(x(t))$ can be either a power spectrum (in which case the so-called power cepstrum is obtained) or a complex spectrum (in which case the so-called complex cepstrum is obtained).

The principal use of the cepstrum for bearing fault detection is in detecting periodicities in the frequency spectrum corresponding to bearing frequency harmonics and associated sideband patterns. A typical example of the use of cepstrum to detect bearing frequencies is shown in Figure 14 [Courrech, 1985] where frequency spectra and corresponding cepstra are shown at various time periods for a gearbox with a developing bearing fault.

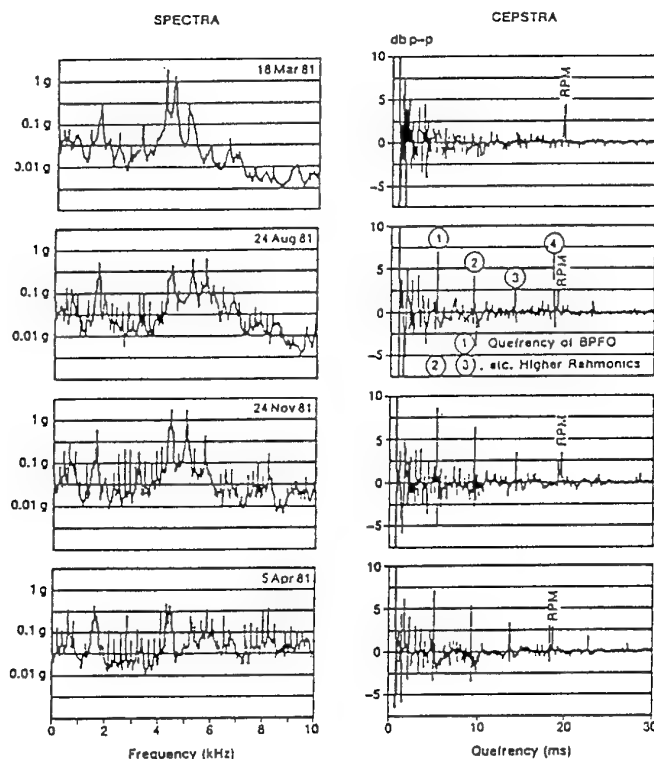


Figure 14. Spectra and cepstra measured on a gearbox following the development of a bearing fault, [Courrech, 1985].

Cepstral analysis has been found to be useful for a number of reasons, including as shown in Figure 14, (a) that the first rahmonic (cepstrum harmonic) indicates directly the harmonic spacing independent of where the harmonics appear in the spectrum, (b) the unknown frequency spacing can often be linked directly back to other known components. eg: it is immediately obvious that the unknown frequency spacing is 4.1 times the shaft frequency which corresponds to a bearing frequency, and (c) the first rahmonic has been found to be a stable trend parameter. In many ways, cepstral analysis is similar to envelope analysis in that both techniques detect periodically spaced frequencies; cepstrum analysis across the whole frequency band of the spectrum, and envelope analysis in a predetermined frequency band. A number of examples of trending based upon cepstra can be found in the literature [Courrech, 1985 and Bruel and Kjaer, 1990].

Although cepstral analysis is a common signal processing technique in other areas of data analysis, it would be fair to say that it has not received widespread acceptance for bearing fault detection and diagnosis as compared to envelope analysis. This is possibly due to the computational complexity in calculating the cepstrum and in interpreting the results. One avenue of cepstrum analysis which is starting to receive more attention is it's ability to deconvolve source and transmission path effects [Lyon, 1985 and Lyon, 1987], which may prove useful for bearing research in the future as it has the potential to be able to remove transmission path effects from the measured vibration signal or at least to enable inverse filters to be designed to minimise their effects [Nathan, et al, 1990].

5.5 *Time-frequency analysis*

A number of time-frequency domain techniques have been developed which show potential for detecting and diagnosing bearing problems in some of the more complex classes of rotating machines where the signal to noise ratio is low and a large number of frequency components are present. These techniques include the Short Time Fourier transform (STFT), the Wigner-Ville distribution (and variants), and the Wavelet transform.

5.5.1 *The short time Fourier transform*

One of the most widely used time-frequency techniques is the short time Fourier transform (STFT). It has been known by a range of different terms such as waterfall plot, isoplot, spectrogram, etc., and has been in common use since the advent of computers fast enough to compute the Fourier transform of a discrete data set within a reasonable time frame, [Allen, et al, 1977 and Chen, 1989]. The STFT is evaluated by applying a windowing function to the original time signal and evaluating the conventional Fourier transform of the resulting finite length time signal. The STFT of a time signal $x(t)$ over a time window T , is given by,

$$STFT(t, f) = \int_{t-T/2}^{t+T/2} x(\tau) \cdot w(\tau - t) \cdot e^{-j2\pi f\tau} \cdot d\tau, \quad (47)$$

where $w(\tau)$ represents the window function which satisfies $w(\tau)=0$, for $|\tau| > T/2$ where the time signal is assumed to be stationary during the short time interval T .

Figure 15 shows examples of two STFT's taken over short time segments of vibration time data from a gear test rig. Figure 15a shows the STFT from the acceleration measured on the gear casing with the bearings in good condition while Figure 15b shows the STFT from the bearing with an inner race defect for which the time signal was shown in Figure 3 and the corresponding power spectrum was shown in Figure 6. A sliding hanning window of length 256 points was used over the signal length of 1024 points with a step size of 4 points.

The STFT magnitude is displayed on a logarithmic scale to enhance the low amplitude components. The depth of the magnitude scale is limited to 25 dB down from the maximum magnitude and the display uses 64 gray scale colours through the magnitude range. The jagged nature of the STFT is caused by the discrete number of lines in the FFT which are then displayed for each time interval.

Two of the obvious details which can be seen from the STFT are the transient nature of impacts which occur at various times and the nature of the excitation of various resonances. From Figure 15b, three transient impacts can be seen corresponding to three ball passes over the implanted inner race defect. Although the duration of the impacts can be seen from the STFT, it is affected by the window length used in the computation. Of more interest is the nature of the excitation of the various resonances which occurs. Figure 6 shows a typical power spectrum from the gear test rig with the implanted inner race defect from which various structural resonances can be identified. As shown in Figure 15b, four main resonances are typically excited from the implanted defect, 15 kHz, 26 kHz, 34 kHz and 39 kHz within the 0-40 kHz range, and as expected, each impact results in a slightly different resonance structure being visible above the STFT noise floor. The various high frequency resonances so revealed could be used to help in the application of envelope analysis, as the precise resonances which are excited by the impacts can be determined and then used to focus envelope analysis upon that frequency region.

The other resonance structure which is apparent is that which occurs in the low frequency range between 5-8 kHz and, as shown in Figure 15a and 15b, there is little short time periodicity to the low frequency resonance excitation. This is to be expected as the frequency content below 8 kHz is dominated by the strong gear mesh harmonics as shown in Figure 6.

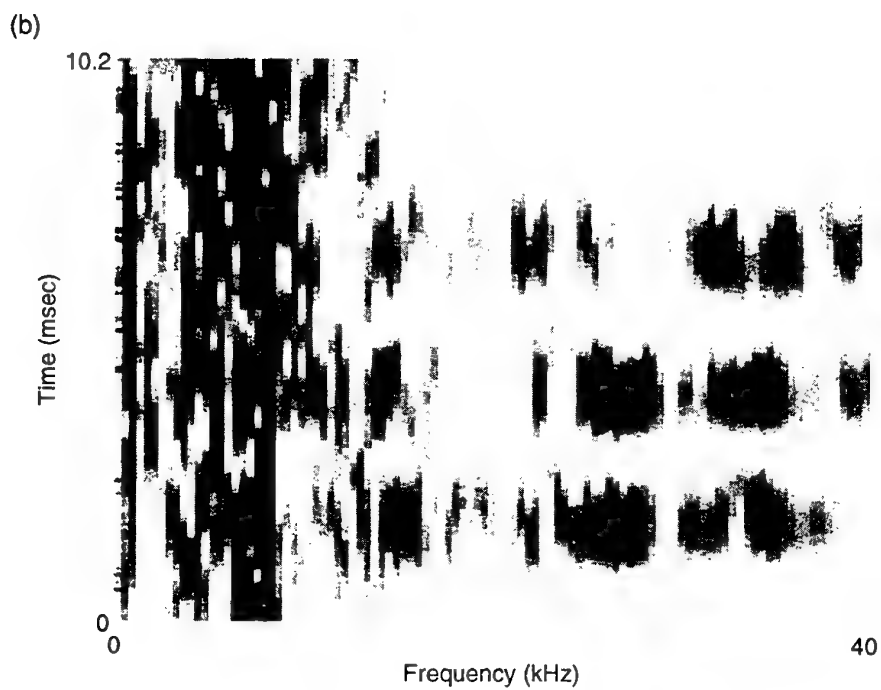
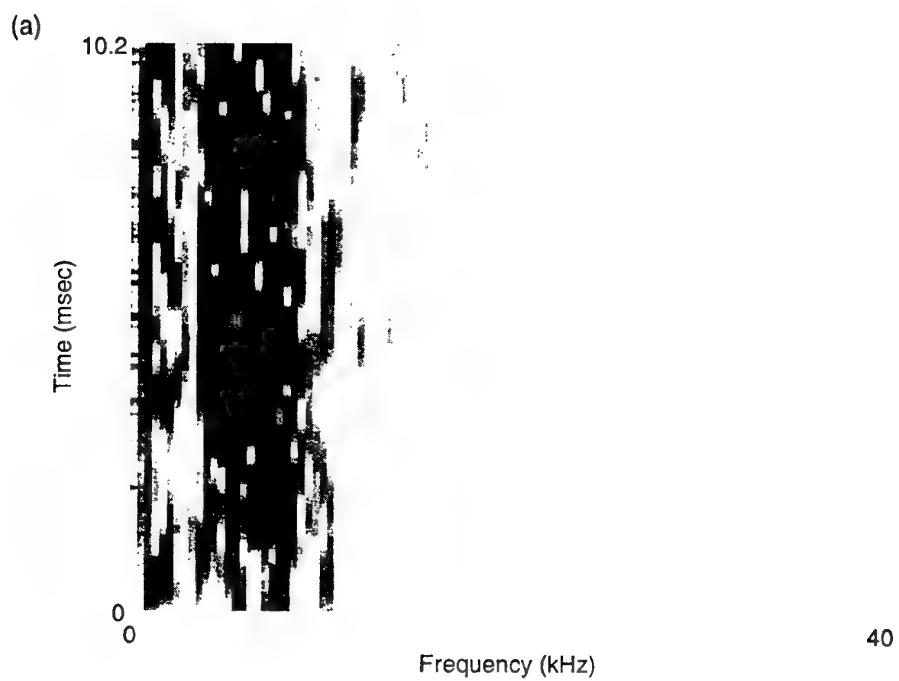


Figure 15. Short time Fourier transform of vibration data measured on a gear test rig. *a)* Bearings in good condition, *b)* Bearings with an inner race defect.

Similar STFT plots can be obtained from the vibration data with outer race and roller related defects. The time period between resonance excitation can be used for diagnostic purposes by relating it to the various characteristic bearing frequencies; however envelope analysis is probably a more effective means.

One of the difficulties with the STFT is the inherent relationship between time and frequency resolution where a finer frequency resolution is achieved at the expense of time resolution and vice-versa. This has led to the development of a number of alternative approaches to time-frequency analysis as detailed in subsequent sections.

5.5.2 The Wigner-Ville distribution

The Wigner-Ville Distribution (WVD) had its earliest developments nearly 50 years ago. More recently it has been extensively used in the areas of speech, radar, sonar and other areas of advanced signal processing [Claasen, et al, 1980, Claasen, et al, 1980, Claasen, et al, 1980, Peyrin, et al, 1986, Boashash, et al, 1987, Boashash, et al, 1990 and Hlawatsch, et al, 1992]. Several papers in particular have been devoted to the use of the WVD for vibration data from rotating machinery [Forrester, 1990, Rao, et al, 1990, Zhuge, et al, 1990 and Meng, et al, 1991]. The WVD and derivatives are particularly useful for diagnosing short time non-stationary events such as impacts, amplitude and phase modulation and resonance excitation [Forrester, 1990].

The Wigner-Ville distribution can be defined using the analytic signal as given in equation (40). If $\hat{a}(t)$ represents an analytic signal then the WVD is defined as,

$$WVD(t, f) = \int_{-\infty}^{\infty} \hat{a}(t + \frac{\tau}{2}) \cdot \hat{a}^*(t - \frac{\tau}{2}) \cdot e^{-j2\pi f\tau} \cdot d\tau \quad (48)$$

where t is the time variable and f is the frequency domain variable. The above derivation implies that the time signal must be known for all time prior to computing the WVD. This limitation can be overcome by applying the WVD analysis to a windowed version of the analytic signal. The definition for the Windowed Wigner-Ville Distribution computed over a time length T , is given by [Boashash, et al, 1987],

$$WVD(t, f) = \int_{-T}^T \hat{a}(t + \frac{\tau}{2}) \cdot \hat{a}^*(t - \frac{\tau}{2}) \cdot w(\frac{\tau}{2}) \cdot w^*(-\frac{\tau}{2}) \cdot e^{-j2\pi f\tau} \cdot d\tau. \quad (50)$$

As defined above, the WVD is real valued with both positive and negative components. Where illustrated in this report, the WVD display uses 64 gray scale colours to represent the logarithmic positive amplitude over a range of 25 dB from the maximum. The negative components of the WVD are not shown.

Figure 16a shows the WVD over 10 msec of vibration data from the gear test rig with the bearings in good condition and Figure 16b shows the WVD for 10 msec of the vibration data with the inner race defect where the time data was shown in Figure 3, and the corresponding power spectrum was shown in Figure 6.

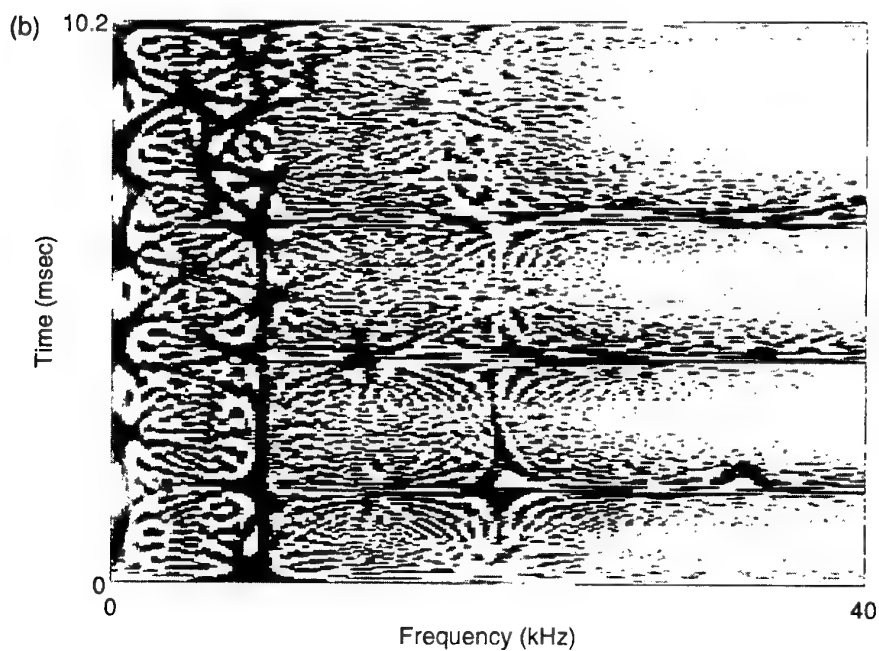
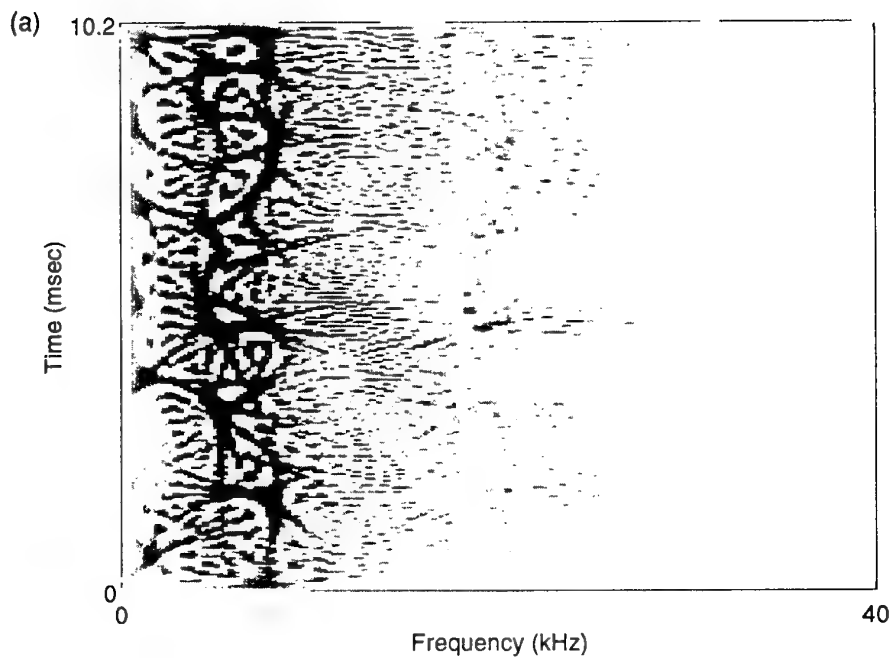


Figure 16. Wigner-Ville Distribution from gear test rig vibration data. a) Bearings in good condition, b) Bearing with an inner race defect.

The WVD for the gear test rig in good condition appears to be dominated by the low frequency resonance structure below approximately 8 kHz. In the high frequency region, the distribution is of low amplitude and appears random in nature. This contrasts sharply with the distribution shown in Figure 16b with the inner race defect where the high frequency region is dominated by the three impulses which occur at discrete times as the rolling elements in the bearing contact the defect in the load zone. The WVD confirms the excitation of the high frequency resonances although the appearance of specific resonances is less clear than that in the STFT shown in Figure 15b. The WVD shows a sharper time localisation when compared to the STFT as the WVD at each time point is relatively independent of the window size.

5.5.3 The continuous wavelet transform

The Wavelet Transform (WT) has received considerable attention over the past decade in signal processing [Combes, et al, 1987, Gram-Hansen, et al, 1989, Dorize, et al, 1989, Mallat, 1989, Daubechies, 1990, Rioul, et al, 1991, Cody, 1992, Daubechies, 1992, Li, et al, 1992]. The WT is similar to the STFT and the WVD in that it provides a time-frequency map of the signal being analysed, the main difference being that the WT studies high frequency components with sharper time resolution than the low frequency components. The continuous wavelet transform of a real signal $x(t)$ is defined with respect to an analysing wavelet $g(t)$ (complex in general) as,

$$WT(b, a) = \frac{1}{\sqrt{a}} \int g^* \left(\frac{t-b}{a} \right) \cdot x(t) \cdot dt, \quad (51)$$

where b represents dimensionless time, a represents the wavelet scale (reciprocal of frequency) and g^* denotes the complex conjugate of g . A large number of analysing wavelet families exist and the results obtained with the WT will depend upon the particular wavelet which is chosen. For the current study, the analysing wavelet which was used was the Morlet wavelet [Combes, et al, 1987],

$$g(b, a) = e^{jct} \cdot \exp\left(-\frac{1}{2}t^2\right), \quad (52)$$

where $c = 5.5$ to assure admissibility and progressivity. Figure 17 shows an example of a Morlet wavelet for a typical scale based upon a sampling time period of 0.00001 secs, (100 kHz sampling frequency) and the corresponding power spectrum on a logarithmic scale. The continuous wavelet transform is computed as defined in equation (51) by convolving the analysing wavelet over the complete time signal of interest, for each scale. For the analysis which follows, the transform was computed over seven octaves, using 12 voices per octave to give a consistent time-scale display. Figure 18a shows the continuous wavelet transform of 10 msec of acceleration data measured from the gear test rig in good condition and Figure 18b shows the WT for the vibration data with the inner race defect. The top 10 dB of the magnitude of the wavelet transform are displayed over the seven octaves corresponding to the frequency range below 40 kHz on a linear frequency scale.

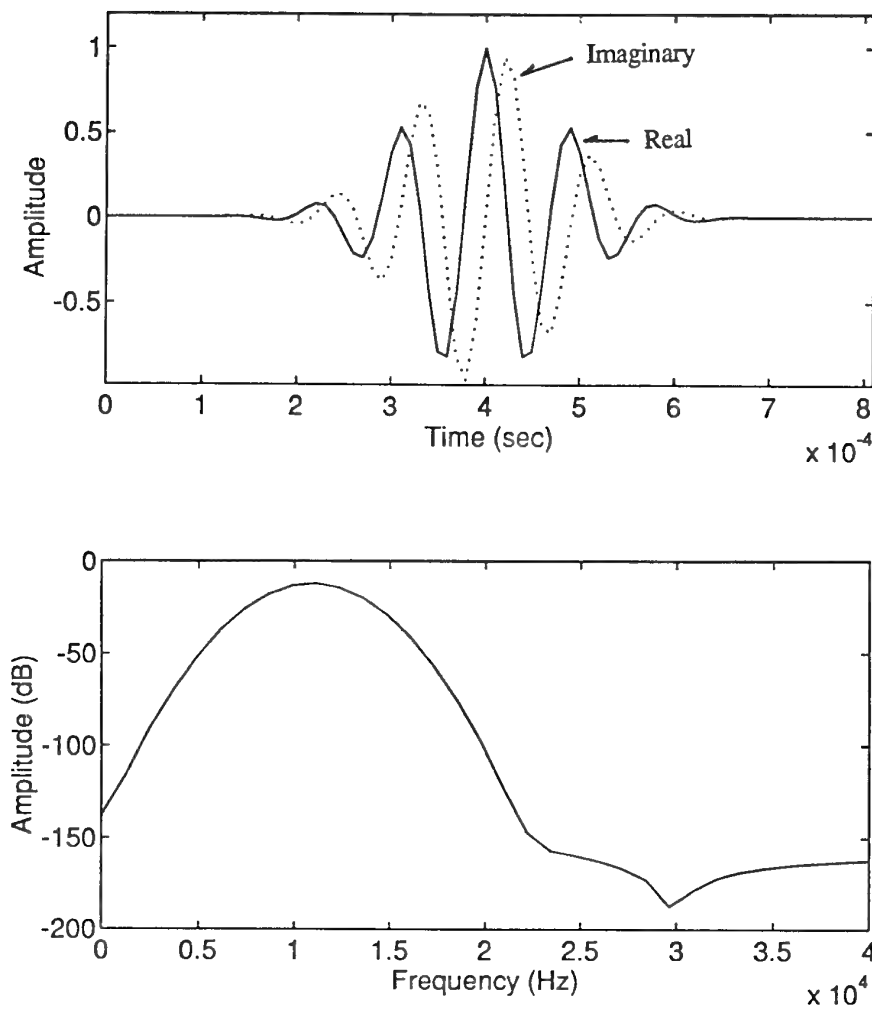


Figure 17. A typical Morlet wavelet and the corresponding power spectrum.

As shown in Figure 18a, the wavelet transform for the gear test rig in good condition is dominated by the low frequency resonances below approximately 8 kHz which are excited by the gear mesh harmonics. No periodic structure is apparent over the short time segment which is being considered. For the bearing with the inner race defect, the high frequency region of the WT as depicted in Figure 18b, is dominated by the excitation of the structural resonances as each rolling element in the load zone contacts the inner race defect. The wavelet transform provides a clear indication of the leading edge of each impulse and then the subsequent damped oscillation across a wide range of high frequencies. Whereas the WT provides a sharp indication of the time response at the higher frequencies, the corresponding frequency response is not very clear and it becomes difficult to detect the individual structural resonances which are excited.

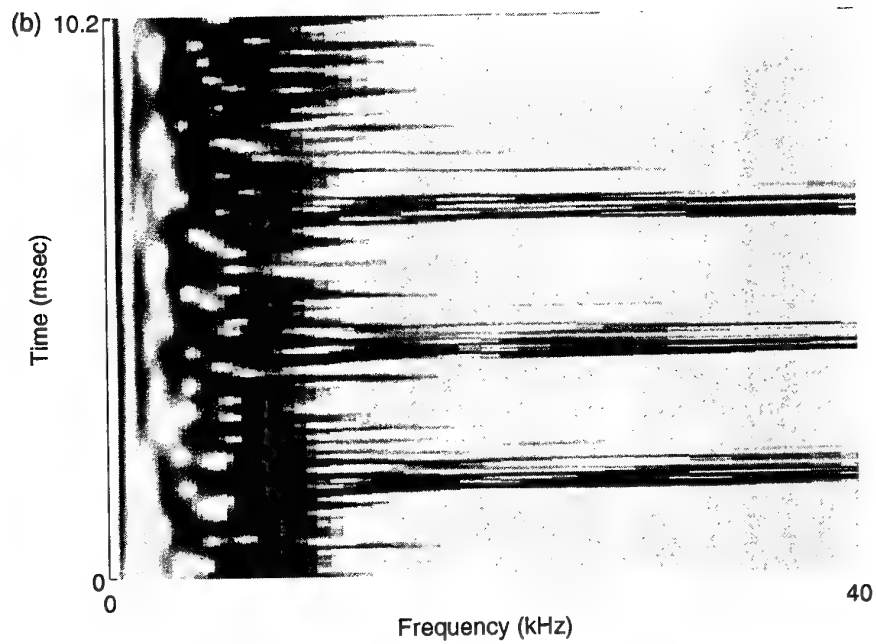
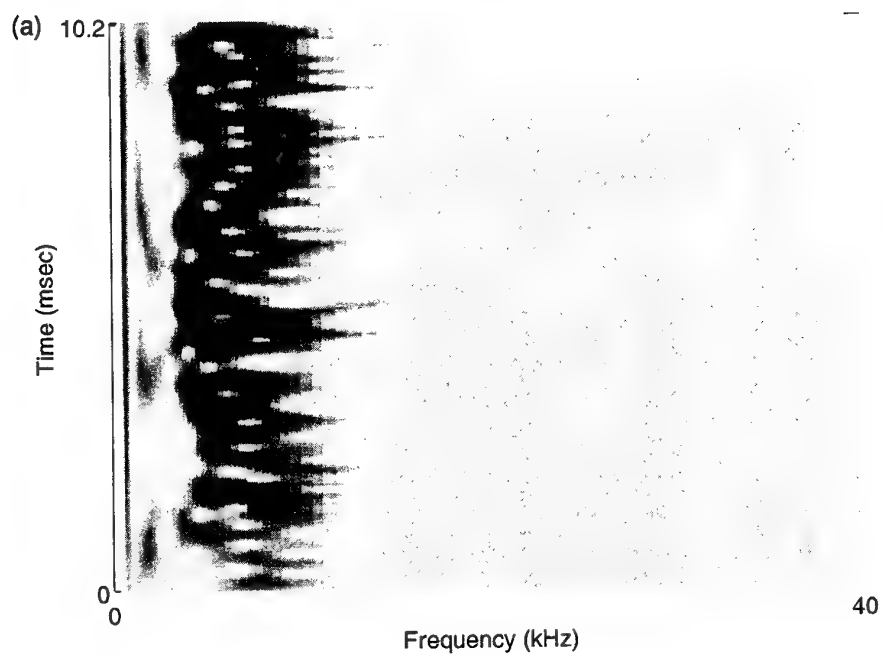


Figure 18. Wavelet Transform computed from gear test rig acceleration. a) Bearings in good condition. b) Bearing with inner race defect.

From a comparison of the results shown in Figures 15, 16 and 18, a number of comments can be made. The STFT appears to be well suited to indicating those structural resonances which respond most to the bearing impacts, whilst it doesn't indicate the precise nature of the resonant response in the time domain. The WT on the other hand, appears to be well suited to indicate the transient nature of the resonant excitation in the time domain, however it doesn't resolve the response of the high frequency resonances very clearly in the frequency domain. In some ways, the WVD tries to get the best of both the time and frequency domain, however, as shown in Figure 16, it is more difficult to interpret than either of the other techniques. The impulses can be identified in the time domain, although not as precisely as in the WT, and the structural resonances are not readily apparent when compared to the results obtained with the STFT.

Time-frequency vibration analysis for machine condition monitoring is growing as an active research area. One of the current areas of interest is its application to gear fault detection [McFadden, et al, 1990, McFadden, et al, 1991, Wang, et al, 1992 and Wang, et al, 1993] where the best approach seems to be the application of the STFT using a gaussian window function.

5.6 *Higher order spectral analysis*

As mentioned above, linear spectral analysis techniques such as the power spectrum have received much attention for condition monitoring of rolling element bearings. Linear spectral analysis techniques are of limited use however, when spectral components interact together due to some nonlinear process. In such a situation, higher order spectral techniques can be used to characterise the signal since the nonlinearities result in new spectral components which are phase coherent. The phase coherence can be detected using higher order spectra since the phase information is retained with the higher order spectral techniques, [Sato, et al, 1977, Kim, et al, 1979, Matsuoka, et al, 1984, Nikias, et al, 1987, Pezeshki, et al, 1990, Li, et al, 1991, Li, et al, 1991, Pezeshki, et al, 1991, Bessios, et al, 1991, Zhang, et al, 1991 and Nikias, et al, 1993]. The higher order spectral techniques are able to determine that nonlinear interactions between spectral components are occurring and to measure the extent of the joint dependence of the various combinations of frequency components. In particular, quadratic phase coupling between three spectral components can be determined using the bispectrum, defined as the Fourier transform of the third order cumulant sequence.

5.6.1 *Definition of bispectrum*

The bispectrum can easily be defined in relation to the power spectrum. If a random time signal is defined as $x(t)$, then the Fourier transform as defined in equation (32) can be rewritten to give,

$$X(f) = |X(f)| \exp(j\theta), \quad (53)$$

where the magnitude and phase angle are given by $|X(f)|$ and θ respectively. The power spectrum of $x(t)$ can then be obtained as given in equation (33),

$$P(f) = E[X(f)X^*(f)],$$

where * denotes the complex conjugate and $E[\]$ represents the expectation operator. Using the same notation, the bispectrum of $x(t)$ can be defined as,

$$B(f_1, f_2) = E[(X(f_1).X(f_2).X^*(f_1+f_2))], \quad (54)$$

where f_1 , f_2 and f_1+f_2 denote the individual complex frequency components obtained from the Fourier transform. Equation (54) demonstrates how the bispectrum measures the statistical dependence between the three frequency components. If the frequency components at f_1 , f_2 and f_1+f_2 are independent components, each frequency will be characterised by statistically independent random phases distributed over $(-\pi, \pi)$. Upon statistical averaging denoted by the expectation operator E in equation (54), the bispectrum will tend toward zero due to the random phase mixing effect. On the other hand, if the three spectral components f_1 , f_2 and f_1+f_2 are nonlinearly coupled to each other, the total phase of the three components will not be random at all, even though each of the individual phases are random. Consequently, the statistical averaging will not lead to a zero value in the bispectrum.

The bispectrum isn't normally computed over the entire two-dimensional frequency plane due to symmetry relationships which exist [Kim, et al, 1979]. Figure 19 shows the region of computation using the constraints of Nyquist and symmetry which are normally used.

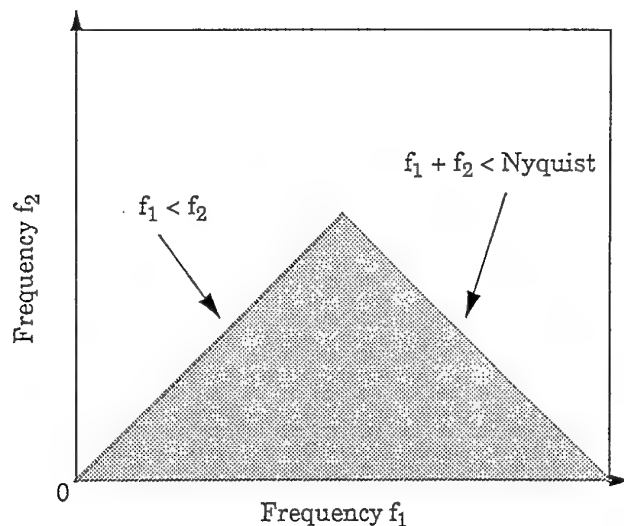


Figure 19. Region of bispectrum computation.

A number of computational procedures exist in the literature for estimating the bispectrum [Kim, et al, 1979, Matsuoka, et al, 1984, Nikias, et al, 1987]. The procedure which was used in this study followed that given by [Kim, et al, 1979] as shown in equation (54) using the FFT and consists of a number of steps as follows,

1. Segment the time series data into m sections of equal length n .
2. Subtract the mean value from each section.
3. Apply an appropriate data window to each section to reduce leakage.
4. Compute the Fourier coefficients for each section using the FFT, (equation (53)).
5. Compute the bispectrum for each section, equation (54).
6. Obtain the statistical estimate of the bispectrum by averaging over each of the data sections.

The estimate of the bispectrum given by equation (54) can be used to determine the presence of quadratic coupling between frequency components. The bicoherence spectrum, which is the normalised bispectrum, can be used to compute the degree of coupling between frequency components. The bicoherence spectrum will be bound by zero and unity, and its square is defined as,

$$b^2(f_1, f_2) = \frac{\left| \sum_{i=1}^m X_{f_1}^i \cdot X_{f_2}^i \cdot X_{f_1+f_2}^{i*} \right|^2}{\left[\sum_{i=1}^m \left| X_{f_1}^i \cdot X_{f_2}^i \right|^2 \right] \cdot \left[\sum_{i=1}^m \left| X_{f_1+f_2}^i \right|^2 \right]}. \quad (55)$$

5.6.2 Determining the existence and strength of quadratic coupling

An example of the bicoherence spectrum and its ability to not only determine the presence of quadratic coupling but also the extent of coupling, can be found in [Kim, et al, 1979] using computer generated signals as outlined below in further detail.

Consider 64 sections of a simulated signal which involves three sinusoidal components f_b , f_c and f_d where $f_b = 0.11x f_s$, $f_c = 0.1875x f_s$ and $f_d = f_b + f_c$ where f_s is the sampling frequency with 256 points per section. The phases of the three components are initially chosen from a set of random numbers uniformly distributed over the range $(-\pi, \pi)$. A small amount of random noise (-20 dB) was also added to the signal. The resulting power spectrum and bicoherence spectrum are shown in Figure 20. As expected the three spectral components appear in the spectrum at the same amplitude and the bicoherence spectrum shows low level random amplitudes across the region of computation.

To illustrate the effects of quadratic coupling, the simulation was changed whereby the phase of the third component f_c was the sum of the phases of the first two components. The resulting power spectrum and bicoherence spectrum are shown in Figure 21. The power spectrum is very similar to that shown in Figure 20 because the power spectrum of a signal is independent of the phases of the individual sinusoidal components. However, the bicoherence spectrum in Figure 21 shows the phase consistency between the three components as a bicoherence amplitude approaching a value of 1.0, $b^2(f_b, f_c) = 0.9993$. The ability of bispectrum analysis to detect phase coherence between frequency components is the major reason why it can be used to detect nonlinearities.

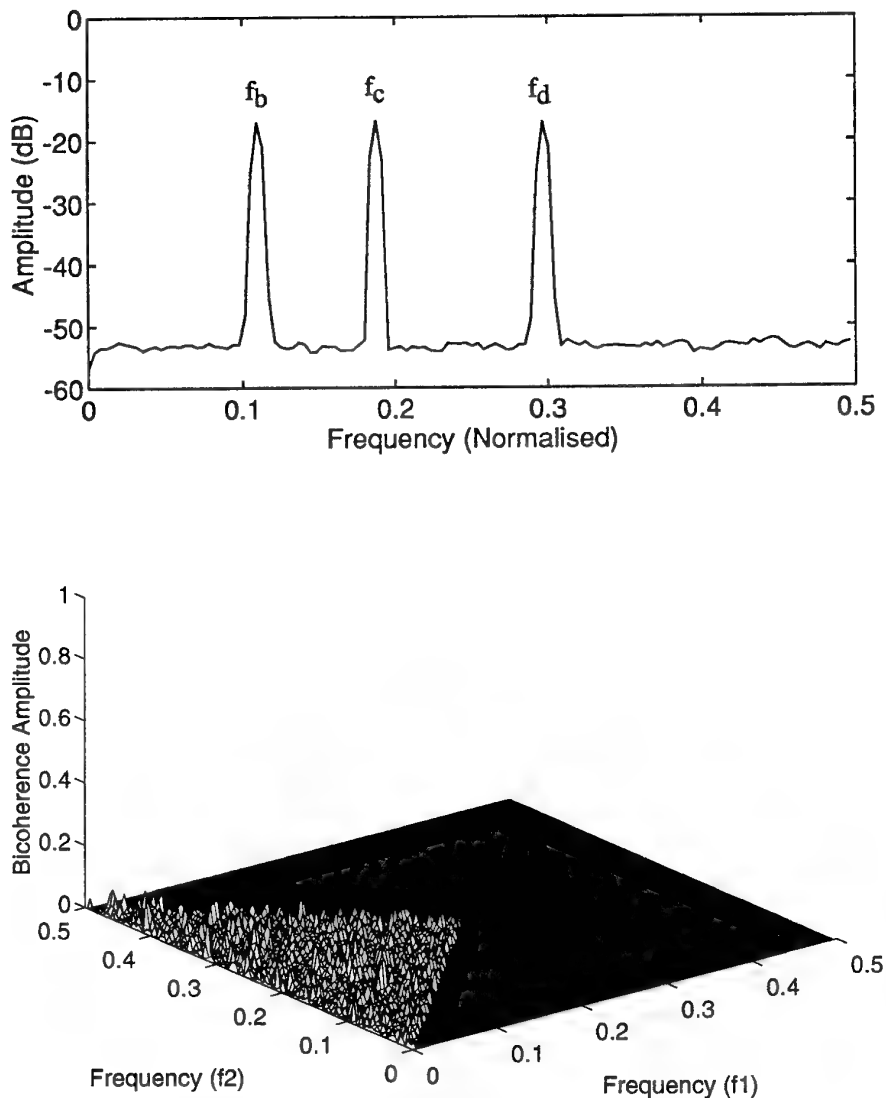


Figure 20. The power spectrum and bicoherence spectrum of three sinusoidal components with independent phases in the presence of random noise.

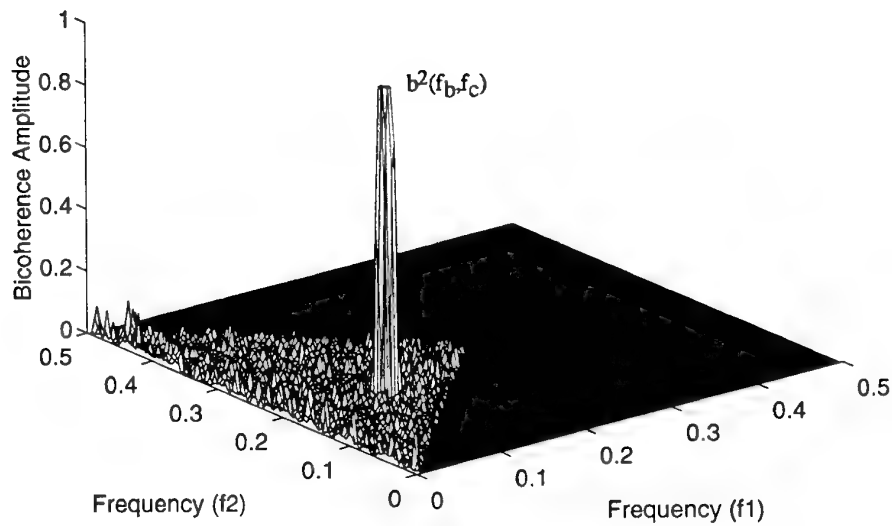
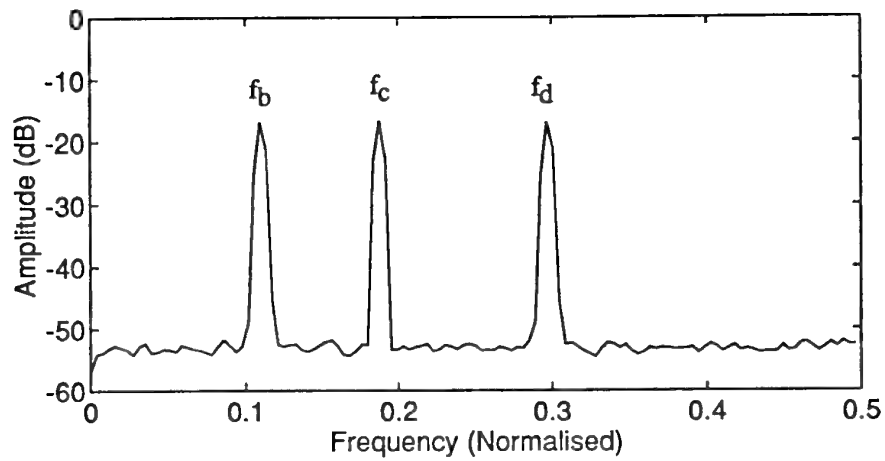


Figure 21. The power spectrum and bicoherence spectrum of three sinusoidal components with coherent phases in the presence of random noise.

A further simulation illustrates the ability of bispectrum analysis to not only detect quadratic phase coupling, but the extent of the phase coupling as given below. Consider the simulated signal $x(t)$,

$$x(t) = \cos(f_b t + \theta_b) + \cos(f_c t + \theta_c) + \frac{1}{2} \cos(f_d t + \theta_d) \\ + \cos(f_b t + \theta_b) \cdot \cos(f_c t + \theta_c) + n(t)$$

where, as before, $f_b = 0.11 \times f_s$, $f_c = 0.1875 \times f_s$ and $f_d = f_b + f_c$ where f_s is the sampling frequency, $n(t)$ is small amplitude random noise (-20 dB) and the phases of each wave are independently chosen from a set of randomly distributed numbers between $(-\pi, \pi)$. The product term in the test signal will generate sum and difference frequencies so that half the power at f_d will be due to the product interaction of frequencies f_b and f_c , $(f_c + f_b)$ and the other half will be due to the independent component at f_d . The power at the difference frequency $(f_c - f_b)$ will be entirely due to the product interaction of frequencies f_b and f_c . Figure 22 shows the power spectrum and the bicoherence spectrum of the signal $x(t)$.

The results from the power spectrum indicate the possible interaction of components f_b and f_c to generate a third component at their sum frequency $f_d = f_c + f_b$ and at their difference frequency, $f_c - f_b$. As there is no phase information in the spectrum, however, a positive and quantitative investigation of any interaction can not be undertaken. On the other hand, the bicoherence spectrum gives a definite and quantitative answer. The computed bicoherence for the sum interaction gives $b^2(f_b, f_c) \approx 0.5$ which implies that only half of the power at f_d is due to the nonlinear interaction of the components f_b and f_c . Furthermore, the computed bicoherence for the difference interaction was $b^2(f_c - f_b, f_b) = 0.99$ which shows that the power at the difference frequency was entirely due to the interaction of the components at f_b and f_c .

As illustrated in the two examples above, a certain amount of phase information which doesn't appear in the power spectrum can be recovered by using a higher order spectrum. For a quadratically nonlinear situation, the bispectrum measures the extent of phase consistency due to the nonlinearity between three components. The bicoherence spectrum, a normalised bispectrum, quantitatively measures the fraction of the power due to the quadratic interaction.

There are three common means of displaying the results of the bicoherence spectrum. The first method is illustrated in Figures 20, 21 and 22 where the bicoherence matrix is displayed as a three-dimensional cube [Kim, et al, 1979]. Although the most visually impressive method for displaying the bicoherence, it is often the most difficult to interpret. The second method involves displaying the three-dimensional matrix seen from above as a contour plot [Howard, 1993]. This provides an accurate indication of the actual frequency components involved, however, the magnitude of the bicoherence is not easily determined. The third method for displaying the bicoherence involves selecting one of the primary frequency components first and then computing the bicoherence for the second frequency axis. The resulting bicoherence is no longer a matrix but a

vector so can be displayed as a two-dimensional spectrum providing precise details of both the magnitude and frequency of the major components [Coffin, et al, 1986]. This method shows greater potential usefulness as a practical diagnostic tool and will be used in the remainder of this section.

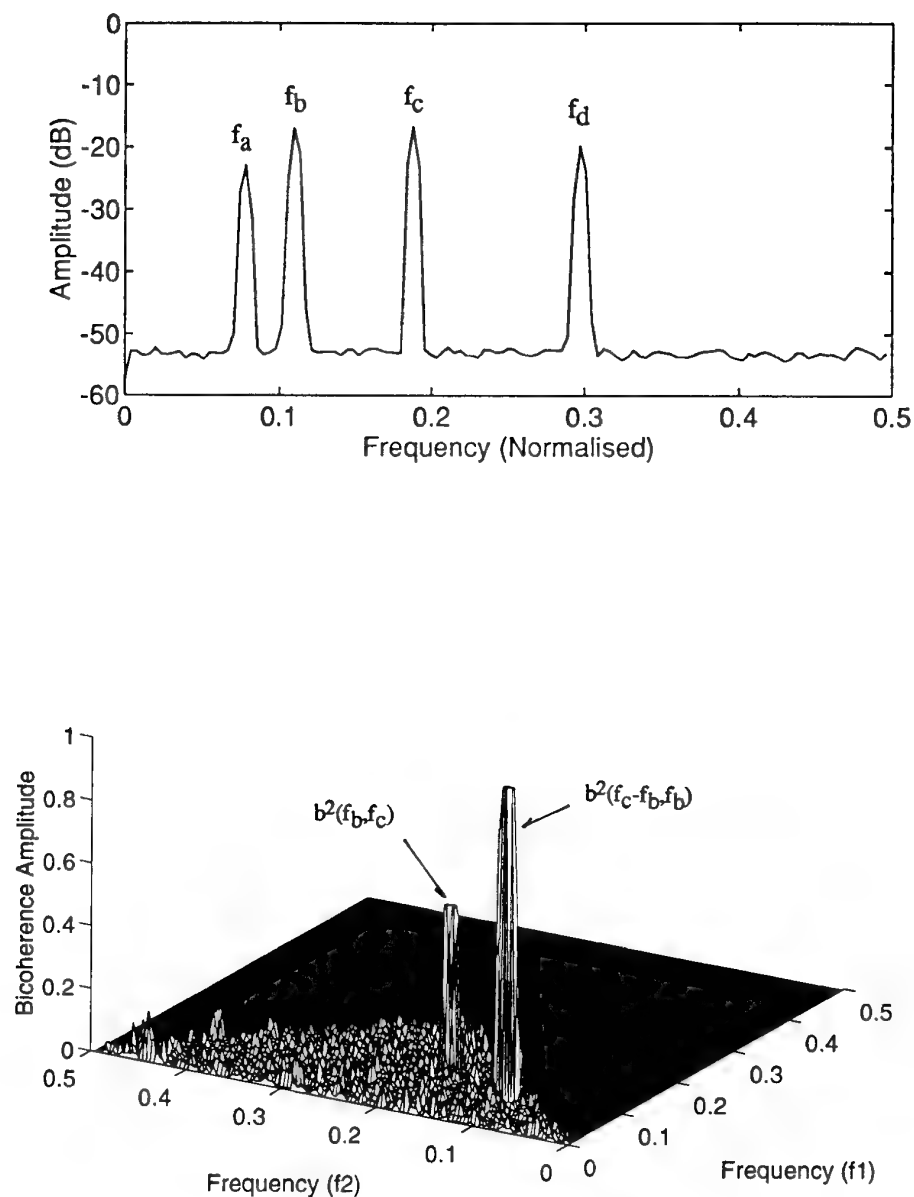


Figure 22. The power spectrum and bicoherence spectrum of a simulated signal involving the quadratic coupling of two components.

5.6.3 Application to bearing fault detection and diagnosis

Higher order spectral analysis has been used with success on the Space Shuttle Liquid Oxygen Turbopump bearings, for fault detection and diagnosis for a number of years [Coffin, et al, 1986 and Howard, 1993]. In particular, bispectrum analysis has been found to provide additional information on mechanical condition that linear techniques such as spectral analysis and envelope analysis are unable to provide. As indicated above, bispectral analysis can identify nonlinear quadratic coupling between frequency components and the strength of that coupling. Frequency components that appear to be sidebands, or modulated components of bearing-related frequencies, can now be identified as quadratically coupled to shaft frequencies, confirming the presence of bearing damage.

A further simulation can be used to illustrate the practical nature of bispectrum analysis and its relationship to bearing fault detection and diagnosis. Consider a rotating shaft and its response to whirl and the effect of waveform clipping due to rubbing [Coffin, et al, 1986], representing the Oxygen Turbopump. Figure 23a shows the displacement of a shaft as a clipped sine wave at a frequency of $N=625$ Hz, representing the unbalance vibration of a rotating shaft, where the wave has been clipped at 50% in the positive direction, to simulate the effect of rubbing. The resulting signal is now amplitude-modulated by another lower (whirl) frequency $W=110$ Hz as shown in Figure 23b. Figure 23c depicts the power spectrum of the second derivative of the displacement signal (acceleration) after random noise has been added and some of the higher frequency modulation sidebands are no longer visible in the spectrum or are difficult to identify.

For early diagnosis of changes in mechanical condition of rotating machinery, it is desirable to identify whether small peaks near the synchronous shaft frequency or harmonics are true sidebands or are from independent sources such as structural resonances. The components from independent sources will be independent of the components associated with the rotational frequencies, while the sideband components will be quadratically coupled to them. Bispectral analysis is able to identify whether an apparent sideband is statistically correlated to the rotational components. Figure 23d shows the bicoherence spectrum computed from the acceleration data with the first frequency fixed at $N+W$, and the second frequency varying across the complete frequency range, ie $b^2(N+W, f)$. The peaks at $b^2(N+W, N-W)$ and $b^2(N+W, N)$, indicate that a quadratic correlation exists among $(N+W, N-W, 2N)$ and $(N+W, N, 2N+W)$, respectively. The other peaks in the bicoherence indicate the quadratic correlation among the higher shaft harmonics and their sidebands. The bicoherence among some of the higher harmonics has also provided significant signal-to-noise enhancement where peaks which were buried in the noise in the power spectrum have appeared in the bicoherence coupled to the frequency $N+W$. This example has clearly shown that bispectral analysis can be used to identify the existence of quadratic coupling among frequency components [Coffin, et al, 1986]. For bearing fault detection and diagnosis, this offers the potential to determine the degree of phase correlation between various frequencies which appear from time to time, section 3.1 and 3.2, and the shaft

rotational frequency or characteristic bearing defect frequencies. This should help confirm the presence of bearing damage at the early stages of incipient failure.

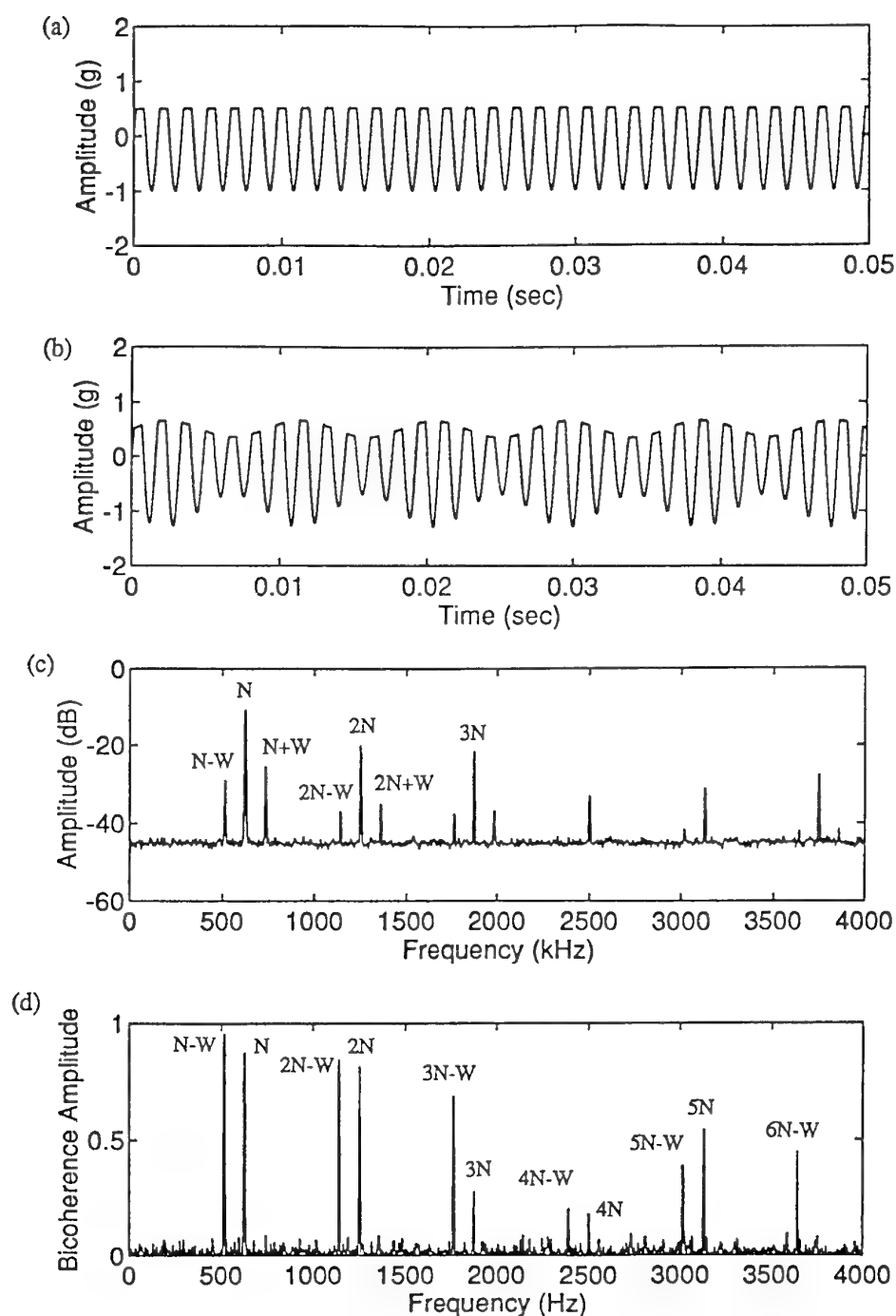


Figure 23. Simulation of a rotating shaft vibration with the effects of unbalance, clipping and whirl. *a)* Shaft displacement due to unbalance and clipping due to rubbing. *b)* Including the effects of whirl. *c)* Shaft acceleration spectra. *d)* Resulting bicoherence.

Bispectrum analysis was used with bearing test rig vibration data to further emphasise its ability to detect phase coupling between frequency components. A bearing accelerated fatigue test was conducted under overload and poor lubrication conditions using the ARL bearing test rig [Swansson, et al, 1984]. Twenty four vibration readings were taken over the duration of the test which went for 18 hours before complete seizure of the test rig occurred. The post-test analysis revealed inner race spalling and cage disintegration, with severe overheating discolouration of the races and balls. Figure 24 shows the power spectrum and bicoherence in the low frequency range (0-5000 Hz) at 2.0, 17.25 and 17.58 hours run time, obtained from acceleration measurements with a shaft frequency of 100 Hz. The bearing defect frequencies were computed from the equations shown in Table 2, $f_{bpf_i}=8.13xf_i$, $f_{bpfo}=5.87xf_i$, $f_{bsf}=2.915xf_i$ and $f_c=0.4193xf_i$, where f_i represents the inner race rotational frequency (shaft frequency). The low frequency range was used to illustrate the phase coupling of various bearing frequency components in the low frequency range as compared to the normal application of envelope analysis which is in the high frequency range [Li, et al, 1991].

Figure 24a, b and c show the progressive development of the power spectrum at the start of the test and then in the final stages. The spectral response in the low frequency range during the final minutes was dominated by the ball spin frequency harmonics, $4xf_{bsf}$ and $6xf_{bsf}$ as shown. No strong evidence of the inner race ball pass frequency was to be found below 5 kHz in the power spectrum. To investigate the nature of the coupling of the ball spin frequencies with other frequencies in the low frequency range, the bicoherence spectrum was computed using the sixth harmonic of ball spin as the fixed frequency component, ie $b^2(6xf_{bsf}, f)$. The results are shown in Figure 24d, e and f for the three power spectra displayed in Figure 24.

Figure 24d shows that for the bearing in the initial condition, the low amplitude ball spin frequency component at $6xf_{bsf}$ is not well correlated with any other frequency components. At 17.25 hours into the test, the frequency at $6xf_{bsf}$ is the largest component below 5 kHz, Figure 24b, and a significant amount of phase coupling occurs between the component at $6xf_{bsf}$ and inner race defect frequency harmonics and shaft frequency sidebands, Figure 24e. At the conclusion of the test, the coupling between the ball spin frequency component and the inner race defect frequency harmonic was further increased, Figure 24f. These results have demonstrated a number of significant points. Although no strong evidence of the inner race defect frequencies was found using the power spectrum, the bicoherence showed strong coupling with a large number of the inner race defect frequency harmonics and the ball spin frequency component. This has also provided further evidence that the component at $6xf_{bsf}$ was in fact a harmonic of the ball spin frequency and not an extraneous resonance.

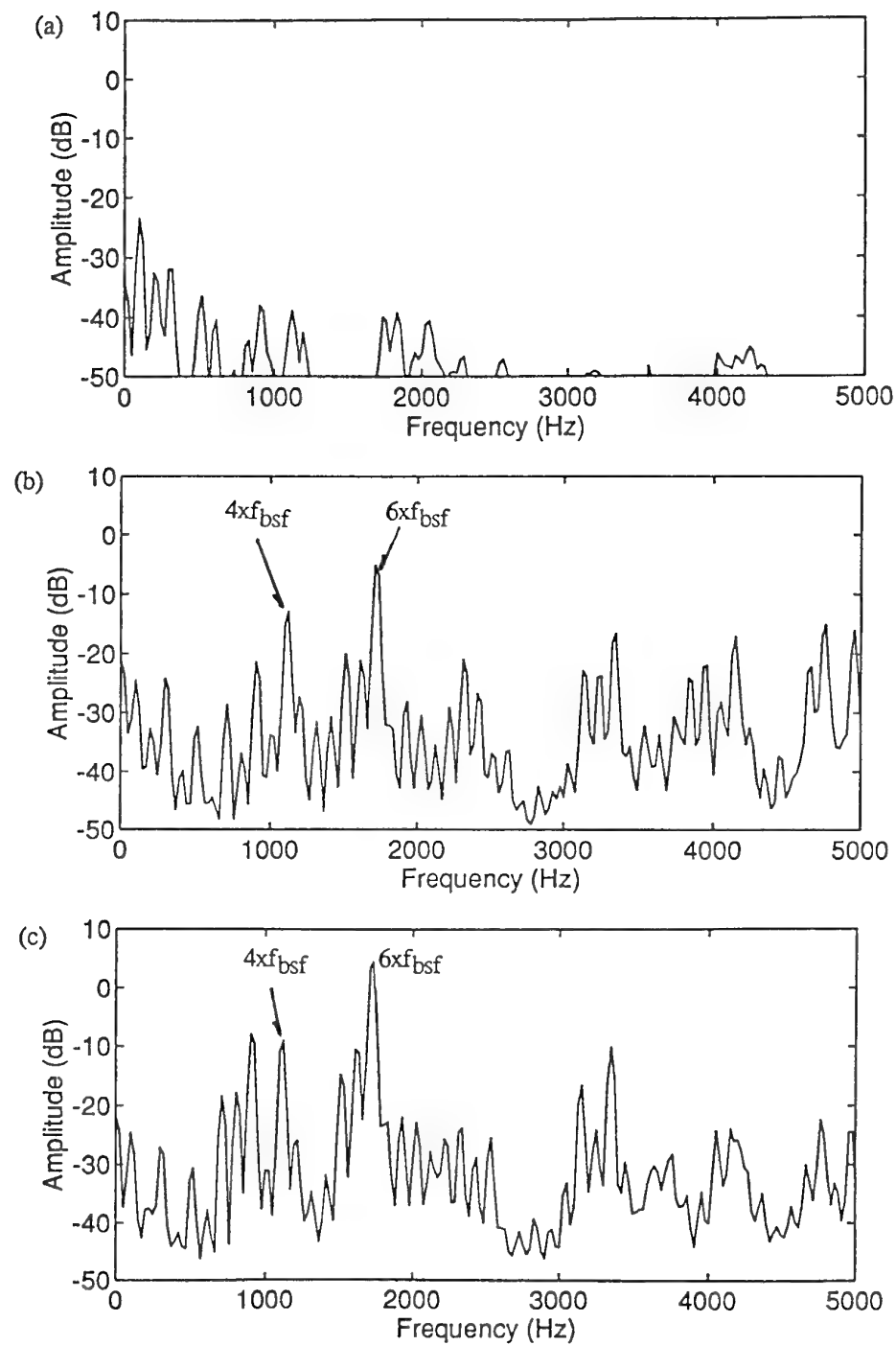


Figure 24. Power spectrum and bicoherence obtained from bearing test under overload and poor lubrication conditions. a) Power spectrum at 2.0 hours run time. b) Power spectrum at 17.25 hours run time. c) Power spectrum at 17.58 hours run time.

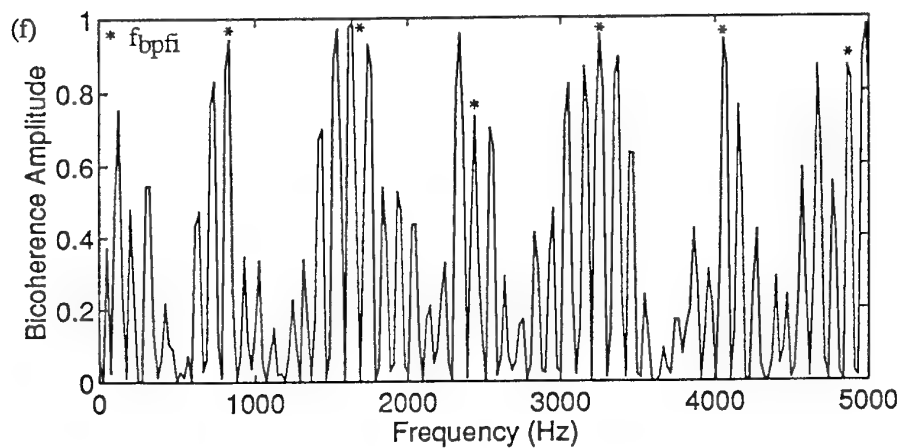
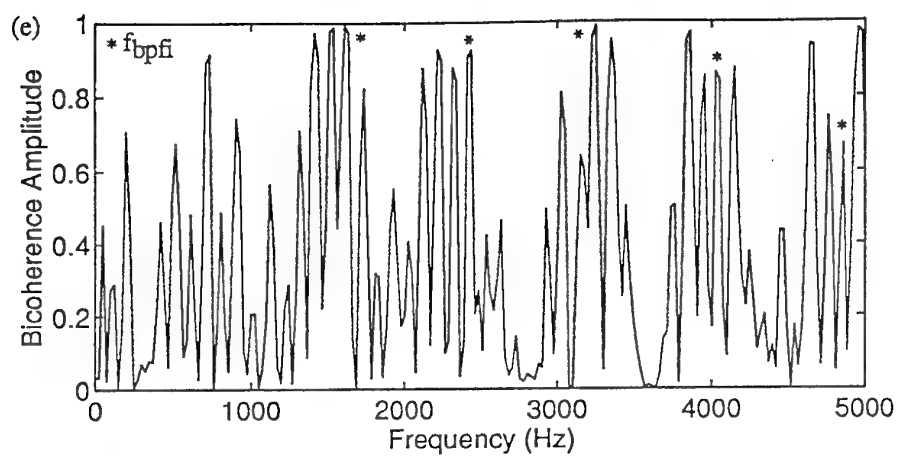
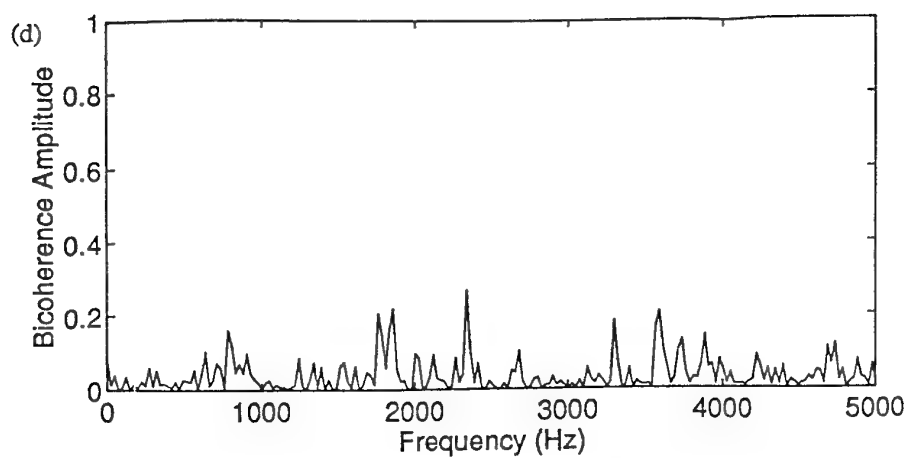


Figure 24(cont). d) Bicoherence at 2.0 hours run time. e) Bicoherence at 17.25 hours run time. f) Bicoherence at 17.58 hours run time.

The sensitivity of bicoherence analysis for bearing vibration analysis has been demonstrated in other publications [Coffin, et al, 1986, Li, et al, 1991]. It has also shown considerable potential to be used for trend purposes [Howard, 1993], which may provide a useful prognostic tool for predicting imminent catastrophic bearing failure.

5.7 Adaptive noise cancellation

A number of papers over the past decade have dealt with the use of adaptive noise cancellation (ANC) for bearing fault detection under low signal-to-noise conditions [Chaturvedi, et al, 1982, Bannister, 1985 and Tan, 1991]. Adaptive noise cancellation is achieved using two transducers. The 'principal' transducer is attached to the machine in the vicinity of the bearing to be monitored. This principal transducer contains the signal carrying the information relating to the fault condition combined with uncorrelated background noise. A secondary 'reference' transducer is also positioned onto the machine, but is located where it is thought the source of the background noise originates, and therefore possesses information correlated in some way to the noise measured by the principal transducer. This secondary position could, for example, be a compressor or gearbox, and should not contain information relating to the fault. The reference transducer is adaptively filtered to produce an output that is close to the principal uncorrelated noise, which is then subtracted from the principal input, resulting in attenuation of the background noise.

The adaptive filter is controlled by a feedback loop, taken from the system output and fed back into the filter, which is continuously adjusted to minimise the system output power. Figure 25 illustrates the adaptive noise cancelling principle [Bannister, 1985].

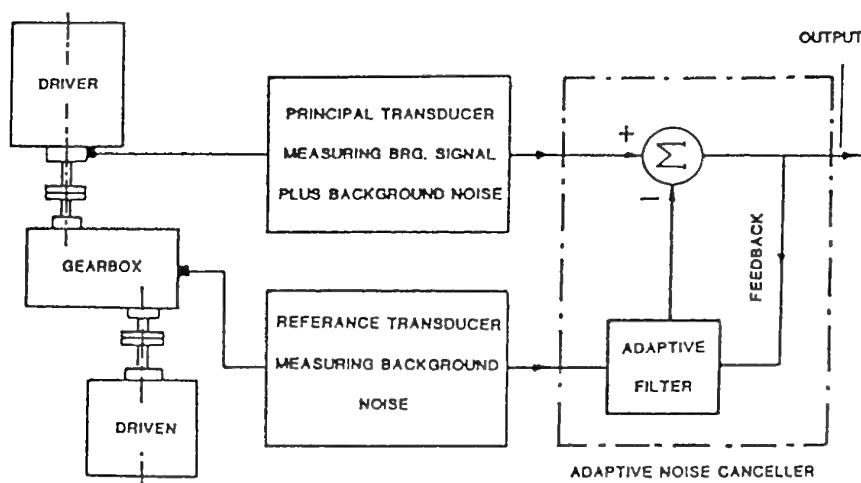


Figure 25. Schematic illustration of the adaptive noise cancellation principle.

The ANC technique can be implemented in conjunction with widely used signature analysis techniques such as spectrum analysis, time domain statistics and cepstrum analysis to improve the overall detection and diagnostic ability of these conventional techniques in the presence of severe noise.

5.8 The Haar transform

Although the FFT is probably the most popular transform used in signal processing, other transforms such as the Haar transform can also be defined [Yan, et al, 1990, Yan, et al, 1991 and Yan, et al, 1992]. The Haar function set forms a complete set of orthogonal rectangular functions, and the finite approximation to a function using the Haar function series converges more efficiently than the Fourier series. An example of the first eight Haar waveforms is shown in Figure 26.

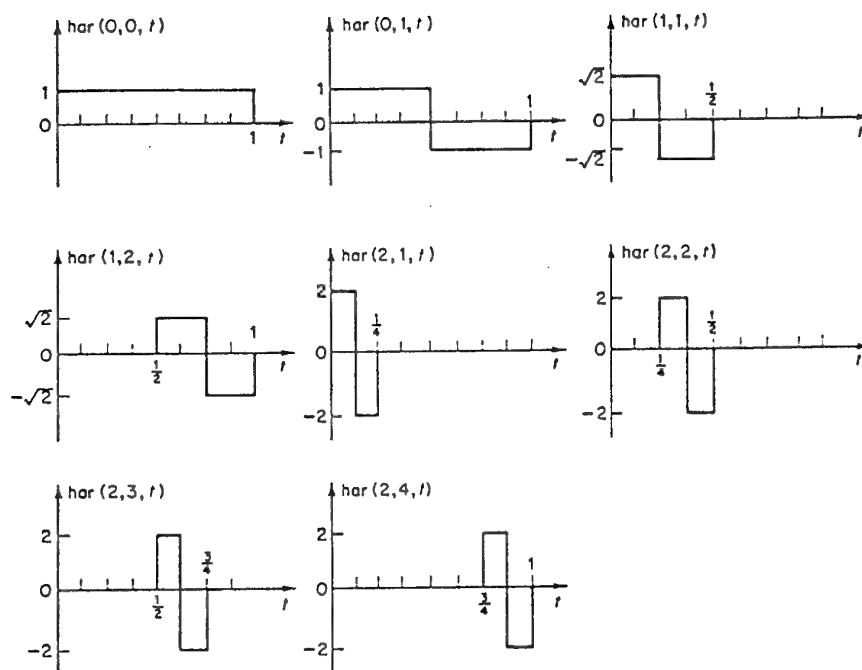


Figure 26. The first eight Haar functions [Yan, et al, 1992].

The Haar transform is especially suitable for detecting signal bursts and is computationally more efficient than the Fourier transform. The impulse index can be defined, based upon the Haar transform, as shown below [Yan, et al, 1990],

$$I(m) = \frac{\sum_{k=2^{m-1}}^{k=2^m-1} H^2(k)}{2^{m-1}}, \quad (56)$$

for $(m=1,2,\dots,M)$, where $M=\log_2 N$ denoting the dimension of the impulse index or the number of sequence groups. N is the dimension of the time series or the number of sampling points in the time history and H represents the Haar transform.

The impulse index represents the average power intensity contained in the Haar transform components falling into the equivalent sequence group [Yan, et al, 1990]. The equivalent sequence of the Haar function series is defined as one half the average number of zero crossings per unit time interval. The specific investigation of the Haar transform [Yan, et al, 1992] has shown that the impulse index compares favourably with the Fourier power spectrum in extracting useful information from vibration signals for bearing fault detection and in particular the index has excellent stability.

5.9 *Summary of techniques*

Section 5 has attempted to review the majority of techniques which have been published in the literature over the past two decades dealing with bearing vibration monitoring. Although the techniques are generally well known, a thorough comparison of the various techniques has not been attempted in the context of the class of machine and the mode of failure. This section attempts to summarise the various techniques, as given above, in the context of the mode of failure and the class of machine and the vibration environment.

The vibration environment and the class of machine as discussed in sections 2.4 and 2.6 will have a dramatic effect upon the types of vibration signal processing techniques which will be required to correctly identify a particular bearing fault. In selecting a technique for application to a particular machine class, the general principle should be, if a simple technique will be effective in providing enough warning of impending failure, then it should be used rather than the more complicated techniques.

In general there are two methods which can be used for machine condition monitoring, one-shot analysis and trending. It has been the author's experience that trending should always be used wherever possible. In the absence of trend data however, one-shot analysis can be effective. A number of techniques can be used for trending as detailed above. These include the time domain statistics, frequency domain parameters, envelope analysis parameters, cepstrum amplitudes and bispectrum amplitudes. The majority of these parameters will require detailed knowledge of the bearing defect frequencies to correctly diagnose bearing failure, while some of the more rudimentary parameters in the time and frequency domain can be used to detect significant changes in machine condition.

The one-shot techniques which have been demonstrated to be useful include some of the time domain statistics such as kurtosis, visual analysis of the time domain signal looking for periodic and transient features as well as the probability density distribution. Detailed frequency analysis can also be used to investigate the appearance of bearing-related frequencies in the baseband along with envelope spectrum analysis, cepstrum analysis and bispectrum analysis.

The time-frequency analysis techniques can also be used to investigate transient features such as impacts exciting resonances. The one-shot approach is much more time consuming than normal trending as it requires detailed knowledge of the class of machine and the range of bearing vibration excitation mechanisms which can occur. It would be normal for a much more thorough investigation to be required with the one-shot analysis than with the trending as it involves so called 'expert' interpretation rather than the blind application of statistics. Often for the more complex machines, the detailed investigation which is obtained by a hands-on look of the one-shot approach is required to correctly determine the presence of bearing damage. Figure 27 shows a flow chart of the approaches which can be used to detect bearing failure depending upon the class of machine, whether the mode of failure is known and whether previous history data is available. The diagnostic route is broken down into one of eight choices.

The actual mode of failure will be the most critical factor in determining the difficulty of vibration detection and diagnosis. As discussed in section 2.1, various modes of failure can occur. Localised fatigue damage of the bearing raceways and rolling elements will be the easiest failure mode to detect because the characteristic bearing defect frequencies are well understood. Wear and geometric form errors of the raceways can also give rise to periodic vibrations as the geometric errors will repeat with the cage rotation. For the majority of other failure modes, such as lubrication starvation, corrosion, excessive looseness or faulty installation, definitive vibration characteristics are not well understood and the use of comprehensive trending and/or the application of advanced signal processing will be required. For those instances where no significant vibration defect parameters can be found prior to failure, other forms of machinery health monitoring such as oil debris monitoring or temperature monitoring will be required. These other forms of monitoring should be used in any event, as no single approach can be guaranteed of detecting all defects, and confirmation of defects from multiple techniques reduces the possibility of false alarms.

The vibration environment in which the vibration transducer is located will also be of major importance in determining the effectiveness of the particular signal processing techniques which are used. The most obvious illustration will be in identifying the vibration defect frequencies using spectrum analysis. If the noise environment is so severe as to bury the frequencies in the spectrum, then spectral analysis may be of no use. The same can be said about the time domain parameters and many of the other techniques. Severe noise applications often require novel signal processing methods before the vibration defect features can be identified.

6.0 *Bearing Prognosis*

The subject of bearing prognosis is not new. A number of publications have addressed the topic over a number of years [Dyer, et al, 1978, Berggren, et al, 1983, Randall, 1985, Frarey, et al, 1986, Smith, et al, 1988, Harker, et al, 1989, Berry, 1991, Khan, 1991, McElroy, et al, 1991, Succi, 1991, Khan, 1992]. This section attempts to summarise the findings obtained from the published literature.

Bearing prognosis using vibration analysis is concerned with using the current and previous vibration data to predict the remaining life of a bearing. Traditionally, three stages of bearing life have been recognised [Frarey, et al, 1986, McElroy, et al, 1991 and Succi, 1991] although at times this has been increased to four [Berry, 1991]. The three stages have been known by different names such as (infant mortality, useful life, wear-out) or (good, damaged, failure imminent), or (prefailure, failure, near catastrophic/catastrophic) and have been defined by the standard 'bath tub' shaped curve which can be associated with systems that fail in a statistical manner. Bearings as an operating mechanical system of several components under favourable operating conditions tend to follow the typical 'bath tub' failure profile. They either fail early in their running life or last a reasonable time and then begin to wear out. It is possible to predict on a statistical basis when a bearing operating under known conditions will fail as detailed in section 4. However, what is required is knowledge of when a particular bearing is going to fail. This is where prognosis can help by providing estimations of the remaining life in the bearing.

Prognosis is based upon trending of vibration parameters. A large number of trend parameters are available as was observed in section 5. The question is, which parameters should be trended for a particular machine class with a particular mode of failure? A number of recent investigations have focused on prognosis of bearings using simple test rig natural bearing failures [Khan, 1991 and Succi, 1991], but it would be difficult to extrapolate the results to general industrial rotating machinery because of the different vibration environment and the range of failure modes which occur in practice. Two papers which have discussed prognosis of bearings in general industrial rotating machinery are [Randall, 1985 and Berry, 1991]. Randall [Randall, 1985], has shown that a range of parameters can be trended including overall levels, specific frequency components, cepstrum amplitudes and integrated frequency band amplitudes. He has suggested the use of fitting a straight line to the dB values (logarithmic scale) against a linear time scale. The estimated lead time can then be obtained by extrapolating the curve to reach a 20 dB change with respect to the baseline level.

A further problem arises when the trend increase is not uniform but step-wise [Randall, 1985]. An example was given for a developing spall within a rolling element bearing. From the trend curves, it was apparent that the fault developed over a period of four months, after which a stabilisation occurred for a further period of four months in operation until the machine was shut down for repair. Had the machine been allowed to continue in operation, the mechanism of sub-surface fatigue would have continued, eventually leading to further loss of metal

and the possibility of a more rapid breakdown. A number of faults such as spalls and cracks result in sudden step-wise changes which make trending extremely difficult.

The detailed investigation by Khan, [Khan, 1991], deserves further comment. He completed a number of endurance tests where bearings in a test rig were run for between 100 and 900 hours before failure. The tests included outer race damage, rolling element damage and inner race damage. A number of time domain parameters were computed and trended throughout the various tests including peak, RMS, Crest factor, Kurtosis, ratio of peak in 5-12.5 kHz to 0-5 kHz frequency band, ratio of RMS in 5-12.5 kHz to 0-5 kHz frequency band and the transducer resonance response measurement (RMS) in the 27-35 kHz frequency band. A number of frequency bands were used for the time domain statistics with the 5-12.5 kHz band found to provide the most sensitive results due primarily to the presence of a number of structural resonances in this region.

The parameters which were found to provide the most consistent trending information were peak and RMS acceleration for incipient detection while RMS band ratio (5-12.5 kHz to 0-5 kHz) and RMS velocity were more useful for advanced stages of damage. For predicting the remaining life left in the bearing, Khan used the criterion of a 20dB change postulated by Randall [Randall, 1985]. In particular, the RMS acceleration in the 5-12.5 kHz frequency band was used as a basis for the prediction. Rather than use a linear trend of dB values, Khan found that a reasonably straight line was obtained by using a double log of the RMS values, $\ln(\ln(\text{RMS}))$, displayed against a linear time scale from which a least squares fit could be used to estimate the safe operating life (20 dB gain) with a definable confidence band.

Bearing prognosis is seen by the author as one of the areas of work where room exists for further development, particularly for the more difficult classes of rotating machinery where a number of modes of failure could be expected. Unfortunately, the amount of vibration data which is available in this area is limited. It is hoped that this will be rectified in the future, particularly for helicopter transmissions and aircraft engines.

7.0 Discussion

This report has attempted to review the current knowledge on rolling element bearing fault detection, diagnosis and prognosis using vibration analysis. Consideration has been given to the basic underlying science of rolling element bearings including factors such as the modes of failure, kinematics, dynamics, stresses and forces generated at the contact points for the different components, transmission path effects and the class of machine. The vibration response resulting from classical localised fatigue failure of the bearing components is reasonably understood. However, a large number of failure mechanisms are known to exist for rolling element bearings such as wear, inadequate lubrication, faulty design, incorrect installation, corrosion damage, etc., for which the

vibration response is not well understood. Although these failure modes might give rise to localised fatigue failure later on, detection of the initial failure mechanism is difficult.

A large number of simple and advanced vibration signal processing techniques exist for detecting changes in mechanical condition of rotating machinery as outlined in this report. However, correct diagnosis of bearing damage requires the identification of the vibration which is generated by the specific mode of failure currently in existence. As mentioned by Bannister [Bannister, 1985], the art of machine condition monitoring is knowing what to look for, and successful diagnosis is having the ability to measure it and to correlate the results with known failure mechanisms.

Over the past decade, the understanding of signal processing techniques and their application to bearing fault detection has increased tremendously. The amount of information which can be gained from the vibration measured on rotating machinery is immense. It would be anticipated that the general use of advanced signal processing techniques will become more widespread in the future.

Advanced dynamic models have been developed for rolling element bearings as outlined in section 3.3. In the future, it is likely that these models will provide significant benefit for those concerned with machine condition monitoring as the effects of the more difficult modes of failure can be simulated. This should provide greater understanding of the vibration generation mechanisms and improve the ability for successful detection and diagnosis. A significant lack of experimental validation of the predictions of the dynamic models exists. Experimental validation of bearing dynamic response is seen as one area of growing importance in the future. In particular, experimental measurement of the transient forces and dynamic motions of the bearing components which arise when various imperfections and defects are encountered would increase our understanding of the underlying science of bearings and their vibration generation mechanisms.

This report has not undertaken a detailed comparison of the various signal processing techniques for bearing fault detection. Rather, an emphasis has been placed upon discussion of the underlying factors associated with bearings, their modes of failure and the vibration environment and class of machine. The next logical step would be to undertake a detailed comparison of techniques for the various modes of failure, class of machine, vibration environment, etc.

The work by Randall [Randall, 1985], Khan [Khan, 1991], and others has laid the foundation for significant progress to be made in the area of bearing prognosis. One of the difficulties in furthering this work will be the lack of vibration data from general industrial rotating machinery. However, it is hoped that the widespread use of electronic data collectors and on-line monitoring equipment which is now occurring, will overcome this problem, even for complex equipment such as helicopter transmissions and aircraft engines.

7.1 *Future research program*

A number of areas where further effort is warranted have come to light as a result of this report and these will be outlined below.

1. Detailed comparison of signal processing techniques.

Most so-called signal processing experts have their own favourite techniques which they use. It is difficult to undertake an objective comparison between the various techniques, particularly when commercial considerations regarding proprietary techniques and intellectual property come into play. The comparison of techniques should cover a range of machine types and a number of modes of failure.

2. Bearing prognosis.

The basic nature of the trends which occur in simple vibration levels over the life of a bearing is reasonably well understood. By undertaking a more advanced study using a variety of signal processing techniques, covering a range of classes of machines and modes of failure, it should be possible to build upon the work already in place to further advance the understanding of bearing prognosis.

3. Advanced dynamic modelling of various modes of failure.

Dynamic modelling of bearings has reached the stage of being able to simulate the effects of changes in raceway and rolling element profile as well as localised damage. This allows various modes of failure to be simulated and the resulting dynamics, forces and stresses to be predicted. This capability should be used along with models of the rotating machinery dynamics, transmission path effects and vibration environment to predict the resulting vibration which could be measured externally on the machine for various modes of failure.

4. Experimental work on the dynamics and forces of bearing components resulting from various modes of failure.

In conjunction with the dynamic modelling, experimental validation is required of the bearing dynamics which occur when various raceway and rolling element interactions occur. These include the effects of cage/roller and raceway/roller interaction, the skidding/slippage of rolling elements and cage instabilities. Further experimental determination of these effects would significantly add to the available knowledge of the underlying science of bearing operation and hence condition monitoring.

8.0 Conclusion

The art of machine condition monitoring is knowing what to look for, and successful diagnosis is having the ability to measure it and to correlate the results with known failure mechanisms [Bannister, 1985]. This report has attempted to address these issues in detail for rolling element bearings, and provide a review of the developments which have taken place over the last two decades.

Rolling element bearing vibration has been investigated by looking at the underlying science, including effects such as the mode of failure, dynamic response of the bearing to damage, transmission path effects, external noise and vibration, vibration measurement and the effect of the class of machine. These factors have been seen to play a most significant role in detection, diagnosis and prognosis of bearing damage. The two most important factors to be considered in bearing vibration monitoring have been seen to be the mode of failure and the class of machine. The vibration resulting from classical localised fatigue failure is relatively well understood and the characteristic bearing frequencies which can be found have been discussed in detail. This is in contrast to most other modes of failure such as wear, lubrication starvation, corrosion or faulty installation, etc., where the expected bearing vibrations are not well known. Much has been made of the effect of the class of machine on the difficulty in determining bearing condition. Simple rotating machinery should require simple diagnostic techniques in general, as contrasted with complex rotating machinery where more sophisticated methods will have to be used to detect incipient bearing failure.

A range of signal processing techniques have been discussed covering the time, frequency, cepstrum domains, envelope analysis, time-frequency analysis, higher order spectra, etc. An immense amount of information can be gleaned from the vibration measured external to rotating machinery. The difficulty lies in correctly transforming the information from the various techniques into knowledge about the condition of the rolling element bearings.

As an outcome of the review detailed in this report, a number of avenues for further work have been given, including a comparison of the signal processing techniques, further work on bearing prognosis, dynamic modelling of various modes of failure and experimental determination of the dynamics and forces resulting from various modes of failure.

Acknowledgments

The author would like to thank the machine dynamics staff at ARL for contributing to this report in a number of ways over the past year. Thanks in particular go to Mr. Brian Rebbeschi for providing the initial encouragement and impetus to undertake this investigation.

References/Bibliography

Acoustic Technology Ltd, "Autoderivative gas turbines - Bearing monitoring using advanced vibration diagnostic techniques". Noise and Vibration Worldwide, September 1990

B., Alavi, "Design optimisation of high speed axially loaded ball bearings of a turbo-pump. Canadian Acoustics, Vol. 19, No 4, September 1991, pp 55-56.

R.J. Alfredson and J. Mathew, "Time domain methods for monitoring the condition of rolling element bearings". Mechanical Engineering Transactions Vol. ME10, No. 2, The Institution of Engineers, Australia, July 1985, pp 102-117.

R.J. Alfredson and J. Mathew, "Frequency domain methods for monitoring the condition of rolling element bearings". Mechanical Engineering Transactions Vol. ME10, No. 2, The Institution of Engineers, Australia, July 1985, pp 108-112.

J.B. Allen and L.R. Rabiner, "A unified approach to short-time Fourier analysis and synthesis". Proceedings of the IEEE, Vol. 65, No. 11, 1977, pp 1558-1564.

F. Andersson, "Practical experience of the Mepa 10 A meter". Special Issue, Ball Bearing Journal, SKF, pp 26 - 31.

W.J. Anderson, "Rolling Element Bearings". Proceedings of the joint American Society of Mechanical Engineers and Society of Tribology and Lubrication Engineers Tribology Conference, Toronto, Ontario, Canada, October 7-10, 1990, pp 75-90.

S. Bagnoli, R. Capitani and P. Citti, "Comparison of accelerometer and acoustic emission signals as diagnostic tools in assessing bearing damage". Proceedings of the 2nd International Conference on Condition Monitoring, London, England, 24-25th May, 1988, pp 117-125.

H.E. Bandow, S.E. Gray and P.K. Gupta, "Performance simulation of a solid-lubricated ball bearing". Proceedings of the 40th Annual meeting of the American Society of Lubrication Engineers, Las Vegas, Nevada, May 6-9, 1985.

R.H. Bannister, "The use of ultrasound to monitor incipient failure of rolling element bearings". Proceedings of the Mechanism Conference, Cranfield, July 1984, Vol. 1.

R. H. Bannister, "A review of rolling element bearing monitoring techniques". IMECH.E Conference on Condition Monitoring of Machinery and Plant, 1985, pp 11-24.

G.H. Bate, "Vibration diagnostics for industrial electric motor drives". Bruel and Kjaer Application Note No. 269-12.

D. Bell, "An enveloping technique for the detection and diagnosis of incipient faults in rolling element bearings". Vibration analysis to improve reliability and reduce failure, Proceedings of the Design Automation Conference, Cincinnati, OHIO, September 10-13, 1985, pp 65-69.

J.C. Berggren, "Malfunction diagnosis of rolling element bearings". Technological advances in engineering and their impact on detection, diagnosis and prognosis methods, Proceedings of the 36th meeting of the Mechanical Failures Prevention Group, Cambridge University Press, 1983, pp 157-172.

J.E. Berry, "How to track rolling element bearing health with vibration signature analysis". Sound and Vibration, November 1991, pp 24-35.

F. Berryman, P. Michie, A. Smulders and K. Vermeiren, "Condition monitoring - a new approach. A method of monitoring machines using a High Frequency Acoustic Emission Technique". SKF Engineering and Research Centre, The Netherlands.

A.G. Bessios and C.L. Nikias, "FFT based bispectrum computation on polar rasters". IEEE Transactions on Signal Processing, Vol. 39, No. 11, November 1991, pp 2535-2539.

A.K. Bhattacharjee, A.K. Chatterjee, B.N. Panda and R. Devanathan, "Condition assessment of antifriction bearings by shock pulse method - Case Studies". Journal of Condition Monitoring and Diagnostic Technology, Vol. 3, No. 2, November 1992, pp 52-56.

B. Boashash and P.J. Black, "An efficient real-time implementation of the Wigner-Ville distribution". IEEE Transactions on Acoustics, Speech, and Signal Processing, Vol. ASSP-35, No. 11, November 1987, pp 1611-1618.

B. Boashash and P. O'Shea, "A methodology for detection and classification of some underwater acoustic signals using time-frequency analysis techniques". IEEE Transactions on Acoustics, Speech, and Signal Processing, Vol. 38, No. 11, November 1990, pp 1829-1841.

E.A. Boesiger, A.D. Donley and S. Loewenthal, "An analytical and experimental investigation of ball bearing retainer instabilities". Transactions of the American Society of Mechanical Engineers, Journal of Tribology, Vol. 114, July 1992, pp 530-539.

B.P. Bogert, M.J.R. Healy and J.W. Tuckey, "The quefrency alalysis of time series for echoes: Cepstrum, pseudo-autocovariance, cross-cepstrum and saphe cracking". Proceedings of the Symposium on time series analysis by Rosenblatt, M., (Ed.), Wiley, N.Y. 1963, pp 209-243.

P.A. Boto, "Detection of bearing damage by shock pulse measurement". Ball Bearing Journal Vol. 167, 1971, pp 1-7.

S. Braun and B. Datner, "Analysis of roller/ball bearing vibrations". Transactions of the American Society of Mechanical Engineers, Journal of Mechanical Design, Vol. 101, January 1979, pp 118-125.

D.N. Brown, "Machine condition monitoring using vibration analysis - A case study from a Nuclear power plant". Bruel and Kjaer Application Note No. 209-11.

D.N. Brown and T. Jensen, "Machine condition monitoring using vibration analysis. The use of crest factor and cepstrum analysis for bearing fault detection - A case study from Kenogami paper mill, Quebec, Canada". Bruel and Kjaer Application Note No. 252-11.

D.N. Brown and T. Jensen, "Machine condition monitoring using vibration analysis. The use of spectrum comparison for bearing fault detection - A case study from Alma paper mill, Quebec, Canada". Bruel and Kjaer Application Note No. 253-11.

D.N. Brown and T. Jensen, "Peak and envelope analysis for bearing fault detection - A case study from a Pacific North-West mill, USA". Bruel and Kjaer Application Note No. 286-11.

Bruel and Kjaer, "Machine Health Monitoring Using Vibration Analysis". Proceedings of the workshop presented by J. Courrech and R.B. Randall, Monash University, 17th September, 1990.

K.M. Cena and R.A. Hobbs, "The effects of ball quality, radial clearance and grease specification on the noise and vibration of an electric motor". I.MECH.E Conference Paper C103/72, 1972, pp 93-102.

J.C. Chann, "Online ultrasonic monitoring of bearing wear". Proceedings of the nineteenth turbomachinery symposium, Dallas, Texas, September 18-20, 1990, pp 91-98.

G.K. Chaturvedi and D.W. Thomas, "Bearing Fault Detection using Adaptive Noise Cancelling". Transactions of the American Society of Mechanical Engineers, Journal of Mechanical design, Vol. 104, April 1982, pp 280-289.

F.H.K. Chen, "Applications of spectrograms to practical signature analysis problems". Proceedings of the 7th International Modal Analysis Conference, Las Vegas, Nevada, January 30th - February 2nd, 1989, pp 1571-1576.

D.G. Childers, D.P. Skinner and R.C. Kemerait, "The Cepstrum: A guide to processing". Proceedings of the IEEE, Vol. 65, No. 10, October 1977, pp 1428-1443.

P. Chivers and P. Gadd, "Monitoring of rolling element bearings using vibration analysis techniques". NGAST 6638 Feasibility Study, June 1986.

T.A.C.M. Claasen and W.F.G. Mecklenbrauker, "The Wigner distribution - a tool for time - frequency signal analysis, Part I: Continuous time signals". Phillips Journal of Research, Vol. 35, No. 3, 1980, pp 217-250.

T.A.C.M. Claasen and W.F.G. Mecklenbrauker, "The Wigner distribution - a tool for time - frequency signal analysis, Part II: Discrete time signals". Phillips Journal of Research, Vol. 35, No. 4/5, 1980, pp 276-300.

T.A.C.M. Claasen and W.F.G. Mecklenbrauker, "The Wigner distribution - a tool for time - frequency signal analysis, Part III: Relations with other time-frequency signal transformations". Phillips Journal of Research, Vol. 35, No. 6, 1980, pp 372-389.

M.A. Cody, "The Fast Wavelet Transform: beyond Fourier Transforms". Dr. Dobb's Journal, April 1992, pp 16-28.

T. Coffin and J.Y. Jong, "Signal detection techniques for diagnostic monitoring of Space Shuttle Main Engine Turbomachinery". Wyle Laboratories Technical Report 66938-01. A final report of work performed for NASA Marshall under contract NAS8-34961. February 1986.

J.M. Combes, A. Grossmann and Ph. Tchamitchian, (Eds.), "Wavelets: Time-Frequency methods and phase space". Proceedings of the International Conference, Marseille, France, December 14-18, 1987.

J. Courrech, "New techniques for fault diagnosis in rolling element bearings". Proceedings of the 40th Mechanical Failures Prevention Group, Maryland, April 1985, pp 83-91.

R. Czaja, "Stress Wave Sensors". Helitune Limited, Private Communication, August 1990.

A. Daadbin and J.C.H. Wong, "Different vibration monitoring techniques and their application to rolling element bearings". International Journal of Mechanical Engineering Education, Vol. 19, No. 4, 1991, pp 295-304.

M.S. Darlow, R.H. Badgley and G.W. Hogg, "Application of high frequency resonance techniques for bearing diagnostics in helicopter gearboxes". US Army Air Mobility Research and Development Laboratory Technical Report-74-77, October 1974.

I. Daubechies, "The Wavelet Transform, time-frequency localization and signal analysis". IEEE Transactions on Information Theory, Vol. 36, No. 5, September 1990, pp 961-1005.

I. Daubechies, "Ten Lectures on Wavelets". CBMS-NSF Regional Conference Series in Applied Mathematics, Philadelphia, Pennsylvania, 1992.

R.R. Davis and C.S. Vallance, "Incorporating general race and housing flexibility and deadband in rolling element bearing analysis". NASA Lewis Research Center, Rotordynamic Instability Problems in High-Performance Turbomachinery, 1988, pp 373-387.

C. Dorize and K. Gram-Hansen, "Related positive time-frequency energy distributions". Proceedings of the International Congress on Wavelets and some of their applications, Marseille, June 1989.

D.A. Dousis, "A vibration monitoring acquisition and diagnostic system for helicopter drive train bench tests". Proceedings of the 48th Annual forum of the American Helicopter Society, Washington, D.C., June 3-5, 1992, pp 355-369.

D. Dyer and R.M. Stewart, "Detection of rolling element bearing damage by statistical vibration analysis". Transactions of the American Society of Mechanical Engineers, Journal of Mechanical Design, Vol. 100, April 1978, pp 229-235.

M.A. Elbestawi and H.J. Tait, "A comparative study of vibration monitoring techniques for rolling element bearings". Proceedings of the 3rd International Modal Analysis Conference, 1985, pp 1510-1517.

I.K. Epps and H. McCallion, "An investigation into the characteristics of vibrations excited by discrete faults in rolling element bearings". Department of Mechanical Engineering, University of Canterbury, New Zealand.

P. Eschmann, L. Hasbargen and K. Weigand, *Ball and roller bearings - Theory, Design and Application*. John Wiley and Sons, 2nd Edition 1985.

R.L. Eshleman, "The role of sum and difference frequencies in rotating machinery fault diagnosis". Proceedings of the 2nd International Conference on Vibrations in Rotating Machinery, I.Mech.E. paper C272/80, 1980, pp 145-149.

R.L. Florom, A.R. Hiatt, J.E. Bambara and R.L. Smith, "Wayside acoustic detection of railroad roller bearing defects". Proceedings of the ASME Winter Annual Meeting, Boston, Massachusetts, December 13-18, 1987.

B.D. Forrester, "Analysis of gear vibration in the time-frequency domain". Proceedings of the 44th meeting of the Mechanical Failures Prevention Group, Virginia Beach, Virginia, April 1990, pp 225-234.

J. Frarey and R.L. Smith, "Acoustic signatures of various roller bearing defects". 1986 IEEE/ASME Joint Railroad Conference.

D. Gore and G. Edgar, "Techniques for the early detection of rolling-element bearing failures". Radio Corporation of America-RCA Engineer, September-October 1984, Vol. 29, No. 5, pp 71-77.

K. Gram-Hansen and C. Dorize, "On the choice of parameters for time-frequency analysis". Proceedings of the International Congress on Wavelets and some of their applications, Marseille, June 1989.

L.M. Greenhill and R.L. Bickford, "Modelling of rolling element bearings". Aerojet Propulsion Division Monthly Report for NASA Marshall, Contract NAS 8-38607, February 1991.

P.K. Gupta, "Transient ball motion and skid in ball bearings". Transactions of the American Society of Mechanical Engineers, Journal of Lubrication Technology, April 1975, pp 261-269.

P.K. Gupta, "Dynamics of rolling element bearings Part I: Cylindrical Roller Bearing Analysis". Transactions of the American Society of Mechanical Engineers, Journal of Lubrication Technology, Vol. 101, July 1979, pp 293-304.

P.K. Gupta, "Dynamics of rolling element bearings Part II: Ball Bearing Analysis". Transactions of the American Society of Mechanical Engineers, Journal of Lubrication Technology, Vol. 101, July 1979, pp 305-311.

P.K. Gupta, "Dynamics of rolling element bearings Part III: Ball Bearing Analysis". Transactions of the American Society of Mechanical Engineers, Journal of Lubrication Technology, Vol. 101, July 1979, pp 312-318.

P.K. Gupta, "Dynamics of rolling element bearings Part IV: Ball Bearing Results". Transactions of the American Society of Mechanical Engineers, Journal of Lubrication Technology, Vol. 101, July 1979, pp 319-326.

P.K. Gupta, "Some dynamic effects in high-speed solid-lubricated ball bearings". Proceedings of the ASLE/ASME Lubrication Conference, New Orleans, Louisiana, October 5-7, 1981.

P.K. Gupta, *Advanced dynamics of rolling element bearings*. Springer Verlag 1984.

P.K. Gupta, J.F. Dill and H.E. Bandow, "Dynamics of rolling element bearings: Experimental validation of the DREB and RAPIDREB computer programs". Transactions of the American Society of Mechanical Engineers, Journal of Tribology, Vol. 107, January 1985, pp 132-137.

P.K. Gupta and T.E. Tallian, "Rolling Bearing Life Prediction - Correction for materials and operating conditions. Part III: Implementation in bearing dynamics computer codes". Transactions of the American Society of Mechanical Engineers, Journal of Tribology, Vol. 112, January 1990, pp 23-26.

B.J. Hamrock and W.J. Anderson, "Rolling element bearings". NASA Lewis Research Center, NASA RP- 1105, June 1983.

R.G. Harker and J.S. Hansen, "Rolling element bearing monitoring using high gain eddy current transducers". Transactions of the American Society of Mechanical Engineers, Journal of Engineering for Gas Turbines and Power, Vol. 107, January 1985.

R.G. Harker and J.L. Sandy, "Rolling element bearing monitoring and diagnostics techniques". Transactions of the American Society of Mechanical Engineers, Journal of Engineering for Gas Turbines and Power, Vol. 111, April 1989, pp 251-256.

M.W. Hawman and W.S. Galinaitis, "Acoustic emission monitoring of rolling element bearings". Proceedings of the IEEE 1988 Ultrasonics Symposium, pp 885-889.

A.G. Herraty, "Bearing vibration - failures and diagnosis". Mining Technology, February 1993, pp 51-53.

M.J. Hine, "Absolute ball bearing wear measurements from SSME turbopump dynamic signals". Journal of Sound and Vibration, Vol. 128, No. 2, 1989, pp 321-331. Also presented at the 59th Shock and Vibration Symposium, Albuquerque, New Mexico, October 1988.

F. Hlawatsch and G.F. Boudreaux-Bartels, "Linear and Quadratic time-frequency signal representations". IEEE Signal Processing Magazine, April 1992, pp 21-67.

M.R. Hoeprich, "Rolling element bearing fatigue damage propogation". Transactions of the American Society of Mechanical Engineers, Journal of Tribology, Vol. 114, April 1992, pp 328-333.

T.J. Holroyd and N. Randall, "Use of acoustic emission for machine condition monitoring". British Journal of Non-Destructive Testing, Vol. 35, No. 2, February 1993.

D.R. Houser and M.J. Drosjack, "Vibration signal analysis techniques". US Army Air Mobility Research and Development Laboratory Technical Report-73-101, December 1973.

I.M. Howard and G.W. Stachowiak, "Detection of surface defects in rolling element bearings". The Institution of Engineers, Australia, Mechanical Engineering Transactions, Vol. 13, 1989, pp 158-164.

I.M. Howard and Y.Y. Link, "Vibration analysis for bearing fault detection". Proceedings of the 1991 Asia-Pacific Vibration Conference, Monash University, Melbourne, Australia, December 1991, pp 5.10-5.17.

I.M. Howard, "Signal processing techniques for mechanical diagnosis of Space Shuttle Main Engine turbomachinery using vibration analysis". Technology Integration Incorporated Report R9301-002-RD. A report on data analysis performed under contract NAS8-38955, January 1993.

T. Igarashi and H. Hamada, "Studies on the vibration and sound of defective rolling bearings (First Report: Vibration of ball bearings with one defect)". Bulletin of the Japanese Society of Mechanical Engineers, Vol. 25, No. 204, June 1982, pp 994-1001.

T. Igarashi and H. Hamada, "Studies on the vibration and sound of defective rolling bearings (Second Report: Sound of ball bearings with one defect)". Bulletin of the Japanese Society of Mechanical Engineers, Vol. 26, No. 220, October 1983, pp 1791-1798.

T. Igarashi and H. Hamada, "Studies on the vibration and sound of defective rolling bearings (Third Report: Vibration of ball bearing with multiple defects)". Bulletin of the Japanese Society of Mechanical Engineers, Vol. 28, No. 237, March 1985, pp 492-499.

V.D., Jayaram and F. Jarchow, "Experimental studies on ball bearing noise". Wear, Vol 46, 1978, pp 321-326.

C.J. Jenkins, L.V. Embling and D.A. Cordner, "The prediction and measurement of bearing transfer functions at high frequencies". Proceedings of the 3rd International Conference on Vibrations in Rotating Machinery. University of York, Heslington, Yorkshire, September 11-13, 1984. IMECH.E. Paper C268/84, pp 295-302.

L. Johansson, "Bearing noise in electric motors". Ball Bearing Journal Vol. 200, pp 28-31.

D.D. Johnson, "Implementing integrated predictive maintenance". Maintenance Technology July 1992, pp 28-31.

J.Y. Jong, T. Coffin, J.H. Jones, J.E. McBride and P.C. Jones, "Correlation identification between spectral components in turbomachinery measurements by generalized hypercoherence". Proceedings of the 3rd International Machinery Monitoring and Diagnostics Conference, Las Vegas, Nevada, December 9-12 1991, pp 243-248.

H. Kanai, M. Abe and K. Kido, "Estimation of the surface roughness on the race or balls of ball bearings by vibration analysis". Transactions of the American Society of Mechanical Engineers, Journal of Vibration, Acoustics, Stress, and Reliability in Design, Vol. 109, January 1987, pp 60-68.

S.M. Kay and S.L. Marple, "Spectrum analysis - A modern perspective". Proceedings of the IEEE, Vol. 69, No. 11, November 1981, pp 1380-1419.

R. Kazikowski, "The effect of lubricants on the vibration of rolling bearings". NLGI Spokesman, February 1977, pp 389-395.

J.E. Keba, "Component test results from the bearing life improvement program for the Space Shuttle Main Engine Oxidizer Turbopumps". Proceedings of the 3rd International Symposium on Rotating Machinery, Honolulu, HI, 1990, pp 303-318.

R.J. Kershaw, "Machine diagnostics with combined vibration analysis techniques". Proceedings of the 41st Meeting of the Mechanical Failures Prevention Group, October 1986, pp 160-168.

A.F. Khan, "Condition monitoring of rolling element bearings: A comparative study of vibration based techniques". Ph.D. Thesis, University of Nottingham, May 1991.

A.F. Khan and E.J. Williams, "Predicting the remaining life of rolling element bearings". Proceedings of IMECH.E. Conference on Vibrations in Rotating Machinery, University of Bath, September 7-10, 1992, pp 403-408.

P.Y. Kim, "A review of rolling element bearing health monitoring (III): preliminary test results on eddy current proximity transducer technique". Proceedings of the 3rd International Conference on Vibrations in Rotating Machinery, York, U.K., September 11-13, 1984, pp 119-125.

P.Y. Kim, "Proximity transducer technique for bearing health monitoring". Journal of Propulsion, Vol. 3, No. 1, 1987, pp 84-89.

Y.C. Kim and E.J. Powers, "Digital bispectral analysis and its applications to non-linear wave interactions". IEEE Transactions on Plasma Science, Vol. PS-7, No. 2, June 1977, pp 120-131.

Y.H. Kim, W.S. Cheung and Y.K. Kwak, "Complex envelope of the vibration signature of ball bearing system and its application to fault detection". Proceedings of the 6th International Congress on Experimental Mechanics, Portland, Oregon. June 1988, pp 1067-1071.

Y.H. Kim, B.D. Lim and W.S. Cheoung, "Fault detection in a ball bearing system using a moving window". Mechanical Systems and Signal Processing, Vol. 5, No. 6, 1991, pp 461-473.

T. Koizumi, M. Kiso and R. Taniguchi, "Preventive maintenance for roller and journal bearings of induction motor based on the diagnostic signature analysis". Transactions of the American Society of Mechanical Engineers, Journal of Vibration, Acoustics, Stress, and Reliability in Design, Vol. 108, January 1986, pp 26-31.

B.T. Kuhnell and J.S. Stecki, "Correlation of vibration, wear debris analysis and oil analysis in rolling element bearing condition monitoring". Maintenance Management International, Vol. 5, 1985, pp 105-115.

M.S. Lai, "Detection of developing bearing failures by means of vibration analysis". Ph. D. Thesis, University of Windsor, Ontario, Canada, 1990.

M.F. Lester, "Minex". Mining Technology, April 1986, pp 115-118.

C.J. Li and S.Y. Li, "Acoustic emission analysis for bearing condition monitoring". Proceedings of the 44th Meeting of the Mechanical Failures Prevention Group, April 1990, Virginia Beach, Virginia, pp 249-258.

C.J. Li, J. Ma, B. Hwang and G.W. Nickerson, "Bispectral analysis of vibrations for bearing condition monitoring". Proceedings of the 3rd International Machinery Monitoring and Diagnostics Conference, Las Vegas, Nevada, December 9-12 1991, pp 225-231.

C.J. Li, J. Ma, B. Hwang and G.W. Nickerson, "Pattern recognition based bicoherence analysis of vibrations for bearing condition monitoring". Proceedings of the Symposium on Sensors, Controls and Quality Issues in Manufacturing, ASME Winter Annual Meeting, Atlanta Georgia, December 1991, pp 1-11.

C.J. Li and J. Ma, "Bearing localized defect detection through wavelet decomposition of vibrations". Proceedings of the 46th Meeting of the Mechanical Failures Prevention Group, April 7-9, 1992, Virginia Beach, Virginia, pp 53-62.

C.J. Li and S.M. Wu, "On-line severity assessment of bearing damage via defect sensitive resonance identification and matched filtering". Mechanical Systems and Signal Processing, Vol. 2, No. 3, 1988, pp 291-303.

C.Q. Li and C.J.D. Pickering, "Robustness and sensitivity of non-dimensional amplitude parameters for diagnosis of fatigue spalling". Condition Monitoring and Diagnostic Technology, Vol. 2, No. 3, January 1992, pp 81-84.

I. Liddle and S. Reilly, "Diagnosing vibration problems with an expert system". ASME Mechanical Engineering Magazine, Vol. 115, No. 4, April 1993, pp 54-55.

T.C. Lim and R. Singh, "Vibration transmission through rolling element bearings, Part I: Bearing stiffness formulation". Journal of Sound and Vibration, Vol. 139, No. 2, 1990, pp 179-199.

T.C. Lim and R. Singh, "Vibration transmission through rolling element bearings, Part II: System Studies". Journal of Sound and Vibration, Vol. 139, No. 2, 1990, pp 201-225.

T.C. Lim and R. Singh, "Vibration transmission through rolling element bearings, Part III: Geared rotor system studies". Journal of Sound and Vibration, Vol. 151, No. 1, 1991, pp 31-54.

M. Luo and B.T. Kuhnell, "Diagnosis of rotating machine fault using grey relational grade analysis". Condition Monitoring and Diagnostic Technology, Vol. 2, No. 4, May 1992, pp 119-124.

R.H. Lyon, "Failure detection and diagnostics using the cepstrum". Proceedings of the 40th meeting of the Mechanical Failures Prevention Group, Maryland, April 1985, pp 112-121.

R.H. Lyon, *Machinery Noise and Diagnostics*. Butterworth Publishers 1987.

S.G. Mallat, "A theory of multiresolution signal decomposition: The Wavelet representation". IEEE Transactions on Pattern Analysis and Machine Intelligence, Vol. 11, No. 7, July 1989, pp 674-693.

B.G. Marchenko, E.P. Osadchii and L.D. Protsenko, "Using a model of rolling-bearing vibroacoustic noise for diagnostics". Power Engineering, Vol. 22, No. 2, 1984, pp 165-172.

H.R. Martin, "Statistic moment analysis as a means of surface damage detection". Proceedings of the 7th International Modal Analysis Conference, Nevada, 1989, pp 1016-1021.

H.R. Martin, F. Ismail and A. Sakuta, "Algorithms for statistical moment evaluation for machine health monitoring". Mechanical Systems and Signal Processing, Vol. 6, No. 4, 1992, pp 317-327.

J. Mathew, "Machine condition monitoring using vibration analysis". Journal of the Australian Acoustical Society, Vol. 15, No. 1, 1987, pp 7-13.

J. Mathew, "Monitoring the vibrations of rotating machine elements - An overview". The Bulletin of the Centre of Machine Condition Monitoring, Monash University, Vol. 1, No. 1, 1989, pp 2.1-2.13.

T. Matsuoka and T.J. Ulrych, "Phase estimation using the bispectrum". Proceedings of the IEEE, Vol. 72, No. 10, October 1984, pp 1403-1411.

A.J. McElroy and I. Fruchtman, "Use statistical analysis to predict equipment reliability". Power, October 1991, pp 39-46.

P.D. McFadden and J.D. Smith, "Vibration monitoring of rolling element bearings by the high frequency resonance technique - a review". Tribology International, Vol. 17, No. 1, February 1984, pp 3-10.

P.D. McFadden and J.D. Smith, "Acoustic emission transducers for the vibration monitoring of bearings at low speeds". Proceedings of the Institution of Mechanical Engineers, Vol. 198C, No. 8, 1984, pp 127-130.

P.D. McFadden and J.D. Smith, "Model for the vibration produced by a single point defect in a rolling element bearing". Journal of Sound and Vibration, Vol. 96, No. 1, 1984, pp 69-82.

P.D. McFadden and J.D. Smith, "Model for the vibration produced by multiple point defects in a rolling element bearing". Journal of Sound and Vibration, Vol. 98, No. 2, 1985, pp 263-273.

P.D. McFadden, "Condition monitoring of rolling element bearings by vibration analysis". Proceedings of the IMECH.E. Machine Condition Monitoring Seminar, January 9th, 1990, pp 49-53.

P.D. McFadden and W.J. Wang, "Time-frequency domain analysis of vibration signals for machinery diagnostics. (I) Introduction to the Wigner-Ville Distribution". University of Oxford, Department of Engineering Science, Report No. OUEL 1859/90, 1990.

P.D. McFadden and W.J. Wang, "Time-frequency domain analysis of vibration signals for machinery diagnostics. (II) The Weighted Wigner-Ville Distribution". University of Oxford, Department of Engineering Science, Report No. OUEL 1891/91, 1991.

S.W. McMahon, "Condition monitoring of bearings using ESP". Condition Monitoring and Diagnostic Technology, Vol. 2, No. 1, July 1991, pp 21-25.

C.K. Mechefske and J. Mathew, "A comparison of frequency domain trending and classification parameters when used to detect and diagnose faults in low speed rolling element bearings". The Bulletin of the Centre of Machine Condition Monitoring, Monash University, Melbourne, Australia, Vol. 3, No. 1, 1991, pp 4.1-4.7.

C.K. Mechefske and J. Mathew, "Automatic fault diagnosis in rolling element bearings using nearest neighbour classification". The Bulletin of the Centre of Machine Condition Monitoring, Monash University, Melbourne, Australia, Vol. 2, No. 1, 1990, pp 8.1-8.5.

C.K. Mechefske and J. Mathew, "Diagnosing faults in rolling element bearings using parametric spectra and snob unsupervised classification". The Bulletin of the Centre of Machine Condition Monitoring, Monash University, Melbourne, Australia, Vol. 3, No. 1, 1991, pp 6.1-6.8.

C.K. Mechefske and J. Mathew, "Bearing gradual deterioration trending using parametric spectra". The Bulletin of the Centre of Machine Condition Monitoring, Monash University, Melbourne, Australia, Vol. 3, No. 1, 1991, pp 2.1-2.6.

C.K. Mechefske and J. Mathew, "Fault detection and diagnosis in low speed rolling element bearings using parametric spectra". The Bulletin of the Centre of Machine Condition Monitoring, Monash University, Melbourne, Australia, Vol. 2, No. 1, 1990, pp 3.1-3.5.

C.K. Mechefske and J. Mathew, "Fault detection and diagnosis in low speed rolling element bearings Part I: The use of parametric spectra". Mechanical Systems and Signal Processing, Vol. 6, No. 4, 1992, pp 297-307.

C.K. Mechefske and J. Mathew, "Fault detection and diagnosis in low speed rolling element bearings Part II: The use of nearest neighbour classification". Mechanical Systems and Signal Processing, Vol. 6, No. 4, 1992, pp 309-316.

C.K. Mechefske and J. Mathew, "Parametric spectral trending and classification for monitoring low speed bearings". Proceedings of the Asia-Pacific Vibration Conference, Monash University, Melbourne, Australia, November 1991, pp 5.42-5.48.

Q. Meng and L. Qu, "Rotating machinery fault diagnosis using Wigner Distribution". Mechanical Systems and Signal Processing, Vol. 5, No. 3, 1991, pp 155-166.

L.D. Meyer, F.F. Ahlgren and B. Weichbrodt, "An analytic model for ball bearing vibrations to predict vibration response to distributed defects". Transactions of the American Society of Mechanical Engineers, Journal of Mechanical Design, Vol. 102, April 1980, pp 205-210.

R. Milne, J. Aylett, S. McMahon and T. Scott, "Portable bearing diagnostics using enveloping and expert systems". Proceedings of COMADEM 91, pp 75-79.

T. Moriuchi and H. Kageyama, "Lubricating grease noise test in ball bearings". Proceedings of the JSLE International Tribology Conference, Tokyo, Japan, July 8-10, 1985, pp 1027-1032.

J.M. de Mul, J.M. Vree and D.A. Mass, "Equilibrium and associated load distribution in ball and roller bearings loaded in five degrees of freedom while neglecting friction, Part II: Application to roller bearings and experimental verification". Transactions of the American Society of Mechanical Engineers, Journal of Tribology, Vol. 111, January, 1989, pp 149-155.

A.J. Mordin and A.J. Penter, "An on-line vibration analysis system for a marine gas turbine". Proceedings of I.MECH.E. Conference on Vibrations in Rotating Machinery, University of Bath, September 7-10, 1992, pp 441-449.

D. Muster, "Condition monitoring and diagnostics of systems and their relationship to some aspects of artificial intelligence". Proceedings of the Acoustical and Vibratory Surveillance Conference, Senlis, France, October 27-29, 1992, pp 245-265.

A. Nagamatsu and M. Fukuda, "Sound noise generated from ball bearing in high speed rotation". Bulletin of the Japanese Society of Mechanical Engineers, Vol. 21, No. 158, August 1978, pp 1306-1310.

R.J.G. Nathan and M.P. Norton, "Bowl-roller mill top radial bearing diagnostic vibration trend analysis utilising the inverse frequency response function". Proceedings of the Institution of Engineers, Australia, Vibration and Noise Conference, Melbourne, 18-20 September 1990, pp 111-114.

C.L. Nikias and M.R. Raghuveer, "Bispectrum estimation: a digital signal processing framework". Proceedings of the IEEE, Vol. 75, No. 7, July 1987, pp 869-891.

C.L. Nikias and A.P. Petropulu, "*Higher order spectral analysis: a non-linear signal processing framework*". Prentice Hall, Englewood Cliffs, New Jersey, 1993.

K. Nishio, S. Hoshiya, T. Miyachi and M. Matsuki, "An investigation of the early detection of defects in ball bearings by the vibration monitoring". Proceedings of the ASME design Engineering Technical Conference, St. Louis, Mo., September 10-12, 1979.

A.V. Oppenheim and R.W. Schaffer, "*Digital signal processing*". Prentice-Hall, 1975.

G. Oreskovic, B. Mesko, S. Volcanjk and E. Prager, "Diagnostics of increased vibration and design of a monitoring system on a 630 MW turbine-generator set in nuclear power plant 'KRSKO' ". Proceedings of the Acoustical and Vibratory Surveillance Conference, Senlis, France, October 27-29, 1992, pp 315-323.

C.C. Osuagwu and D.W. Thomas, "Effect of inter-modulation and quasi-periodic instability in the diagnosis of rolling element incipient defect". Transactions of the American Society of Mechanical Engineers, Journal of Mechanical Design, Vol. 104, April 1982, pp 296-302.

A. Palmgren, *Ball and Roller Bearing Engineering*. S.H. Burbank and Co. Inc., Philadelphia, 1947.

E.F. Pardue, K.R. Piety and R. Moore, "Elements of reliability based machinery maintenance". Sound and Vibration, May 1992, pp 14-20.

F. Peyrin and R. Prost, "A unified definition for the discrete-time, discrete frequency, and discrete-time/frequency Wigner distributions". IEEE Transactions on Acoustics, Speech, and Signal Processing, Vol. ASSP-34, No. 4, August 1986, pp 858-866.

C. Pezeshki, S. Elgar and R.C. Krishna, "Bispectral analysis of systems possessing chaotic motion". Journal of Sound and Vibration, Vol. 137, No. 3, 1990, pp 357-368.

C. Pezeshki, W.H. Miles and S. Elgar, "Signal processing techniques for nonlinear structural dynamical systems". Applied Mechanics Review, Vol. 44, No. 11, part 2, November 1991, pp S214-S218.

G.J. Philips, "Bearing performance investigations through speed ratio measurements". ASLE Transactions, Vol. 22, No. 4, pp 307-314.

G.J. Philips, "The fibre optic bearing monitor". Proceedings of the 28th International Instrumentation Symposium, Pittsburg, PA, USA, 1982, pp 379-395.

G.J. Philips, "Measuring the size of rolling element bearing flaws". Sound and Vibration, April 1989, pp 6-16.

S.Y. Poon and F.P. Wardle, "Running quality of rolling bearings assessed". Chartered Mechanical Engineer, Vol. 25, April 1978, pp 74-77.

J.V. Poplawski, "Merging technologies solve rolling-mill bearing failures". Power Transmission Design, November 1992, pp 22-24.

H. Prashad, M. Ghosh and S. Biswas, "Diagnostic monitoring of rolling-element bearings by high-frequency resonance technique". ASLE Transactions, Vol. 28, No. 4, pp 439-448.

H. Prashad, "The effect of cage and roller slip on the measured defect frequency response of rolling element bearings". ASLE Transactions, Vol. 30, No. 3, pp 360-367.

H. Rahnejat and R. Gohar, "The vibrations of radial ball bearings". Proceedings of the Institution of Mechanical Engineers, Vol. 199, No. C3, 1985, pp 181-193.

R.B. Randall, "Advances in the application of cepstrum analysis to gearbox diagnosis". Proceedings of the 2nd International Conference on Vibrations in Rotating Machinery.

R.B. Randall, "The application of cepstrum analysis to machine diagnostics". Proceedings of the 36th meeting of the mechanical failures prevention group, Cambridge University Press, 1983, pp 64-72.

R.B. Randall, "Computer aided vibration spectrum trend analysis for condition monitoring". Maintenance Management International, Vol. 5, 1985, pp 161-167.

R.B. Randall, *Frequency Analysis*. Bruel and Kjaer, September 1987.

R.B. Randall, "Introduction to condition monitoring". Journal of the Australian Acoustical Society, Vol. 18, No. 1, 1990, pp 15-18.

R.B. Randall, Private Communication, August 1993.

P. Rao, F. Taylor and G. Harrison, "Real time monitoring of vibration using the Wigner Distribution". Sound and Vibration Magazine, May 1990, pp 22-25.

G.A. Ratcliffe, "Condition monitoring of rolling element bearings using the enveloping technique". Proceedings of the I.MECH.E. Machine Condition Monitoring Seminar, January 9th, 1990, pp 55-65.

A.G. Ray, "Monitoring rolling contact bearings under adverse conditions". Proceedings of the 2nd International Conference on Vibrations in Rotating Machinery, I.MECH.E., 1980, pp 187-194.

J.J. Reis, "Program for experimental investigation of failure prognosis of helicopter gearboxes". US Army Air Mobility Research and Development Laboratory Technical Report-76-13, August 1976.

O. Rioul and M. Vetterli, "Wavelets and Signal Processing". IEEE Signal Processing Magazine, October 1991, pp 14-38.

J.C. Robinson, F.E. LeVert and J.E. Mott, "The acquisition of vibration data from low-speed machinery". Sound and Vibration, May 1992, pp 22-28.

E. Ryckalts, "Effective enhanced techniques for early detection, monitoring, trending and diagnosis of bearing damage". Proceedings of the Acoustical and Vibratory Surveillance Conference, Senlis, France, 27-29th October 1992, pp 345-356.

N.W. Sachs, "Logical failure analysis in rolling element bearings". Power Transmission Design, October 1992, pp 22-25.

R.R. Sanders, "Design considerations to limit noise and vibrations in limit applications". Noise and Vibration Control Worldwide, Vol. 13, No. 6, September 1982, pp 268-269.

T. Sato, K. Sasaki and Y. Nakamura, "Real-time bispectral analysis of gear noise and its application to contactless diagnosis". *Journal of the Acoustical Society of America*, Vol. 62, No. 2, August 1977, pp 382-387.

R.S. Sayles and S.Y. Poon, "Surface topography and rolling element vibration". *Precision Engineering*, 1981, pp 137-144.

W. Scheithe, "Better bearing vibration analysis". *Hydrocarbon Processing*, Vol. 71, No. 7, July 1992, pp 57-64.

R.L. Schiltz, "Forcing frequency identification of rolling element bearings". *Sound and Vibration*, May 1990, pp 16-19.

M. Serridge, "What makes vibration condition monitoring reliable". *Noise and Vibration Worldwide*, September 1991, pp 17-24.

S.K. Sharma, "Traction behavior of some lubricants and hydraulic fluids". *Transactions of the American Society of Mechanical Engineers, Journal of Tribology*, Vol. 109, April 1987, pp 372-373.

J.M. Shea and J.K. Taylor, "Spike energy in fault analysis / machine condition monitoring". *Noise and Vibration Worldwide*, February 1992, pp 22-26.

B. Sheppard, "Diagnosing bearings using vibration data". *Maintenance Technology*, August 1992, pp 30-32.

P.J. Sherman and K.N. Lou, "A new spectral approach for identification of defects in rotating machinery". *Proceedings of the 43rd Meeting of the Mechanical Failures Prevention Group*, San Diego, California, October 1988, pp 99-105.

J.D. Smith, "Vibration monitoring of bearings at low speeds". *Tribology International*, June 1982, pp 139-144.

R. L. Smith and J. Bambara, "Acoustic detection of defective rolling element bearings". *Proceedings of the 43rd Meeting of the Mechanical Failures Prevention Group*, San Diego, California, October 1988, pp 79-88.

R.L. Smith, "Railcar bearing end-life failure distances and acoustical defect censuring methods". *Proceedings of the ASME Winter Annual Meeting*, Chicago, Illinois, November 27-December 2, 1988.

R. L. Smith, "Rolling element bearing diagnostics with lasers, microphones and accelerometers". *Proceedings of the 46th Meeting of the Mechanical Failures Prevention Group*, San Diego, California, April 1992, pp 43-52.

R.M. Stewart, "Application of signal processing techniques to machinery health monitoring". *Noise and Vibration*, Halsted Press, 1983, Chapter 23, pp 607-632.

Y.T. Su and S.J. Lin, "On initial fault detection of a tapered roller bearing: Frequency domain analysis". *Journal of Sound and Vibration*, Vol. 155, No. 1, 1992, pp 75-84.

Y.T. Su, M.H. Lin and M.S. Lee, "The effects of surface irregularities on roller bearing vibrations". *Journal of Sound and Vibration*, Vol. 163, No. 3, 1993, pp 455-466.

Y.T. Su, Y.T. Sheen, M.H. Lin, "Signature analysis of roller bearing vibrations: Lubrication effects". *Proceedings of the Institute of Mechanical Engineers, Part C: Journal of Mechanical Engineering Science*, Vol. 206, 1992, pp 193-202.

Y.T. Su, Y.T. Sheen, "On the detectability of roller bearing damage by frequency analysis". *Proceedings of the Institute of Mechanical Engineers, Part C: Journal of Mechanical Engineering Science*, Vol. 207, 1993 pp 23-32.

G.P. Succi, "Prognostic methods for bearing condition monitoring". *Proceedings of the 3rd International Machinery Monitoring and Diagnostics Conference*, Las Vegas, Nevada, December 1991, pp 335-342.

M. o'Sullivan, "Diagnosis of vibration problems in Holland - Case studies from the Groenpol vibration consultancy". *Brueel and Kjaer Application Note No. 297-11*.

M. o'Sullivan, "Systematic machine condition monitoring - A case study from Parenco paper mill in Holland". *Brueel and Kjaer Application Note No. 299-11*.

C.S. Sunnersjo, "Rolling bearing vibrations - The effects of geometrical imperfections and wear". *Journal of Sound and Vibration*, Vol. 98, No. 4, 1985, pp 455-474.

N.S. Swansson and S.C. Favaloro, "Applications of vibration analysis to the condition monitoring of rolling element bearings". *Aeronautical Research Laboratory, Propulsion Report 163*, January 1984.

T.E. Tallian and O.G. Gustafsson, "Progress in rolling bearing vibration research and control". *ASLE Transactions*, Vol. 8, 1965, pp 195-207.

C.C. Tan, "Adaptive noise cancellation of acoustic emission noise in ball bearings". *Proceedings of the Asia-Pacific Vibration Conference*, Monash University, Melbourne, Australia, November 1991, pp 5.28-5.35.

N. Tandon and B.C. Nakra, "Defect detection in rolling element bearings by acoustic emission method". *Journal of Acoustic Emission*, Vol. 9, No. 1, 1990, pp 25-28.

N. Tandon and B.C. Nakra, "Vibration and acoustic monitoring techniques for the detection of defects in rolling element bearings - A review". *The Shock and Vibration Digest*, Vol. 24, No. 3, March 1992, pp 3-11.

N. Tandon and B.C. Nakra, "Comparison of vibration and acoustic measurement techniques for the condition monitoring of rolling element bearings". *Tribology International*, Vol. 25, No. 3, 1992, pp 205-212.

M. S. Tavakoli, "Bearing fault detection in the acoustic emission frequency range". *Proceedings of Noise Con 91*, Tarrytown, New York, July 14-16, 1991, pp 79-86.

J.I. Taylor, "Determination of antifriction bearing condition by spectral analysis".

J.I. Taylor, "Identification of bearing defects by spectral analysis". *Transactions of the American Society of Mechanical Engineers, Journal of Mechanical Design*, Vol. 102, 1980, pp 199-204.

S. Teo, "Advances in the condition monitoring of slow speed rolling element bearings". *International Noise and Vibration Conference*, 1989.

S. Teo, "Condition monitoring of slow speed rolling element bearings in a mechanically noisy environment". *Appita*, Vol. 42, No. 3, May 1989, pp 206-208.

N. Tsushima, "Rolling contact fatigue and fracture toughness of rolling element bearing materials". *JSME International Journal, Series C*, Vol. 36, No. 1, 1993, pp 1-8.

W.J. Wang and P.D. McFadden, "Time-frequency domain analysis of vibration signals for machinery diagnostics. (III) The present power spectral density". *University of Oxford, Department of Engineering Science, Report No. OUEL 1911/92*, 1992.

W.J. Wang and P.D. McFadden, "Early detection of gear failure by vibration analysis -I. Calculation of the time-frequency distribution". *Mechanical Systems and Signal Processing*, Vol. 7, No. 3, 1993, pp 193-203.

W.J. Wang and P.D. McFadden, "Early detection of gear failure by vibration analysis -II. Interpretation of the time-frequency distribution using image processing techniques". *Mechanical Systems and Signal Processing*, Vol. 7, No. 3, 1993, pp 205-215.

F.P. Wardle and S.Y. Poon, "Rolling bearing noise - Cause and cure". *Chartered Mechanical Engineer*, July-August 1983, pp 36-40.

F.P. Wardle, "Vibration forces produced by waviness of the rolling surfaces of thrust loaded ball bearings, Part I: Theory". *Proceedings of the Institution of Mechanical Engineers*, Vol. 202, No. C5, 1988, pp 305-312.

F.P. Wardle, "Vibration forces produced by waviness of the rolling surfaces of thrust loaded ball bearings, Part II: Experimental validation". *Proceedings of the Institution of Mechanical Engineers*, Vol. 202, No. C5, 1988, pp 313-319.

M.F. While, "Rolling element bearing vibration transfer characteristics: Effect of stiffness". Transactions of the American Society of Mechanical Engineers, Journal of Applied Mechanics, Vol. 46, September 1979, pp 677-684.

G. White, "Amplitude demodulation - A new tool for predictive maintenance". Sound and Vibration, September 1991, pp 14-19.

D.J. Whitehouse, "Beta functions for surface typology". Annals of the CIRP, Vol. 27, No. 1, 1978, pp 491-497.

E. Yhland, "A linear theory of vibrations caused by ball bearings with form errors operating at moderate speeds". Transactions of the American Society of Mechanical Engineers, Journal of Tribology, Vol. 114, April 1992, pp 348-359.

T. Yoshioka, "Detection of rolling contact sub-surface fatigue cracks using acoustic emission technique". Lubrication Engineering, Journal of the Society of Tribologists and Lubrication Engineers, Vol. 4, No. 4, April 1993, pp 303-308.

A. Yuasa, H. Kanai, M. Abe and K. Kido, "Detection of flaws in ball bearings by analysis of vibration signals detected by two pick-ups". Journal of the Acoustical Society of Japan, Vol. 9, No. 2, 1988, pp 81-87.

Y. Yan and T. Shimogo, "An application of the impulse index in knocking detection in the reciprocating engine". Proceedings of the Asia-Pacific Vibration Conference, Monash University, Melbourne, Australia, November 1991, pp 5.36-5.41.

Y. Yan and T. Shimogo, "The application of HAAR transform in signature extraction and condition monitoring of mechanical systems". JSME International Journal, Series III, Vol. 33, No. 2, 1990, pp 191-197.

Y. Yan and T. Shimogo, "Application of the impulse index in rolling element bearing fault diagnosis". Mechanical Systems and Signal Processing, Vol. 6, No. 2, 1992, pp 167-176.

E.V. Zaretsky, "Lubricant effects on bearing life". NASA Lewis Research Center Technical Memorandum TM-88875, 1986.

W. Zhang and M.R. Raghuveer, "Nonparametric bispectrum based time delay estimators for multiple sensor data". IEEE Transactions on Signal Processing, Vol. 39, No. 3, March 1991, pp 770-774.

Q. Zhuge, Y. Lu and S. Yang, "Non-stationary modelling of vibration signals for monitoring the condition of machinery". Mechanical Systems and Signal processing, Vol. 4, No. 5, 1990, pp 355-365.

A Review of Rolling Element Bearing Vibration
"Detection, Diagnosis and Prognosis"

Ian Howard
DSTO-RR-0013

DISTRIBUTION

AUSTRALIA

Defence Science and Technology Organisation

Chief Defence Scientist	}	shared copy
FAS Science Policy		
AS Science Corporate Management		
Counsellor Defence Science, London (Doc Data Sheet only)		
Counsellor Defence Science, Washington (Doc Data Sheet only)		
Senior Defence Scientific Adviser (Doc Data Sheet only)		
Scientific Advisor Policy and Command (Doc Data Sheet only)		
Navy Scientific Adviser		
Scientific Adviser - Army (Doc Data Sheet only)		
Air Force Scientific Adviser (Doc Data Sheet only)		

Aeronautical and Maritime Research Laboratory

Director
Library, Fishermens Bend
Library, Maribyrnong
Chief Airframes and Engines Division
Author: I.M. Howard
Machine Dynamics: B.R. Rebbechi
B.D. Forrester

Electronics and Surveillance Research Laboratory

Director
Main Library - DSTO Salisbury

Defence Central

OIC TRS, Defence Central Library
Document Exchange Centre, DIS (8 copies)
Defence Intelligence Organisation
Library, Defence Signals Directorate (Doc Data Sheet Only)

HQ ADF

Director General Force Development (Sea)

Navy

Aircraft Maintenance and Flight Trials Unit
Director Aircraft Engineering - Navy
Director of Aviation Projects - Navy
Director of Naval Architecture
RAN Tactical School, Library
Superintendent, Naval Aircraft Logistics

Army

Engineering Development Establishment Library
US Army Research, Development and Standardisation
Group (3 copies)

Air Force

Aircraft Research and Development Unit
Scientific Flight Group
Library
PDR AF
DENGPP-AF
AHQ CSPT
CLSA-LC
OIC ATF, ATS, RAAFSTT, WAGGA (2 copies)

UNIVERSITIES AND COLLEGES

Australian Defence Force Academy
Library
Head of Aerospace and Mechanical Engineering

Adelaide
Head Mechanical Engineering

Flinders
Library

LaTrobe
Library

Melbourne
Engineering Library

Monash
Hargrave Library
Director, Centre for Machine Condition Monitoring

Newcastle
Library
Head Mechanical Engineering

New England
Library

Sydney
Engineering Library
Head, School of Mechanical Engineering

NSW
Physical Sciences Library
Head, Mechanical Engineering
Mr R.B. Randall, Mechanical Engineering

Queensland
Library

Tasmania
Engineering Library

Western Australia
Library
Head, Mechanical Engineering

RMIT
Library
Head, Aerospace Engineering

University College of the Northern Territory
Library

OTHER GOVERNMENT DEPARTMENTS AND AGENCIES

Department of Transport & Communication, Library
Civil Aviation Authority
Gas & Fuel Corporation of Vic., Manager Scientific Services
SEC of Vic., Herman Research Laboratory, Library

OTHER ORGANISATIONS

NASA (Canberra)
AGPS
ASTA Engineering, Document Control Office
Ansett Airlines of Australia, Library
Qantas Airways Limited
Hawker de Havilland Aust Pty Ltd, Victoria, Library
Hawker de Havilland Aust Pty Ltd, Bankstown, Library
Rolls Royce of Australia Pty Ltd, Manager
Australian Nuclear Science and Technology Organisation
Ampol Petroleum (Vic) Pty Ltd
Australian Institute of Petroleum Ltd
BHP Melbourne Research Laboratories
BP Australian Ltd, Library

CANADA

NRC, Ottawa
Division of Mechanical Engineering, Mr J. Ploeg
Engine Laboratory, Dr G. Krishnappa
NRC, Vancouver
Tribology and Mechanics Laboratory, Dr P. Kim

DENMARK

Brueel and Kjaer
Dr J. Courrech

ISRAEL

Technion-Israel Institute of Technology
Prof S. Braun, Engineering Department

NEW ZEALAND

Defence Scientific Establishment, Library
Transport Ministry, Airworthiness Branch, Library

Universities

Canterbury
Head, Mechanical Engineering

UNITED KINGDOM

Ministry of Defence, Research, Materials and Collaboration
Defence Research Agency (Aerospace)
Head Airworthiness Division
Defence Research Agency (Naval)
Holton Heath, Dr N.J. Wadsorth
St Leonard's Hill, Superintendent
Naval Aircraft Material Laboratory
Mr P. Gadd
British Aerospace
Kingston-upon-Thames, Library
Hatfield-Chester Division, Library
Civil Aviation Authority, Safety Regulation Group,
Mr S.L. James
Mr J.E. Witham

Universities and Colleges

Bristol
Engineering Library

Cambridge
Library, Engineering Department

Cranfield Inst. of Technology
Library
Dr R.H. Bannister, School of Mechanical Engineering

Imperial College
Aeronautics Library

Manchester
Professor Applied Mathematics
Head Dept of Engineering (Aeronautical)

Oxford
Library
Dept of Engineering Science, Dr P.D. McFadden

Southampton
Library
Professor J. Hammond Institute of Sound & Vibration Research

UNITED STATES OF AMERICA

NASA Scientific and Technical Information Facility
United Technologies Corporation
Library
Mr M. Hawman Research Center
Nondestructive Testing Information Analysis Center
Naval Aircraft Test Center (Patuxent River)
Mr M. Hollins
United Technologies Sikorsky Aircraft
Dr Ray Carlson
Bell Helicopter Textron
Mr J. Cronkhite
McDonnell Douglas Helicopter Company
Boeing Helicopter Company
NASA Lewis Research Center
Mr Jim Zakrajsek
NASA Marshall Space Flight Center
Mr Preston Jones, ED 23
Naval Air Propulsion Center
Mr D. Rawlinson
US Army Aviation Technology Directorate
Technology Integration Inc.
Dr Jim Gottwald
Dr Sam Ventres
Mr Dick Hayden
Vibration Institute
Dr R.L. Eshleman
Mechanical Technology Inc.
Mr R.L. Smith

Universities and Colleges

Chicago
John Crerar Library

Florida
Aero Engineering Department
Head, Engineering Sciences

Johns Hopkins
Head, Engineering Department

Iowa State
Head, Mechanical Engineering

Purdue
Library

Princeton
Head, Mechanics Department

Massachusetts Inst. of Technology
MIT Libraries

SPARES (5 COPIES)

TOTAL (139 COPIES)

PAGE CLASSIFICATION
UNCLASSIFIED

PRIVACY MARKING

DOCUMENT CONTROL DATA

1a. AR NUMBER AR-008-399	1b. ESTABLISHMENT NUMBER DSTO-RR-0013	2. DOCUMENT DATE OCTOBER 1994	3. TASK NUMBER NAV 92/119				
4. TITLE A REVIEW OF ROLLING ELEMENT BEARING VIBRATION "DETECTION, DIAGNOSIS AND PROGNOSIS"		5. SECURITY CLASSIFICATION (PLACE APPROPRIATE CLASSIFICATION IN BOX(S) IE. SECRET (S), CONF. (C), RESTRICTED (R), LIMITED (L), UNCLASSIFIED (U)).					
		<table border="1"> <tr> <td>U</td> <td>U</td> <td>U</td> </tr> <tr> <td>DOCUMENT</td> <td>TITLE</td> <td>ABSTRACT</td> </tr> </table>		U	U	U	DOCUMENT
U	U	U					
DOCUMENT	TITLE	ABSTRACT					
6. NO. PAGES 102		7. NO. REFS. 239					
8. AUTHOR(S) I.M. HOWARD		9. DOWNGRADING/DELIMITING INSTRUCTIONS Not applicable.					
10. CORPORATE AUTHOR AND ADDRESS AERONAUTICAL AND MARITIME RESEARCH LABORATORY AIRFRAMES AND ENGINES DIVISION GPO BOX 4331 MELBOURNE 3001 VICTORIA AUSTRALIA		11. OFFICE/POSITION RESPONSIBLE FOR: NAVY SPONSOR _____ SECURITY _____ DOWNGRADING _____ APPROVAL _____ CAED					
12. SECONDARY DISTRIBUTION (OF THIS DOCUMENT) Approved for public release. OVERSEAS ENQUIRIES OUTSIDE STATED LIMITATIONS SHOULD BE REFERRED THROUGH DSTIC, ADMINISTRATIVE SERVICES BRANCH, DEPARTMENT OF DEFENCE, ANZAC PARK WEST OFFICES, ACT 2601							
13a. THIS DOCUMENT MAY BE ANNOUNCED IN CATALOGUES AND AWARENESS SERVICES AVAILABLE TO No limitations							
14. DESCRIPTORS Roller bearings Vibration analysis Machinery Condition monitoring		15. DISCAT SUBJECT CATEGORIES 1309					
16. ABSTRACT Rolling element bearings are among the most common components to be found in industrial rotating machinery. They are found in industries from agriculture to aerospace, in equipment as diverse as paper mill rollers to the Space Shuttle Main Engine Turbomachinery. There has been much written on the subject of bearing vibration monitoring over the last twenty five years. This report attempts to summarise the underlying science of rolling element bearings across these diverse applications from the point of view of machine condition monitoring using vibration analysis. The key factors which are addressed in this report include the underlying science of bearing vibration, bearing kinematics and dynamics, bearing life, vibration measurement, signal processing techniques and prognosis of bearing failure.							

PAGE CLASSIFICATION
UNCLASSIFIED

PRIVACY MARKING

THIS PAGE IS TO BE USED TO RECORD INFORMATION WHICH IS REQUIRED BY THE ESTABLISHMENT FOR ITS OWN USE BUT WHICH WILL NOT BE ADDED TO THE DISTIS DATA UNLESS SPECIFICALLY REQUESTED.

16. ABSTRACT (CONT).

17. IMPRINT

**AERONAUTICAL AND MARITIME RESEARCH LABORATORY,
MELBOURNE**

18. DOCUMENT SERIES AND NUMBER

DSTO Research Report 0013

19. WA NUMBER

43 432A

20. TYPE OF REPORT AND PERIOD COVERED

21. COMPUTER PROGRAMS USED

22. ESTABLISHMENT FILE REF.(S)

23. ADDITIONAL INFORMATION (AS REQUIRED)